Development of a Low-Cost, Rapid-Cycle Hot Embossing System for Microscale Parts

by

Melinda Hale

B.S., Mechanical Engineering
Oklahoma State University, 2007

MASSACHUSETTS INSTITUTE
OF TECHNOLOGY
JUN 16 2009
LIBRARIES

Submitted to the Department of Mechanical Engineering
in partial fulfillment of the requirements for the degree of

Master of Science

ARCHIVES

at the

MASSACHUSETTS INSTITUTE OF TECHNOLOGY

June 2009

© Massachusetts Institute of Technology 2009. All rights reserved.

Author ....
Department of Mechanical Engineering
May 8, 2009

Certified by..
David E. Hardt
Ralph E. and Eloise F. Cross Professor of Mechanical Engineering
Thesis Supervisor

Accepted by..
David E. Hardt
Chairman, Department Committee on Graduate Students

Development of a Low-Cost, Rapid-Cycle Hot Embossing System for Microscale Parts

by

Melinda Hale

Submitted to the Department of Mechanical Engineering
on May 8, 2009, in partial fulfillment of the
requirements for the degree of
Master of Science

Abstract

Hot embossing is an effective technology for reproducing micro-scale features in polymeric materials, but large-scale adoption of this method is hindered by high capital costs and low cycle times relative to other technologies, and a general lack of manufacturing equipment. This work details a hot embossing machine design strategy motivated by maximum production speed and quality with minimal capital cost. The approach is to "right-size" the machine for specific product needs while making the design flexible and scalable. Toward this end, a minimal number of components were used, commercially available off-the-shelf components were chosen where possible, system layout was designed to be modular, and system size was scaled for the intended products (in this case microfluidic devices). Innovative design aspects include the use of new ceramic substrate heaters for electrical heating, use of a moveable heat sink to minimize heat load during the heating cycle, and the careful design of the thermal elements to minimize the heating and cooling cycle times. The capital cost and the cost per part produced with this machine are estimated to be an order of magnitude less than currently available hot embossing manufacturing options. The hot embossing machine has been tested extensively to characterize the process variability. The minimum cycle time is two minutes, and microstructures are replicated within a maximum of a 25mm by 75mm area with very low relative variance in dimensions.

Thesis Supervisor: David E. Hardt
Title: Ralph E. and Eloise F. Cross Professor of Mechanical Engineering

Acknowledgments

I would like to thank my family for their encouragement and support - my sister for taking late night phone calls, my brothers for making sure I go home every once in a while, and my mother for her impeccable grammar edits and sympathetic ear. I am especially grateful to my father for his thoughts during long rides in the car - my best ideas are almost certainly his, through either suggestion or the genes.

I would like to thank my advisor, Professor David Hardt, for his mentorship and the opportunity to work under his direction.

I would like to thank my labmates Matt Dirckx and Aaron Mazzeo, for their patience and advice in answering questions, and for the excellent example they have set.

I am eternally grateful to the staff of the machine shop - especially Gerry Wentworth - who all ensured that the "build" phase of my project was of high quality and completed with no loss of fingers.

None of this work would have been possible without funding from the Singapore-MIT Alliance, whose support is much appreciated.

Contents

1 Introduction **15**

1.1 What is micromanufacturing . . . 15

1.1.1 History . . . 16

1.1.2 Applications . . . 17

1.2 Overview of thesis . . . 17

2 Background **19**

2.1 Micromanufacturing Processes . . . 19

2.1.1 Hot Embossing . . . 19

2.1.2 Ultraviolet Casting . . . 20

2.1.3 Injection Molding . . . 21

2.1.4 Soft Lithography . . . 22

2.1.5 Thermoforming . . . 23

2.2 Why Hot Embossing . . . 23

2.3 History of Hot Embossing Machines . . . 25

2.3.1 MIT Generation 1 Equipment . . . 25

2.3.2 MIT Generation 2 Equipment . . . 27

2.3.3 Research Hot Embossing Equipment . . . 29

2.3.4 Commercial Hot Embossing Equipment . . . 30

2.4 Motivation for new equipment . . . 33

3 Goals and Design Approach **35**

3.1 Functional Requirements . . . 35

3.1.1 Workpiece Size . . . 35

3.1.2 Force capacity . . . 36

3.1.3 Heating 36

3.1.4 Cooling 37

3.1.5 Cycle Time 38

3.1.6 Manufacturing considerations 39

3.1.7 Summary 39

3.2 Manufacturing Motivations 39

3.3 Design Approach 40

4 Concepts **43**

4.1 Frame design concepts 43

4.1.1 Frame design requirements 43

4.1.2 Concept: Gantry 44

4.1.3 Concept: Triangular Pyramid 44

4.1.4 Concept: Curved Cantilever 45

4.1.5 Concept: Double Curved Cantilever 45

4.1.6 Concept: Two Stage Process 47

4.1.7 Comparison of Frame Concepts 47

4.2 Force application concepts 49

4.2.1 Force requirements 49

4.2.2 Concept: Hydraulic 49

4.2.3 Concept: Pneumatic 49

4.2.4 Concept: Piezomaterial 49

4.2.5 Concept: Mechanical Lead Screw 50

4.2.6 Comparison of Force Concepts 50

4.3 Heating concepts 51

4.3.1 Heating requirements 51

4.3.2 Concept: Cartridge heaters 51

4.3.3 Concept: Ceramic heaters 51

4.3.4 Concept: Fluidic heating 52

4.3.5 Concept: Peltier Heating 52

4.3.6 Comparison of Heating Concepts 52

4.4 Cooling concepts 53

4.4.1 Cooling Requirements 53
4.4.2 Concept: Air cooling 53
4.4.3 Concept: Oil cooling 53
4.4.4 Concept: Water cooling 54
4.4.5 Compare concepts 54
4.5 Summary of concepts chosen 55

5 Design **57**
5.1 Overview of Design Process 57
5.2 Thermal Design 57
5.2.1 Elements of the stack 58
5.2.2 Heat Sink Design 58
5.2.3 Analysis of Heating 61
5.2.4 Analysis of Cooling 64
5.3 Structural and Force Application Design 67
5.3.1 Pneumatic Cylinder Design 67
5.3.2 Load cell design 67
5.3.3 Support design 68
5.4 Control System Design 70

6 Fabrication **75**
6.1 Structural Components 75
6.2 Thermal Stack Components 77
6.3 Force Components 79
6.4 Cooling Components 82
6.5 Control System Elements 83
6.6 Assembly 84

7 Results and Discussion **87**
7.1 Microfactory Project 87
7.2 Iterations A, B, and C 88
7.3 Temperature Control 88
7.4 Force control 94

7.4.1 Simulink Model of Force Control System 99
7.5 Channel Variability Analysis 103

8 Conclusions 113

8.1 Future Work 113

A Material Properties 115

B Part Height and Width Measurements 117

C Drawings 127

List of Figures

2-1 Schematic for Hot Embossing [15] 20

2-2 Schematic for UV Casting [15] 21

2-3 Schematic for Micro-Injection Molding [15] 22

2-4 Schematic for Soft Lithography [15] 23

2-5 Schematic for Thermoforming [9] 24

2-6 Generation 1 Machine Overview [17] 26

2-7 Generation 1 Machine Platens [17] 26

2-8 Generation 2 Machine Overview 28

2-9 Generation 2 Machine Platens 28

2-10 Commercial Hot Embossing Machines 32

4-1 Gantry Frame Concept 44

4-2 Pyramid Frame Concept 45

4-3 Curved Cantilever Frame Concept 46

4-4 Double Curved Cantilever Frame Concept 46

4-5 Two Stage Frame Concept 47

5-1 Thermal Stack 59

5-2 Possible Heat Sink Support Configurations 60

5-3 CAD Model used for Heating Analysis 63

5-4 Results of FEA Heating Analysis showing a minimum of 35 seconds needed to reach embossing temperature 63

5-5 FEA Plot of Thermal Stack During Heating 64

5-6 CAD Model used for Cooling Analysis 65

5-7 Results of FEA Cooling Analysis showing a minimum of 50 seconds needed to reach demolding temperature 66
5-8 FEA Plot of Thermal Stack During Cooling 66
5-9 Possible Ceramic Pin Configurations 69
5-10 Control System Layout (see Section 6.5 for part numbers) 74

6-1 Overall CAD model 75
6-2 Press Frame 76
6-3 Structural Components 77
6-4 Thermal Stack Components 78
6-5 Embossing Tools 80
6-6 Actual Thermal Stack 81
6-7 Force Components 81
6-8 Cooling Components 82
6-9 Actual Cooling Components 83
6-10 Fabricated Hot Embossing Equipment 85

7-1 Part Blank 89
7-2 Embossed Part 89
7-3 Embossed Part with Frame 90
7-4 Heating Response at Varying Heater Powers 91
7-5 Temperature of Heaters and the Workpiece during Embossing Cycle 92
7-6 Temperature Profiles for PMMA Run A 93
7-7 Temperature Profiles for PMMA Run B 94
7-8 Temperature Profiles for PMMA Run C 95
7-9 Force Profiles for PMMA Run A, Using a +/- 5000 lbf Load Cell 96
7-10 Force Profiles for PMMA Run B 97
7-11 Force Profiles with Incorrect Gain Setting, Showing Oscillation 97
7-12 Broken Ceramic 98
7-13 Force Profiles for PMMA Run C 100
7-14 Simulink Model of Embossing System in Force Feedback 101
7-15 Simulink Force Response Graph 101
7-16 Simulink Model of Embossing System in Force Feedback with Filter 101

7-17 Simulink Force Response Graph with Filter or with Added Spring Layer . . . 102
7-18 Simulink Model of Embossing System with Pressure Source 102
7-19 Simulink Force Response Graph with Pressure Control Valve 103
7-20 Force Profiles for PMMA Run C 104
7-21 Measurement Sites on Micromixer Pattern 105
7-22 Run A Site 1 Height and Width 106
7-23 Run A Site 2 Height and Width 107
7-24 Run A Site 3 Height and Width 107
7-25 Run C Site 1 Height and Width 109
7-26 Run C Site 2 Height and Width 109
7-27 Run C Site 3 Height and Width 110
7-28 Comparison of Tool Dimensions with Average PMMA Part Run Dimensions . 111

B-1 Run A Site 1 Height and Width Including Outliers 124
B-2 Run A Site 2 Height and Width Including Outliers 124
B-3 Run A Site 3 Height and Width Including Outliers 125
B-4 Run C Site 1 Height and Width Including Outliers 125
B-5 Run C Site 3 Height and Width Including Outliers 126

C-1 Solidworks Cylinder Adapter 128
C-2 Solidworks Base 129
C-3 Solidworks Steel Backing Plate 130
C-4 Solidworks Top Ceramic Spacer 131
C-5 Solidworks Force Adapter 132
C-6 Solidworks Heat Sink 133

List of Tables

2.1 Commercial Hot Embossing Machines 31

3.1 Geometry and Thermal Mass of Thermal Stack Elements 37
3.2 Minimum Cycle Time 38
3.3 Functional Requirements 39

4.1 Frame Concept Pugh Chart 48
4.2 Force Concept Pugh Chart 50
4.3 Heating Concept Pugh Chart 53
4.4 Cooling Concept Pugh Chart 54
4.6 Final Concept Choices 55

5.1 Calculation of Diameter of Heat Sink Cooling Passages 61
5.2 Parameters of Heating FEA Components 62
5.3 Parameters of Cooling FEA Components 65
5.4 Bending Analysis Constants 70
5.5 Determining Bending Limiting Case: Pin-to-Pin or Pin-to-Free 70
5.6 Maximum Deflection of Backing Plate vs. Thickness for Aluminum and Steel 71
5.7 Comparison of Thermal Mass of Aluminum and Steel Backing Plates 71
5.8 Determining Worst Case Bending of Simply Supported Beam 71
5.9 Bending Analysis Constants 71
5.10 Critical Force for Buckling 72

7.1 Simulink Parameters 99
7.2 Variability of Measurement System 105
7.3 Actual Measurement of BMG Tool used for all PMMA Runs 105

7.4 Summary of PMMA Run A Height and Width Data 108
7.5 Summary of PMMA Run C Height and Width Data 108

A.1 Material Properties 115

B.1 PMMA Run A Sites 1, 2, 3 Height and Width Data 119
B.2 PMMA Run A Repeatability of Zygo 120
B.3 PMMA Run C Sites 1, 2, 3 Height and Width Data 123

Chapter 1

Introduction

This thesis presents equipment specifically designed from a manufacturing point of view to produce microscale plastic parts using hot embossing. This is important because a new area of technology - microfluidic devices - is nearing a critical period of development: the transition between laboratory use and industry application. Microfluidic devices cannot begin to be mass produced until two things happen: an effective application and an economically viable manufacturing process. This author aims to address the latter. The impact of this work is both short-term and long-term. An immediate effect is that the ability to quickly make microfluidic devices will allow researchers to be more productive - to spend more time on research and less on making the devices. The long-term impact of this work is to push microfluidic technology from the lab into industry by providing manufacturing equipment that allows companies to produce products not currently economically or technologically possible. Pharmaceutical companies may be able to do drug combinatorial trials orders of magnitude faster and cheaper. Homeland security could produce disposable chips to detect explosives and biochemical agents in public places. Third world countries might in the future test for HIV and malaria with disposable, at-home chips using the prick of a finger. All of these possibilities for applications of microfluidic devices require a method of production that is economical at a large scale - they require micromanufacturing.

1.1 What is micromanufacturing

Manufacturing in general is defined "to make from raw materials by hand or by machinery ...a product suitable for use" [1]. Common processes for manufacturing can be additive, subtractive (laser ablation, X-ray lithography), or formative (injection molding, casting, hot embossing) [24]. Micromanufacturing is simply an extension of these principles to parts with features on the order of microns. There are analogous processes (micromachining and micro-injection molding, for instance) and some new processes (ultraviolet embossing, for example) unique to micromanufacturing.

1.1.1 History

Scientific advances have consistently driven technology to be faster, cheaper, and smaller. In the past few decades, this is most easily seen in the case of computer chips. Each new generation of computer chip has had exponentially more functionality, gained by miniaturizing and tightly integrating the electronic components on each chip. In 1990 Manz and Widmer [27] envisioned applying the same principle to biochemistry - taking standard chemical tools such as beakers, test tubes, tubing, pipettes and valves, then miniaturizing and packaging them on a small biochemical chip to do a particular job. The first attempts in the 1990s at making these biochemical chips used mostly the same methods used for computer chips: silicon tools, glass substrates, and MEMS manufacturing technology such as wet-etching and photolithography [26, 18]. There are some companies now that make microfluidic products using these legacy methods (including Caliper Life Sciences, Microline, Micronit, and Dolomite). However, by early in the 2000s, there was a growing consensus that polymeric substrates had significant advantages over quartz, silicon, and glass, and were likely the future of commercial microfluidics [14, 10].

There are many ways to make microscale features in polymeric materials, such as hot embossing, injection molding, soft lithography, laser photoablation, X-ray lithography, and ultraviolet embossing [10]. The majority of these methods are either conventional processes being modified to produce microscale features, or are still experimental and the subject of ongoing research. Commercialization of microfluidic devices from plastic has been slower than commercialization using glass and silicon because polymeric microfabrication does not yet have the body of knowledge that other microfabrication methods have acquired over the years.

1.1.2 Applications

Some of the oldest applications of microfluidic devices are optical waveguides and diffraction gratings in the 1970s [21]. In more recent years, the most mature applications are ink-jet printing, followed closely by lab-on-a-chip assays. Microfluidic devices now commercially exist for DNA sorting, drug-discovery applications, fertility testing, immunoassays, and other flow-through processes in chemistry [30]. Devices have been proven in research to handle jobs such as sample manipulation through mixing and T-junctions, capillary electrophoresis, miniaturized polymerase chain reaction (PCR) for DNA amplification, clinical chemistry and diagnostics, micro-reactions and containment, and cell handling [10]. However, there are many more potential applications in fields that include pharmaceuticals, biotechnology, the life sciences, defense, public health, and agriculture. The market for microfluidic devices is still small, but has steadily grown to $84.3 million in US Revenue in 2005, and is predicted to be $200 million by 2012 [3]. The worldwide market for microfluidic devices was $128 million in 2002 [2], but credible estimates of the potential market size are on the order of billions of dollars [10].

1.2 Overview of thesis

In this thesis, hot embossing equipment specifically for manufacturing microfluidic devices is designed, fabricated, and tested. The design of the equipment keeps the capital cost as low as possible by using the minimum number of components, using simple technologies, and keeping the overall size of the system small. The design also maximizes production speed by careful choices relating to the thermal mass of critical components, using a moving heat sink, and using new ceramic heaters. Testing of the fabricated equipment shows that sub-micron variation in feature dimensions can be obtained across runs of parts manufactured at a rate of two minutes per part.

This thesis was completed in the Polymer Micromanufacturing Laboratory, a division of the Laboratory for Manufacturing and Productivity. The work was completed under the direction of Professor David E. Hardt, in collaboration with the Singapore-MIT Alliance. The historic focus of this lab has been to apply process control to manufacturing processes, including sheet metal forming, welding, thermal set polymer casting and hot embossing. This thesis continues the tradition of the lab by designing manufacturing equipment for, and applying process control to, a process currently using prototyping and fabrication methods. This thesis is also funded by an overarching project with the goal of creating "a fundamental basis for the design and optimal operation of the various processes used to produce microfluidic devices" [6]. Chapter 2 discusses the background and motivation for the project, Chapter 3 presents the goals and requirements for the design, and Chapter 4 reviews the concept selection process. Chapter 5 documents the design of the equipment, Chapter 6 the fabrication, and Chapter 7 reports the testing results and suggests future work. The final Chapter 8 concludes the project and summarizes the key contributions of the work.

Chapter 2

Background

2.1 Micromanufacturing Processes

Some traditional manufacturing methods have been adapted to micromanufacturing, such as machining and injection molding [16]. Other processes, such as lithography, have been borrowed from the semiconductor industry. Manufacturing techniques can be broadly categorized into direct fabrication methods and replication methods. Direct fabrication includes laser ablation, reactive ion etching, X-ray lithography, and mechanical micromachining. Replication methods include hot embossing, ultraviolet embossing, injection molding, soft lithography, and thermoforming. Hot embossing falls under the replication class, so a summary of those methods is presented below.

2.1.1 Hot Embossing

Hot embossing is a three-step process where a thermoplastic polymer is deformed visco-plastically by a micro-patterned tool. A schematic of the process is shown in Figure 2-1. The polymer workpiece and the micro-patterned tool begin at ambient temperature. In step 1, the tool and the workpiece are heated above the glass transition temperature of the polymer. In step 2, pressure is applied and held constant while the workpiece conforms to the tool. Finally, the polymer and tool are cooled below the polymer's glass transition temperature and the workpiece is demolded from the tool. The advantages of hot embossing include limited bulk flow of the material (which minimizes shrinkage and residual stresses), flexibility of tool changes, and potentially low capital cost. Hot embossing is especially

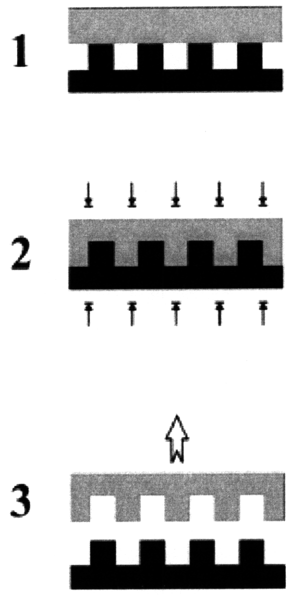

Figure 2-1: Schematic for Hot Embossing [15]

useful for optical applications where high precision and quality are necessary [20]. The major disadvantage is cycle time (as compared to injection molding), which is largely dominated by cooling rate. Important parameters for the process include glass transition temperature, forming pressure, and duration of hold time.

2.1.2 Ultraviolet Casting

In ultraviolet casting, shown in Figure2-2, a UV-curable epoxy resin is applied between a substrate and a micro-patterned tool. In step 2, the tool is brought into contact with the resin and the resin conforms to its shape. The resin is exposed to a UV light source and cured. In step 3, the polymer part is removed from the tool. The advantages of this process are that it involves only ambient temperature and low pressures, and does not require a clean room environment. The disadvantages are that only UV-curing resins may be used, and there must be a UV-transparent path to the part (i.e. the tool or substrate must be UV transparent). Also, when the embossed microstructure exceeds an aspect ratio of 2 or more, demolding of the cured polymer can cause failure of the tool or mold [11]. This process has been applied to produce precise micro-lenses [31].

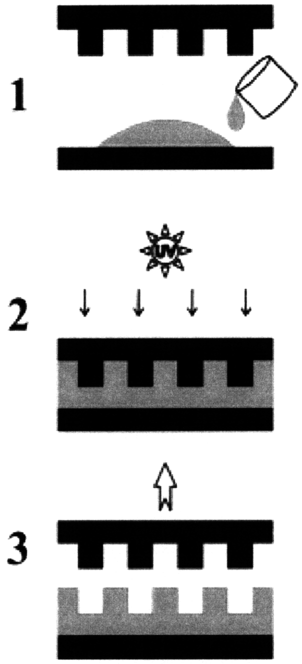

Figure 2-2: Schematic for UV Casting [15]

2.1.3 Injection Molding

Injection molding has historically been a macro-scale process, but only needs slight adaptation (a higher mold temperature and sometimes a vacuum across the mold cavity) to produce micro-scale features [32]. A basic schematic is shown in Figure 2-3. In step 1, a molten polymer is forced into an evacuated mold cavity containing a micro-patterned tool insert. In step 2, the polymer is rapidly cooled. In step 3, the polymer is demolded from the tool insert and removed from the opened mold. The major advantage of injection molding is the fast cycle time, typically on the order of less than a minute, which is possible because the small polymer part cools quickly through conduction to the large metal mass of the mold. Other advantages include the ability to make three-dimensional structures and embed pre-formed elements into the final part. Disadvantages include a higher capital cost, less flexibility than hot embossing, and relaxation of the polymer after release from the mold, causing distortion [10]. Process parameters such as as injection velocity, injection pressure, holding pressure, cooling time and melt temperature must be carefully controlled to achieve optimal performance. The final quality of the part is particularly sensitive to mold temperature [32].

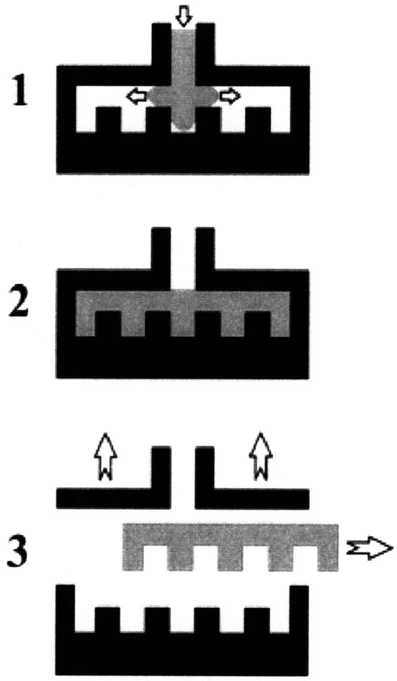

Figure 2-3: Schematic for Micro-Injection Molding [15]

2.1.4 Soft Lithography

Soft lithography differs from the above methods in that a thermoset polymer is used. Microfeatures are created by casting an elastomeric polymer against a micro-patterned tool. The most common material by far is polydimethylsiloxane (PDMS), because it is optically transparent, thermally stable, and bio-compatible - although other materials have been used [35]. A basic process schematic is presented in Figure 2-4. In step 1, a two-part mixture of PDMS or other resin and curing agent is poured over a micro-patterned tool. In step 2, the resin mixture, which has easily conformed to the tool, is cured by heating or by simply waiting. Curing time depends on the ratio of resin to curing agent and the ambient temperature, but is typically on the order of hours. In step 3, the cross-linked elastomer is demolded and removed from its container, typically by gently peeling off the flexible structure by hand. Advantages of soft lithography include readily available and simple equipment, the unique ability to produce elastomeric parts, and a highly robust process. The major disadvantage is the cycle time, dominated by the degassing and curing time [28], and the limited material selection (other processes must be used if a rigid part is desired). Process parameters to control include ratio of curing agent to resin and curing temperature.

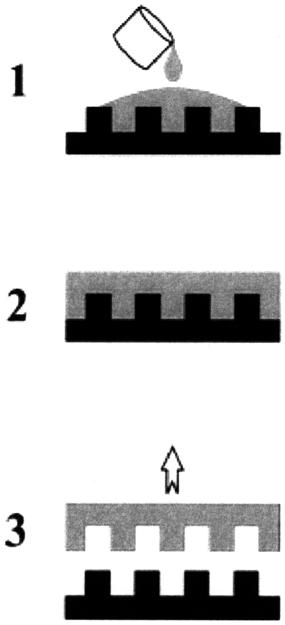

Figure 2-4: Schematic for Soft Lithography [15]

2.1.5 Thermoforming

Thermoforming is another process which has been adapted to produce micro-scale features. The process is shown in Figure 2-5 [9]. In step 1, a thin polymer film is clamped inside an evacuated mold containing a micro-patterned tool. In step 2, the film is heated above its glass transition temperature, and a pressurized gas is forced into the mold to conform the film to the tool. In step 3, the mold and film are cooled below the glass transition temperature and the part is demolded from the tool and removed from the opened mold. The advantages of this process are the simplicity of the mechanical process and fast cycle time. The disadvantage is the poor replication accuracy, especially with high aspect ratios and sharp angles. However, rounded geometries, even undercut features, can be easily demolded because of the flexibility of the film [9, 21]. The most important process parameter is the temperature of the film during forming, because the temperature impacts the flexibility of the film, the stresses in the film, and the permeability of the polymer to gases [21].

2.2 Why Hot Embossing

From the possible methods of micromanufacturing discussed above, hot embossing was chosen as the subject of further research. There are several reasons why hot embossing is

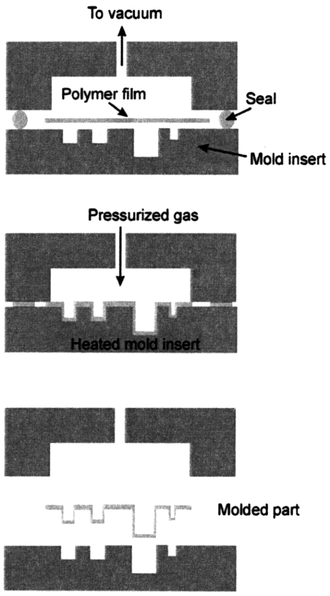

Figure 2-5: Schematic for Thermoforming [9]

particularly suited to manufacturing. First, hot embossing has rather simple mechanical and thermal needs and should have a low capital cost, and does not require a clean room environment. The footprint of currently available hot embossing machines varies substantially, but the process has the potential for a very small footprint as compared to an injection molding machine. There is also the potential for integrated automation of the hot embossing process, provided reliable demolding can be implemented and material handling can be addressed. Hot embossing is also a more flexible process than injection molding; tooling is less expensive than a mold set, and can be simply changed. Compared to ultraviolet embossing and thermoforming, hot embossing has a much more flexible choice of materials, processing parameters, and tooling. The cycle time of hot embossing is not currently quite as fast as injection molding, but this thesis attempts to close that gap.

These reasons, taken in conjunction, mean that hot embossing sits nicely between PDMS casting and injection molding on a cost/volume and flexibility basis. If only one part is needed, PDMS might be the most economical, and if one million parts are needed, injection molding might be the better option, but there is no current market for millions of microfluidic devices. In addition, from discussions with Dr. Holger Becker in the microfluidics industry (personal communication, April 22nd, 2009), there are also cases where devices cannot be fabricated using injection molding because of stringent optical property or dimensional requirements. For these cases or for prototyping, custom manufacturing runs, quick changes of material and tooling, and parts in the volume of hundreds to thousands, hot embossing is the best choice.

There are also reasons why hot embossing is an excellent technical process: the process uses local deformation rather than bulk material flow, which avoids internal stresses, and a low flow rate so that structures with a higher aspect ratio can be fabricated. Hot embossing also does not produce birefringence, which alters the optical properties. These properties make it particularly suited to optical applications where high precision and high quality are necessary [20].

2.3 History of Hot Embossing Machines

The majority of research papers that mention hot embossing are focused on prototype or proof-of-concept devices, and are not concerned with optimizing the hot embossing equipment. More recently there have been some papers dedicated to equipment design [Chang:12, Chang:13, Liu:25, Wang:34]. Chang and Yang [12, 13] as well as Liu et. al [25] focus on improving and modifying the hot embossing process, while Wang et. al [34] have designed an entire integrated production system using hot embossing as the forming process. Ganesan [17] and Dirckx [15] built successive generations of hot embossing equipment as their S.M. theses. There are also several options for current commercially available hot embossing equipment (see Section 2.3.4).

2.3.1 MIT Generation 1 Equipment

Ganesan designed and built a hot embossing machine for the purpose of testing the dimensional variations in embossed parts. The work was for the completion of a S.M. in 2004 in the Polymer Micromanufacturing Laboratory (PML) at MIT [17]. An Instron model 5869 electromechanical load frame provided force and position control for the embossing platens. The platens were constructed from blocks of copper; heating was supplied electrically with cartridge heaters and cooling was by tap water. The heaters were controlled with temperature feedback using Chromalox 2110 controllers. The overall hot embossing setup is shown in Figure 2-6. A detail of the platens and workpiece area is shown in Figure 2-7.

The generation 1 machine has a force capacity up to 50 kN and a temperature capacity up to about 300°C. Position of the crosshead can be controlled with a resolution of 0.0625

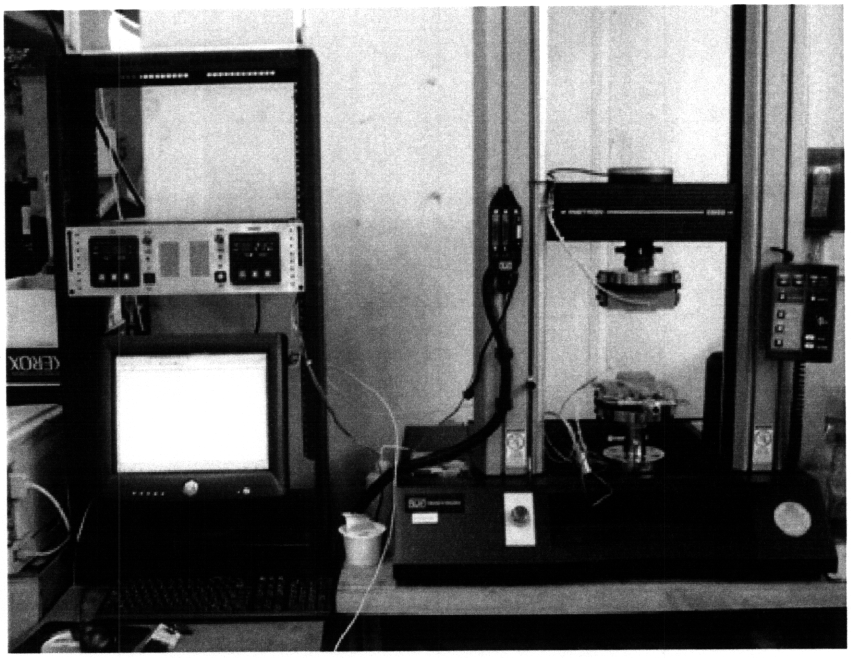

Figure 2-6: Generation 1 Machine Overview [17]

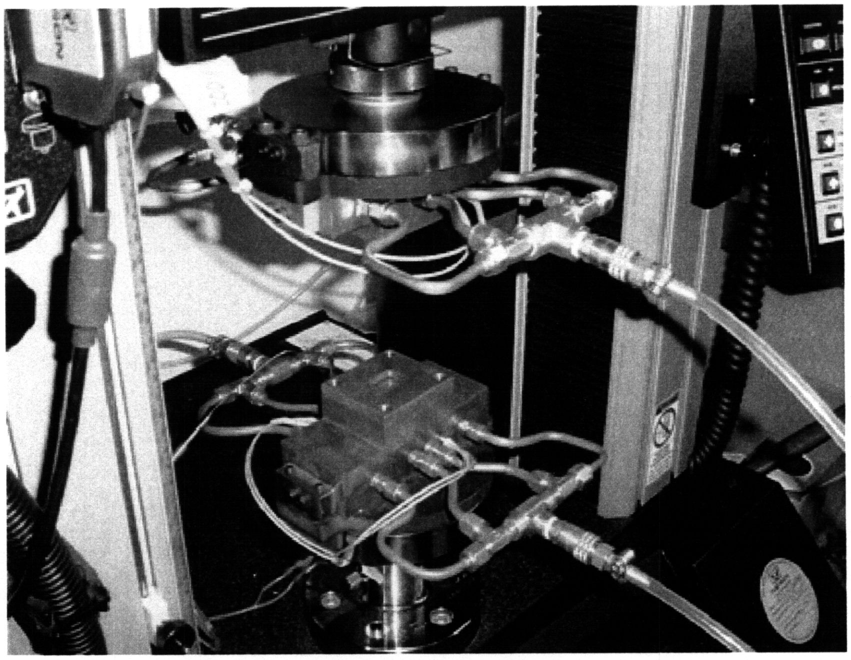

Figure 2-7: Generation 1 Machine Platens [17]

μm up to a speed of 250 mm/min. This capability allows the machine to follow arbitrary position or force trajectories within its limits, so the full range of process parameters in the position and force domains can be investigated. These parameters include embossing force, embossing strain rate, hold force, maximum tool displacement, and others. The cooling rate and demolding temperature are not well controlled parameters and are only as repeatable as manual valves will allow. The heating rate is not controllable at all.

The overall cycle time of the equipment is about 20 minutes - 15 minutes for heating, and 5 minutes for cooling. The cycle time is limited by the heat transfer rate through the large copper mass (needed for the platens in order to ensure even heat distribution to the workpiece and tool). The largest workpiece that can fit in the fixturing area is about 45mm by 40mm, although in practice this has been limited to about 25mm. The tool was affixed using high-temperature epoxy to a post mounted to the upper platen. The workpiece was clamped around its periphery by a copper plate with a hole through which the tool post could pass. [17]

2.3.2 MIT Generation 2 Equipment

Dirckx built on the knowledge contributed by Ganesan to design and build the second generation of hot embossing equipment in the PML in 2005. The Generation 2 machine was intended to explore the limits of hot embossing from a manufacturing process control perspective. The same Instron model 5869 electromechanical load frame was used to provide force and position control, so the force capacity remained 50kN and the position remained controllable with a resolution of 0.0625 μm up to a speed of 250 mm/min.

The embossing platens were again constructed from blocks of copper, but the thermal mass was minimized as much as possible within the design constraints. The temperature of the platens and workpiece were controlled by mixing hot and cold streams of Paratherm MR oil using electro-pneumatic three-port globe valves. The equipment was designed for a temperature capacity up to about 250°C. The hot stream was heated by a 30kW electric circulation heater, and the cold stream was cooled by tap water in a plate-and-frame heat exchanger. The overall hot embossing setup is shown in Figure 2-8. A detail of the platens and workpiece area is shown in Figure 2-9.

The automation of the heating and cooling process of the hot embossing cycle allowed this generation 2 machine to follow arbitrary temperature profiles in addition to the generation 1

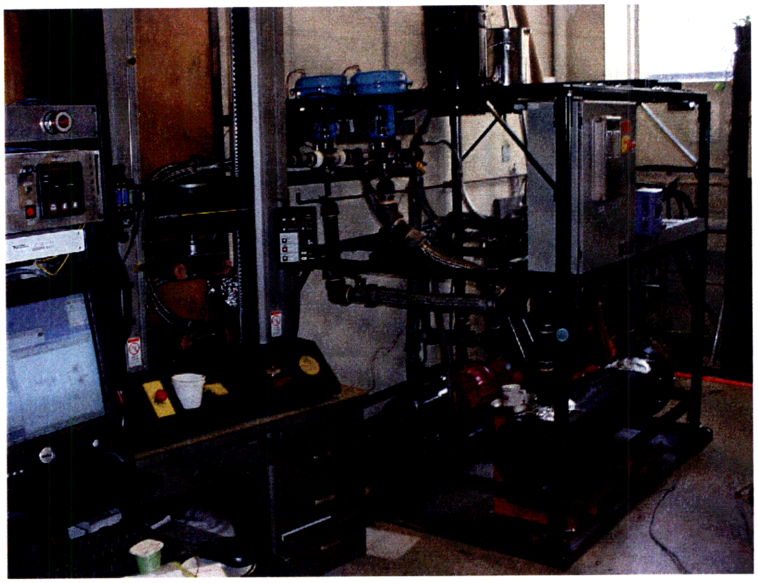

Figure 2-8: Generation 2 Machine Overview

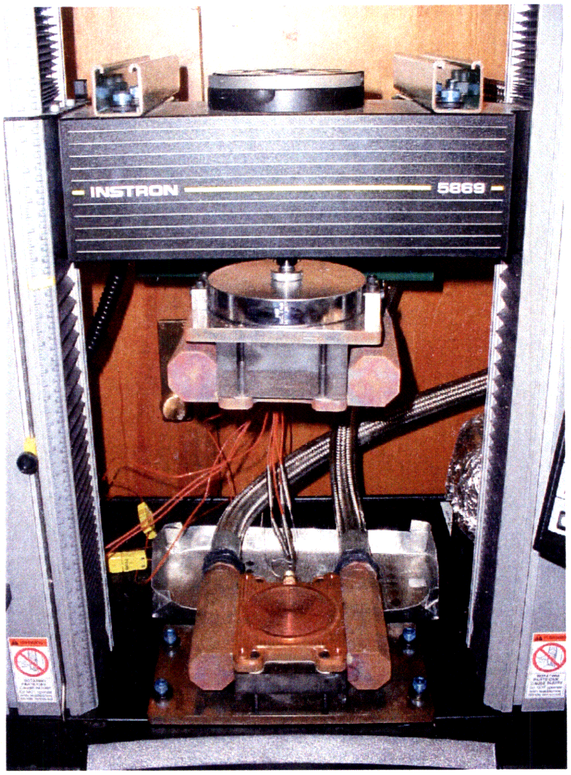
INSTRON
5869

Figure 2-9: Generation 2 Machine Platens

capability of following arbitrary force and displacement profiles. This allowed investigation into the effects of additional parameters on final part quality. The overall cycle time was designed to be on the order of 5 minutes - approximately 2 minutes for heating and 2 for cooling. The cycle time is limited by the heat transfer rate through the platens and by the rate of temperature change in the mixing of the Paratherm oil.

Workpiece and tool fixturing was also improved from generation 1 to allow simpler tool changes and to eliminate the need to re-align the workpiece clamp and the tool chuck after a tool change. The workpiece capacity is a 100mm diameter circle. A vacuum chuck held the tool, and a perimeter clamp held the workpiece. [15]

2.3.3 Research Hot Embossing Equipment

In 1998 Heckele and Bacher [20] designed a hot embossing apparatus based on standardized components taken over from other technologies. The central portion was a universal material testing machine, which was modified by adding a vacuum chamber . Most hot embossing equipment in subsequent papers was similar - repurposed equipment which served as a means to an end, usually prototyping a device. Juang et. al [23] used a typical hot embossing setup: a pneumatic cylinder to provide a constant compression force, cartridge heaters to provide heating, air or water to cool the mold and workpiece, and an LVDT and thermocouples to measure position and temperature . By the 2000s, however, different groups began researching ways to improve the hot embossing process. In 2003 Chang and Yang [12] moved away from a mechanical press setup to use nitrogen to provide forming pressure, which gave a uniform pressure distribution and allowed brittle silicon tools to be used . In 2005 the same authors expanded their idea to include using other working fluids such as steam and oil. In addition, they developed a rapid heating technique using infrared heating to improve the cycle time of the gas pressurization method. They found each method to have its own advantages, but that all methods significantly reduced cycle time to a minimum of about two minutes [13].

Liu and Kimerling et. al in 2004 [25] continued to use a mechanical press setup, using an Instron model 1011 universal testing machine as the basis for their equipment. Their goal was to reduce the cycle time to 30 seconds or less by applying a Rapid Thermal Response (RTR) molding process to hot embossing. They concluded the RTR hot embossing technology showed promise, but did not report experimental cycle times . Yao and Yi et. al in 2006

[36] presented a hot embossing strategy which separated the heating and cooling cycles into two pneumatic press stations in an effort to reduce cycle times, with an ideal cycle time of around 10 seconds for a microlens array .

The main focus of the above papers is minimizing cycle time and improving accuracy, which are both important process considerations. However none of the work mentioned so far significantly addresses common manufacturing concerns such as repeatability data for large runs of parts, automation, capital cost, or equipment size. Wang et. al in 2004 [?] worked from more of a manufacturing perspective to develop an automatic fabrication system for batch production of microfluidic devices, which included hot embossing, alignment of the workpiece and a cover slip, and thermal bonding of the final device. The hot embossing equipment used delivered force through a motor with a mechanical ball bearing screw jack with a force sensor for feedback control. Peltier devices were used for both heating and cooling of the platens, in conjunction with a heat sink. The cycle time was not reported .

2.3.4 Commercial Hot Embossing Equipment

There are several commercial companies which offer hot embossing machines currently on the market. German company Jenoptik-Mikrotechnik has an entire line of hot embossers [8], one of which is shown in Figure 2-10 a), which increase in both capability and degree of automation from model 01 to 04. The EV Group [4] has three machines which are adapted from the semiconductor industry, shown in Figure 2-10 b), including one fully automated system intended for high volume embossing. Wickert [7] has very high force capacity presses in a multitude of sizes from 800 to 60,000 kN capacities, which can include heating and cooling, but are not intended specifically for embossing. The Obducat machines [5] are particularly suited to nano-embossing, and are able to produce structures in very thin polymer layers. This is because of the company's proprietary STU (Simultaneous Thermal and UV Imprint) and IPS (Intermediate Polymer Stamp) processes [5]. The Obducat product catalog did not quote cooling performance.

All but the Obducat machines offer enclosed embossing chambers permitting processing under vacuum, and many have built-in automatic alignment systems for the tool and workpiece. All are able to control steady-state temperature to about ±1%. Most offer active cooling as an option. The key capabilities and specifications of these machines are summarized in Table 2.1.

Supplier	Machine	Cost ($k)	Max. Embossing Force (kN)	Max. Process Temp. (C)	Heating Time (min)	Cooling Time (min)	Maximum Workpiece Size (mm)
Jenoptik [8]	HEX 01	$250	20	320	7	7	100 diam
Jenoptik	HEX 02	$350	200	320	7	7	150 diam
Jenoptik	HEX 03	$450	200	500	2	3	150 diam
Jenoptik	HEX 04	$600-$1000	400	350	2	3	300 diam
Obducat [5]	NIL-2.5		23	250	1 C/s		65 diam
Obducat	NIL-4		26	300	5 C/s		102 diam
Obducat	NIL-6		26	300	5 C/s		152 diam
EV Group [4]	510HE	$300-400	10	550			150 diagonal
EV Group	520HE		40, 60	550	6	5	200 diagonal
EV Group	750		360	250			250 x 250
Wickert [7]	WLP S 230		230	500	6	6	200 x 200
Wickert	WKP S 800		800	500	6	6	300 x 400

Table 2.1: Commercial Hot Embossing Machines

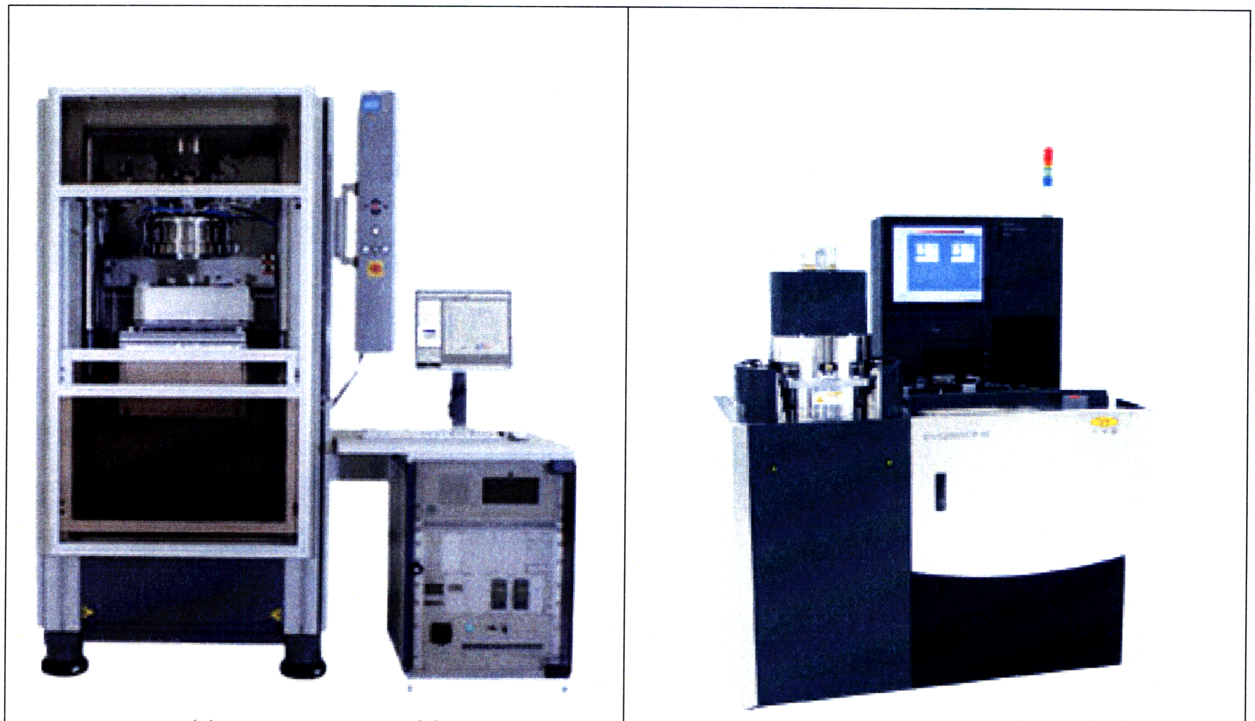

(a) Jenoptik HEX 03 [8]

(b) EVG 520HE [4]

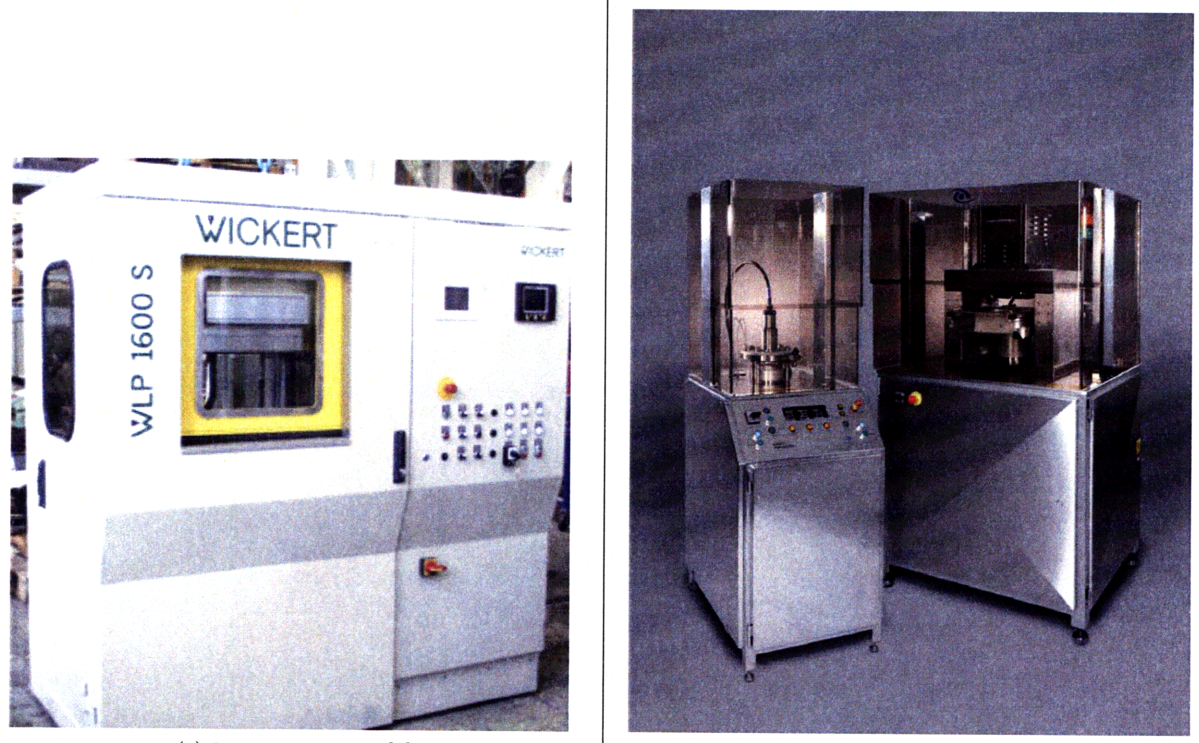
WICKERT
WLP 1600 S
WICKERT

(c) Wickert WLP S [7]

(d) Obducat NIL [5]

Figure 2-10: Commercial Hot Embossing Machines

2.4 Motivation for new equipment

There are certainly capable hot embossing machines available, and much research work has gone into exploring the best techniques and process parameters to use during the hot embossing process. However the commercially available options fail to utilize the knowledge gained in microfluidics research, and the groups doing research are not interested in making equipment for practical use in industry. There has yet to develop an equipment industry for hot embossing machines specifically for microfluidic devices - equipment designed precisely for its purpose using knowledge from research, from a manufacturing point of view.

Research equipment tends to be custom - designed with a set of experiments in mind and difficult to adapt to different tooling, process parameters, or workpiece materials and sizes. The fact that there are not yet industry standards for connections, material handling, or processing parameters only increases the need for equipment flexibility. Research equipment also rarely takes size into consideration - for example, the generation 2 MIT hot embossing machine takes up half of a room. Commercial equipment, on the other hand, is costly and has cycle times too slow to compete with injection molding. There may be room to cut costs and lower the capital investment necessary for production equipment.

The current work addresses this need for a new embossing machine in the Polymer Micromanufacturing Laboratory. The remainder of this thesis presents the development of functional requirements and manufacturing considerations, generation and selection of conceptual designs, design and analysis of predicted performance, fabrication of all hardware, and finally testing results of production runs.

Chapter 3

Goals and Design Approach

The purpose of this thesis is to design, build, and test a hot embossing machine suitable for manufacturing microfluidic devices in a production setting. It is important to define the functional requirements before beginning the design process, and to know what factors are most important when making design decisions. The following chapter outlines the goals for the equipment and the design approach.

3.1 Functional Requirements

Hot embossing has three major process inputs: temperature, forming pressure, and time. These parameters are all related to final part quality, and are interconnected. For instance, the hotter the workpiece material is, the faster it conforms to the tool and the less time it must be held under pressure. Or, a higher pressure could be used at that same temperature with a shorter hold time. When defining capacity requirements for these parameters, it is important to keep the ranges as flexible as possible to allow the user to make choices between these trade-offs.

3.1.1 Workpiece Size

It is difficult to judge what the most useful workpiece size and form factor might be, as there an no standards for design of microfluidic devices. The MIT Generation1 hot embossing machine most frequently used 25mm x 25mm square tools, and the MIT Generation 2 machine was designed for 100mm circular wafers. In the interest of making a production, "right-sized" machine with as low as possible capital cost and footprint size, the new equipment should use the minimum useful workpiece area. Glass microscope slides are often used as cover plates for PDMS microfluidic devices, and out of convenience and practicality researchers tend to design their devices within that 25mm x 75mm area. A 25mm x 75mm area is a good compromise between 25mm x 25mm and an 100mm wafer, and ceramic heaters are available in that size, so that dimension was chosen as the target workpiece area.

3.1.2 Force capacity

One of the most common materials used in hot embossing is polymethylmethacrylate (PMMA), so this plastic was chosen as a baseline for design. Previous research has shown that pressures as low as 1 MPa can be suitable for embossing PMMA (if higher forming temperatures and longer hold times are used), while 2 MPa is a commonly used value [15, 33]. Rarely is pressure over 4 MPa necessary. From this historical data, an overall pressure requirement of 5 MPa was chosen. If unforeseen needs arises requiring more pressure, varying the other process inputs of forming temperature and hold time may be able to accomplish the same results as higher pressure. Over the original workpiece design area of 25mm by 75mm, this gives a required force of 9375 N (or 2100 lbf). It is desired to control the pressure within %2, or +/- 0.1 MPa (+/- 187 N or +/- 42 lbf). Other materials such as Zeonex require even lower pressures during forming than PMMA, so this chosen force capacity should be sufficient for a wide range of possible materials.

3.1.3 Heating

The glass transition temperature of PMMA is around 100ºC, depending on the particular molecular weight from the supplier and the grade of material. Above approximately 200ºC, PMMA is in a molten state unsuitable for embossing. Thus our heating temperature capacity can be safely placed at 200ºC. Other materials such as polystyrene and polycarbonate (PC) have similar glass transition and molten temperatures and can be easily embossed in the same temperature range. Some grades of Zeonex have a higher glass transition temperature than PMMA, but are still well below 200ºC. Prior work focused on very precise control of temperature, but discovered that as long as the process is well away from the glass transition point of the material, the hot embossing process is robust to temperature fluctuations [33]. Therefore it is only necessary to control the temperature to +/- 2-3ºC.

Material	Thickness (mm)	Width (mm)	Length (mm)	Quantity	Thermal Mass (J/ºC)
PMMA	2	25	75	1	6.69
Nickel	1.5	25	95	2	29.10
AlN	2.5	25	75	2	25.34
Steel	2	25	95	1	18.08
				Total Thermal Mass:	79.21

Table 3.1: Geometry and Thermal Mass of Thermal Stack Elements

3.1.4 Cooling

Cooling capacity here is not defined as a temperature but as a cooling *power*, considering the amount of time it takes to bring the workpiece from a forming temperature to a demolding temperature. For a PMMA workpiece, forming temperature can be estimated at 120ºC, and demolding temperature can be conservatively set at 50ºC (though as high as 80ºC might be acceptable). Other materials might have a higher glass transition temperature requiring higher forming temperatures, but then the demolding temperature would also be higher, so these values are sufficient for estimation.

The thermal load that must be cooled can be estimated as follows, using the material properties found in Table A.1. The exact design of the parts that must be cooled is not yet known, but can be estimated assuming a minimal thermal stack has at least one workpiece, two heaters, two tools, and a structural backing plate. PMMA comes in common thicknesses of 1, 1.5, and 2mm, so conservatively a 2mm thick workpiece is used. The most promising heater design uses ceramic heaters with dimensions of 25mm x 75mm x 2.5mm; basic aluminum nitrate ceramic data is used in place of exact material properties. Tooling might potentially be silicon, aluminum, steel, or electroformed nickel - silicon and steel are less likely, and nickel is the conservative choice when compared to the thermal conductivity of aluminum. Table 3.1 gives a summary of the geometry of the thermal stack.

To calculate the thermal load from the thermal mass, equation 3.1 is used:

$$Load = \sum_{i=1}^{4} \rho_i V_i C_{P_i} (T_{form} - T_{demold}) \tag{3.1}$$

where ρ is the density in kg/m^3, V is the volume of material, and Cp is the specific heat of the material. Using $(T_{form} - T_{demold}) = 120 - 50 = 70$, the load is calculated to be $5545J$.

The cooling system of the hot embossing equipment must be able to dissipate this thermal

Event	Time Required (s)
Loading	3
Heating	10
Holding	20
Unloading	3
Total	**36**

Table 3.2: Minimum Cycle Time

energy in an amount of time that keeps the cycle time under the cycle time requirement of 120s. To be conservative, this calculation will assume a somewhat arbitrary design safety factor of 0.6 and aim for a cycle time of 72s instead. Please see Table 3.2 below for an estimate of minimum possible cycle time for all steps *other than* the cooling. Assuming 36s is needed for everything besides cooling, that leaves 36s for cooling to meet a cycle time of 72s.

Then power required becomes:

$$Power(W) = \frac{Energy(J)}{Time(s)} = \frac{5545J}{36s} = 154W \tag{3.2}$$

The required cooling capacity is defined as $154W$.

3.1.5 Cycle Time

The cycle time of the new hot embossing machine should ideally exceed the cycle time of previous versions. The MIT Generation 2 equipment had cycle times on the order of five minutes, so this is taken as the upper bound on cycle time. Since the goal is to be a production machine, it is useful to consider cycle time in parts per shift. In a standard eight hour shift, a reasonable goal might be to make 100 parts. This gives us a cycle time of 4.8 minutes per part, which is again close to the 5 minute upper limit. But in a production environment there is also time spent on material handling, unscheduled machine maintenance or failure, and other delays. Setting a goal substantially faster than 5 minutes per part would allow for these eventualities, position hot embossing to better compete against injection molding cycle times, and make a contribution to current state-of-the-art in hot embossing. Therefore a design cycle time of 2 minutes per part is chosen.

	Capacity	Tolerance
Workpiece Area	25mm x 75mm	
Force	9375 N	+/- 187.5 N
Heating	200 ºC	+/- 2-3 ºC
Cooling Power	154W	$+\infty/-0$
Cycle Time	120 s	no more than 5 minutes
Footprint	1m x 0.5m	$+0/-\infty$
Cost	$10,000	
Connectivity	USB and commercially available software	

Table 3.3: Functional Requirements

3.1.6 Manufacturing considerations

The MIT Generation 2 hot embossing machine was designed to explore process control, so sacrifices were made in other areas such as physical size and cost ($80,000). Commercial hot embossing machines are all designed to be floor standing models, around 1m x 2m or so, depending on the brand and model. Median cost is around $350k (see Table 2.1). This work would like to change those numbers by almost an order of magnitude, and more importantly change the mindset about microfluidic manufacturing equipment. The footprint only needs to be desktop- or benchtop-sized, and the capital cost can be minimized to roughly $10,000 or less. In addition, the equipment needs to be mostly, if not completely automated, and needs to be able to run on well known, commonly available software with a simple connections to a computer or laptop. Therefore requirements of a 1m x .5m benchtop footprint, maximum of $10,000 cost, and USB controllable, commercially available software are added to the list.

3.1.7 Summary

A summary of the functional requirements for the new hot embossing equipment is given in Table 3.3.

3.2 Manufacturing Motivations

The design of this hot embossing setup was motivated by three concerns: right-size design, cost, and modularity. The Toyota Production System and the concept of lean manufacturing inspired right-size design [24]. Lean manufacturing is a systematic approach to identifying and eliminating waste. A machine designed with more capacity than necessary, more parts than necessary, or more complexity than necessary is not optimal and therefore wasteful. To maximize added value, each component of the hot embossing setup was chosen carefully to meet a specific need. This right-sized principle also led to the decision to make the equipment a serial process, producing one part at a time, as opposed to a batch process making multiple parts in a cycle.

To minimize the cost of the equipment, first the basic technology was kept as simple as possible – electric heating and water cooling. Air cooling was considered as an even simpler choice, but fins and forced convection did not provide enough cooling power for the anticipated design operating range. The number of components in the overall setup was kept to a minimum, which reduces both initial cost and possibly future cost in the form of replacements and possibility of errors. Finally, off-the shelf components were used where possible (load cell, pneumatic cylinder, electronic control equipment) to take advantage of established technologies and equipment already in the market.

The third manufacturing motivation was modularity. The tooling was designed to be easily replaceable for quick changes in a production line. Each subsystem (force application, heating, and cooling) is a decoupled module, so that each can be tuned for optimum performance without affecting the other processes. In addition, the entire hot embossing system is itself a module, so additional units can be seamlessly added to the production line if an increase in either capacity or variety of products is required.

3.3 Design Approach

These manufacturing motivations led to several design decisions for this setup. First, the thermal mass involved in the thermal embossing cycle was strictly minimized. A smaller thermal mass requires less power to heat, a shorter time to cool, and minimizes thermal cycle time. The force actuation system (a pneumatic cylinder) was sized to provide just enough force (with a suitable safety margin) to emboss common plastic substrates in a 25mm x 75mm size. Oversizing the actuation would require a larger equipment footprint, slow down the cycle time, and defeat the right-size machine manufacturing motivation. The heating and cooling elements are kept separate to avoid coupling of responses, and to avoid wasted heat during the thermal cycle. If the heating elements were always in contact with the heat sink used for cooling purposes, heat energy would be added to the heat sink unnecessarily.

This could be a significant portion of heat because the thermal mass of the system is kept small. Finally, the size of the entire system is kept to a minimum. Not only does this follow the low-cost and right-size machine manufacturing motivations, it simplifies construction and provides a compact form factor for benchtop work.

Chapter 4

Concepts

The new production hot embossing machine is intended to meet ambitious goals: control of force application up to 5 MPa and control of temperature up to 200ºC, with cycle time of two minutes. In addition, the physical equipment must fit on a small benchtop area, be controllable through a USB connection to a laptop or computer, and cost less than $10,000. Careful consideration of conceptual designs is key to meeting all of these requirements. The following chapter works through the generation and selection of possible concepts, and details how the final choices were made.

4.1 Frame design concepts

4.1.1 Frame design requirements

The frame here refers to the overall design of the machine - the shape of the basic structure, footprint, layout of mechanical elements, and load-bearing structural path. Each concept is briefly described, a picture is provided, and advantages and disadvantages are stated. The frame of the hot embossing equipment must be as compact as possible (with a maximum size of 1m x 0.5m), provide structure to attach a force application system, a cooling system, and a platen system with a tool and workpiece, and resist errors due to deflections caused by force application. It must also be easily accessible for maintenance and adjustments, flexible enough to adapt to changes during the design process, and as simple and cheap to manufacture as possible.

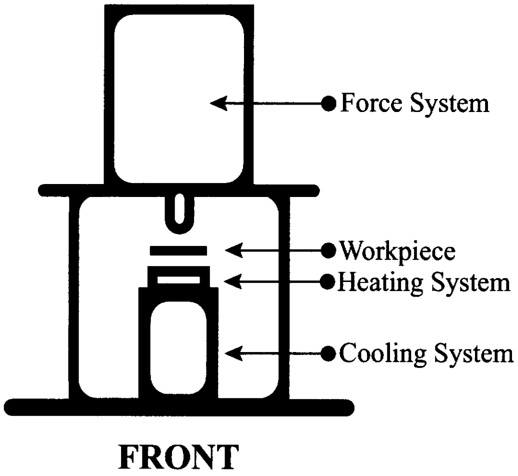

Figure 4-1: Gantry Frame Concept

4.1.2 Concept: Gantry

The first concept considered was a gantry system, with two vertical supports connected by a cross-piece at the top, and bolted to a plate at the bottom. Please see Figure 4-1. This is a standard configuration for presses in general. The advantages are that it is easy to manufacture (simple welding of I-beams or angle iron), and could quite possibly be purchased off-the shelf if needed. The major disadvantage is that mounting the force application system (whether a hydraulic cylinder, pneumatic cylinder, or piezo stack) to the top cross-piece creates a bending moment which will cause deflection of the frame, however small. The wider the vertical supports are placed, the more bending will occur, but closely spaced vertical supports would limit access.

4.1.3 Concept: Triangular Pyramid

The triangle is the most stable configuration of truss members, so a triangular pyramid would create a very robust frame (see Figure 4-2). In an ideal setup, (all joints perfectly pinned), all members would be in tension with no bending, which would minimize deflections. However this frame would be more difficult to manufacture, and needs a wider base (larger footprint).

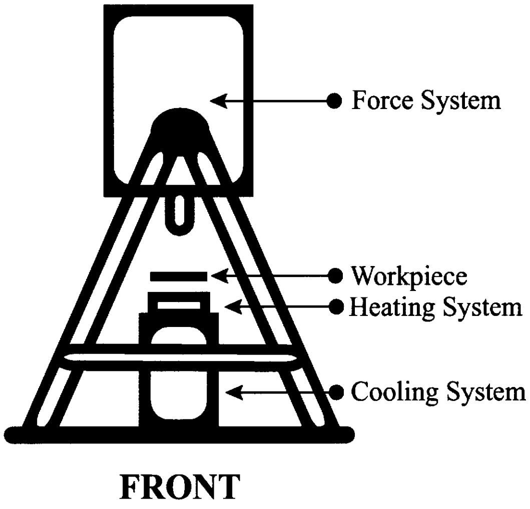

Figure 4-2: Pyramid Frame Concept

4.1.4 Concept: Curved Cantilever

A curved cantilever design (see Figure 4-3) has the force application system suspended over the workpiece and thermal stack, supported by a curved member. A variant of this design might have a "Γ" shaped member instead of the curved brace, but this would have higher stresses in the right-angle joint. The advantages of this design are that it leaves the area around the workpiece open and easily accessible for maintenance, material handling and tool changes, and it has a convenient skinny footprint. Disadvantages are that it is prone to Abbé error due to deflection of the frame when force is applied to the workpiece, and that the curves make it slightly harder to manufacture than the gantry concept.

4.1.5 Concept: Double Curved Cantilever

The double curved cantilever is a variant on the curved cantilever in section 4.1.4. The force application system is supported above the workpiece and thermal stack on two sides by identical curved braces at right angles, as shown in Figure 4-4. This still leaves 270º around the workpiece open for access, and decreases the amount of deflection in the frame from Abbe error. It adds complexity and cost to the system, however, and more than doubles the footprint with no added functionality.

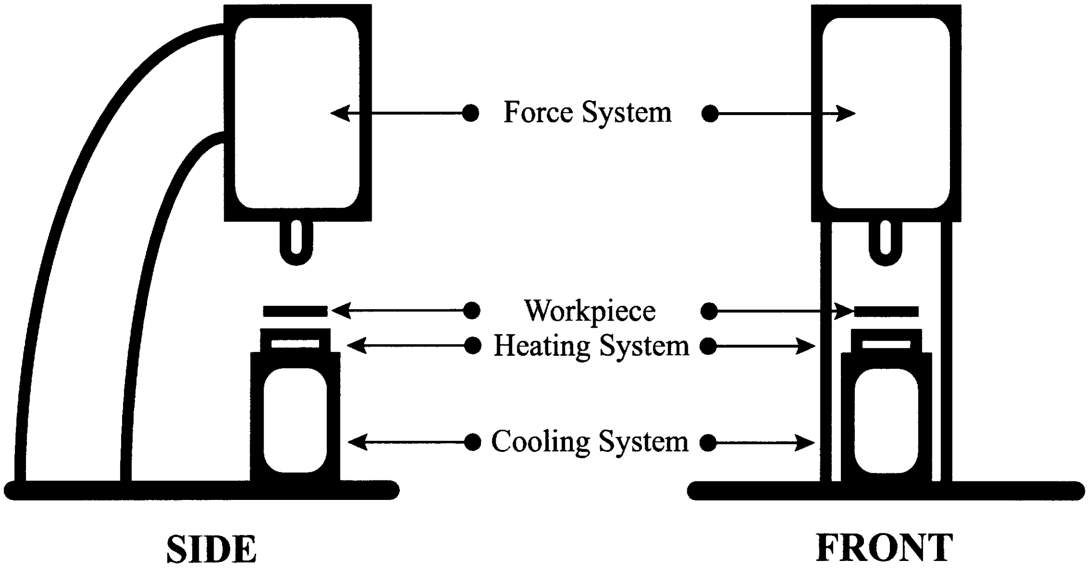
Force System
Workpiece
Heating System
Cooling System
SIDE
FRONT

Figure 4-3: Curved Cantilever Frame Concept

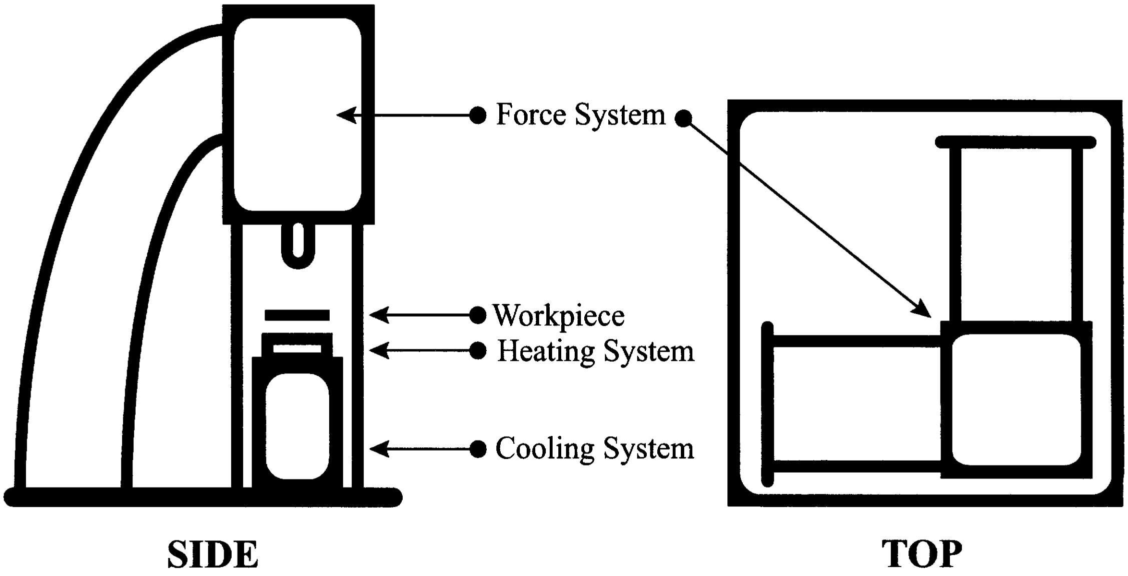
Force System
Workpiece
Heating System
Cooling System
SIDE
TOP

Figure 4-4: Double Curved Cantilever Frame Concept

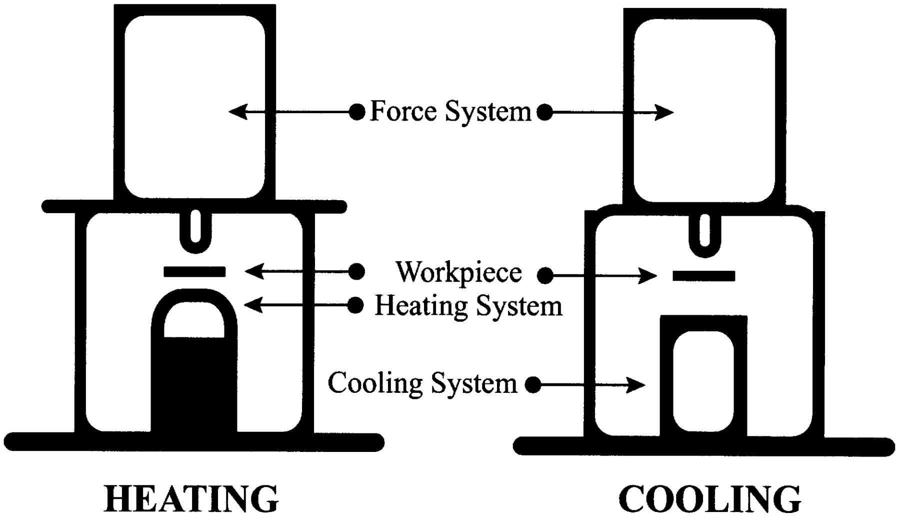

Figure 4-5: Two Stage Frame Concept

4.1.6 Concept: Two Stage Process

A two stage process would separate the heating and the cooling portions of the embossing cycle into two different machines (see Figure 4-5). This is an idea proposed by Yao and Yi [36]. The advantage of this method is that the throughput of parts is higher - a new part can start heating while the first part is cooling. This approach also decouples the heating and cooling completely, potentially allowing better optimization of each stage. Disadvantages include the problem of maintaining forming force while switching the workpiece between stages, and the added complexity and cost of two pieces of equipment.

4.1.7 Comparison of Frame Concepts

A Pugh chart was used to compare the different concepts for overall frame design. In Table 4.1, each design is rated against the gantry concept as a baseline in the categories of footprint, structural deflection, accessibility, flexibility, complexity, and cost.

The total row shows clearly that the Curved Cantilever design is the best choice. Although a Pugh chart cannot be used on its own for decision making, taken in conjunction with the advantages and disadvantages listed in the previous sections, the curved cantilever is chosen as the final frame layout for the new hot embossing equipment.

	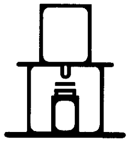	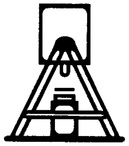	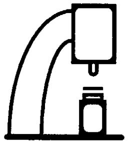	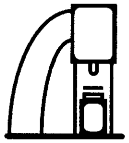	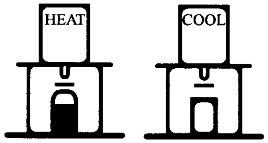
	Gantry	Triangular Pyramid	Curved Cantilever	Double Curved Cantilever	Two-Stage Process
Footprint	0	-	+	-	-
Structural Deflection	0	+	0	+	0
Accessibility	0	+	+	+	0
Flexibility	0	0	+	+	-
Complexity	0	-	0	-	-
Cost	0	-	0	-	-
Total	0	-	+ + +	0	- - - -

Table 4.1: Frame Concept Pugh Chart

4.2 Force application concepts

4.2.1 Force requirements

The second step of the hot embossing process (after heating the workpiece) is to apply force to press a patterned tool into the softened workpiece. Each concept for force application is discussed and compared to find the best solution. For this hot embossing system, the required force capacity is 9375N (5MPa of pressure over a 25mm by 75mm area). Additional concerns include low cost and simplicity of the force application system.

4.2.2 Concept: Hydraulic

Hydraulic cylinders are a common way of applying force, and have been used previously for other projects in this laboratory. They are commonly available on the market, and not very expensive relative to other force application options. The hydraulic cylinder itself might be the smallest physical size of any of these concepts, but hydraulic systems require a large amount of auxiliary equipment for pumping and transporting the hydraulic fluid. From previous experience, they also tend to be messy and prone to leaks. The range of motion varies depending on the design of the cylinder, but is generally less than about five inches. The repeatability of the system is dependent on the controller used, and is potentially limited by the internal friction and bearing alignment,

4.2.3 Concept: Pneumatic

Pneumatic cylinders are also commonly used to apply force, and are very similar to hydraulic cylinders in function, range of motion, and cost. Pneumatic cylinders are larger than hydraulic cylinders for the same capacity, because of the compressible nature of air. However pneumatic cylinders do not require auxiliary pumping or piping, only a shop air connection already usually available in manufacturing environments.

4.2.4 Concept: Piezomaterial

Piezoelectric actuators are created with piezomaterials, solid materials which change volume when a voltage is applied. Piezoelectric materials can provide linear motion in several ways, but for this application stacks of piezoelectric disks would be epoxied together with electrodes between the disks. Applying a voltage across the stack produces an expansion of the stack,

	Hydraulic	Pneumatic	Piezomaterial	Lead Screw
Footprint	0	-	-	0
Repeatability	0	0	+	-
Range of Motion	0	0	-	+
Complexity	0	+	-	0
Cost	0	+	-	0
Total	0	+	- - -	0

Table 4.2: Force Concept Pugh Chart

which translates to pressure applied to the workpiece. The advantages of piezoactuators are that they are very precise and extremely repeatable. However a piezoelectric stack that outputs the required force does not provide enough displacement. The range of travel is quite small, only several millimeters at most. This is all the range needed for embossing, but it doesn't leave enough room for material handling. Adding a linkage of some kind could improve the range, but then the force is reduced and the system has become more complicated. Even if a system meeting the requirements for both force and displacement could be created with piezoelectric stacks, (at least three stacks and corresponding controllers would be necessary), piezos are are also several times more expensive than hydraulic and pneumatic actuators.

4.2.5 Concept: Mechanical Lead Screw

There are several related options for mechanically applying a force: lead screw, ball screw, or gear train. The advantages of any of these options are plentiful inexpensive options already commercially available, an unlimited range of travel, and simple technology only requiring an electrical connection. A disadvantage is that friction and backlash in threaded rods limit the repeatability and precision of the system. In general, these options are not a good fit to the technology needed: these excel at providing lower force over a long distance, whereas this application requires a high force over a small range.

4.2.6 Comparison of Force Concepts

A Pugh chart was used to compare the different concepts for force application. In Table 4.2, each design is rated against the hydraulic cylinder concept as a baseline in the categories of footprint, repeatability, range of motion, complexity, and cost.

From both the results of the Pugh chart and an analysis of the advantages and disadvantages listed in each section, a pneumatic cylinder was chosen as the force application method for the new hot embossing equipment.

4.3 Heating concepts

4.3.1 Heating requirements

The first step in the hot embossing process is to heat the polymer workpiece above its' glass transition temperature. This section discusses ways of accomplishing this, and the pros and cons of each. The maximum temperature of the equipment must be 200ºC, and the rate of heating must be close to 2ºC/s to meet the cycle time goal of two minutes.

4.3.2 Concept: Cartridge heaters

Cartridge heaters use electrical current to heat resistive elements, usually packaged inside round tubes with attached leads. The advantages to this design are cheap, readily available options and very simple technology and operation - just an electrical connection is required. Cartridge heaters have been used in several previous projects in this laboratory, including the MIT Generation 1 hot embossing equipment [17]. The disadvantages are that the heaters are too fragile to be placed in the load path, it is difficult to create uniform heating, and the tube shape takes up a lot of volume.

4.3.3 Concept: Ceramic heaters

Ceramic heaters are similar to cartridge heaters in that they use electrical resistive heating, but instead of being packaged in a tube the resistive elements are embedded into a ceramic substrate. In 2006, Watlow Inc. introduced a new line of ceramic heaters with a maximum temperature of 600ºC and a ramp rate of up to 150ºC/s, in a variety of flat, thin shapes and sizes. The advantages of these heaters are the fantastic heating capacity and power, and the unique form factor in exactly the 25mm by 75mm size needed for uniform heating. The heaters are also capable of withstanding the 5MPa of pressure during the embossing cycle, so they can be placed in the load path. The disadvantages are the cost, the brittleness of the ceramic substrate, and the risk of a new technology.

4.3.4 Concept: Fluidic heating

Fluidic heating refers to flowing a heated fluid stream continuously through platen passages, and using conduction to heat the polymer workpiece. The MIT Generation 2 hot embossing equipment used fluidic heating (Paratherm oil), so a base of knowledge already exists for this option [15]. Another option is to use steam to pressurize a bladder [13], which couples heating and force application. The disadvantages of fluidic heating are a more complicated system, possibility of leaks, and a slow time constant and heating rate. Also, the platens must be carefully designed to ensure uniform heating.

4.3.5 Concept: Peltier Heating

A temperature difference can be created by current passing through dissimilar materials, known as the Peltier effect. This effect can be used for both heating and cooling in the hot embossing process by simply reversing the current in the same hardware. There are Peltier effect devices available with enough power to meet the functional requirements, and a few of these can even operate under embossing temperatures. An all-electric heating and cooling system is technologically simple, and no moving parts is especially attractive. However, commercially available thermoelectric devices are not designed to withstand tension and compression loads, so additional supporting structure would have to be used. This supporting structure would also have to be heated and cooled, creating more thermal mass and limiting the cycle time. Also, Peltier devices simply move heat energy from one place to another, so additional equipment such as a heat sink for cooling and a secondary heating source would be necessary to create bulk heating and cooling of the workpiece.

4.3.6 Comparison of Heating Concepts

The possible methods of heating discussed in the above sections are summarized in Table 4.3. The results of this Pugh chart confirm the analysis of pros and cons of each concept, and lead to the final selection of ceramic heaters.

	Cartridge	Ceramic	Fluidic	Peltier Heating
Maximum Temperature	0	+	0	0
Rate of Heating	0	+	-	-
Complexity	0	0	-	-
Cost	0	-	-	-
Total	0	+	- - -	- - -

Table 4.3: Heating Concept Pugh Chart

4.4 Cooling concepts

4.4.1 Cooling Requirements

The final step in the hot embossing process before removing the finished workpiece is to cool the workpiece from embossing temperature to below its glass transition temperature. This should happen as quickly as possible, and for our given process parameters of two minutes cycle time and 70ºC temperature differential, the cooling power must be at least 154W (see Section 3.1.4). Of course, manufacturing considerations such as cost and footprint should also be minimized.

4.4.2 Concept: Air cooling

Air cooling is attractive because it is a cheap, clean, no-mess technique and because most manufacturing environments will have compressed air lines readily accessible. However, it is uncertain whether air cooling has enough power in a practical size. A typical setup might be a heat sink in contact with the bottom of the thermal stack, cooled between cycles by forced convection across fins. With enough surface area, any cooling power could be attained, but the volume heat sink required might be impractical. Even if it was a feasible design, it would be highly inflexible - if additional power was required or if power requirements were incorrectly estimated, the system could not scale.

4.4.3 Concept: Oil cooling

Cooling the workpiece using variable temperature oil running through platens is the method used for the MIT Generation 2 hot embossing equipment [15], so it is a well understood concept. Oil cooling provides very precise control and can be designed to give uniform heating, but it requires multiple pieces of auxiliary equipment and can be prone to messy

	Air	Oil	Water
Cooling Power	0	+	+
Complexity	0	- -	-
Cost	0	- -	-
Scalability	0	+	+
Total	0	- -	0

Table 4.4: Cooling Concept Pugh Chart

leaks and piping. Mixing two streams of oil to create a temperature difference also has a very slow time constant, so if oil cooling were used it would be best to keep the oil at a constant temperature. It is easier to scale than air cooling, as the cooling power can be changed by increasing the temperature delta or increasing flow rate.

4.4.4 Concept: Water cooling

Water cooling is similar to oil in that both use fluidic convection to cool the workpiece, and that it is messier than air with the possibility for leaks. However, water is easier to clean than oil, and is a more common resource in manufacturing environments. Water cooling capacity can also be scaled by increasing flow rate, chilling the water, or increasing the surface area available for convection. For the MIT Generation 2 hot embossing equipment, Paratherm oil was used partly because it does not boil like water would at the operating temperatures. But because for this equipment the heat sink always stays cool, boiling is not an issue.

4.4.5 Compare concepts

Each of the three cooling methods in this section are compared in Table 4.4. Note that Peltier cooling was not discussed in this section, because it has already been mentioned in conjunction with Peltier heating in section 4.3.5.

Although in this Pugh chart air and water cooling receive the same score, the considerations discussed in the preceding sections push the decision towards water cooling. Water cooling can provide the same cooling power in a smaller package than a large finned heat sink, is more flexible (flow rate can be adjusted, chilled water can be added), and transfers the heat energy in a more controllable fashion (transporting heat energy away in fluid to a specified location, instead of blowing heat into the environment).

	Concept Selected	
Overall Frame	Curved Cantilever	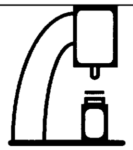
Force Application	Pneumatic Cylinder	
Heating	Ceramic Electric Heaters	
Cooling	Water	

Table 4.6: Final Concept Choices

4.5 Summary of concepts chosen

In this chapter, concepts for the overall frame design of the new hot embossing equipment were discussed, as well as concepts for force application, heating, and cooling. Table 4.6 summarizes the final selection of concepts. The next chapter will cover the detailed design of the new hot embossing equipment, building on these design choices.

Chapter 5

Design

5.1 Overview of Design Process

The concepts chosen for the new hot embossing equipment at the end of Chapter 4 were summarized in Table 4.6. These concepts were to have an open, curved cantilever frame with a pneumatic cylinder for force application, ceramic electric heaters for heating, and a water-cooled heat sink for cooling. Chapter 5 discusses the detailed design decisions and calculations necessary to build these concepts into a physical machine with the required specifications. The design is broken into four subsystems for clarity (thermal, structural, material handling and control system design), although the actual design of these subsystems happened in parallel. Each subsystem was first modeled and analyzed with an appropriate method (CAD for geometric modeling, FEA for stress modeling, thermal software for heating and cooling modeling, MatLab and Simulink for force modeling). Then parameters for each system were chosen to fulfill its functional requirements (see Table 3.3), and the overall design simplified wherever possible.

5.2 Thermal Design

The manufacturing considerations discussed in Section 3.2 (right-size design, cost, and modularity) suggest that the thermal mass involved in the thermal embossing cycle should be strictly minimized. A smaller thermal mass requires less power to heat, a shorter time to cool, and minimizes thermal cycle time (as mentioned in Section 3.3). The heating and cooling elements should be kept separate to avoid coupling of responses, and to avoid wasted heat during the thermal cycle.

5.2.1 Elements of the stack

The first step in designing the thermal subsystem of the hot embossing equipment was to decide what components were going to be involved in the thermal cycle. The minimum necessary components are listed below.

- First, the workpiece, which will most commonly by PMMA, but could also be polycarbonate, Zeonex, or Topas.
- Then, micro-patterned tools for embossing the workpiece. One tool on top of the workpiece, and one underneath the workpiece. For initial testing of the hot embossing equipment, the second tool under the workpiece will be featureless.
- Two ceramic heaters (the chosen concept for heating), to be placed behind the tools.
- A backing plate behind the bottom heater to provide structural support.
- A ceramic block behind the top heater to prevent the heat for traveling outside the thermal stack, and
- A heat sink to provide cooling.

Figure 5-1 depicts the elements of the thermal stack. All of the components between the top ceramic block and the heat sink will be referred to as the thermal stack. The configuration of the heat sink and the pins is discussed in the next section.

5.2.2 Heat Sink Design

Now that the components of the thermal stack have been decided, the configuration of the heat sink must be addressed. Table 4.6 already stated that the heat sink is going to be water cooled. One of the key innovations in this design for hot embossing equipment is that the heat sink is dynamic. During the heating cycle, it is not in contact with the thermal stack, so thermal energy is not lost in heating the sink. During the cooling part of the embossing cycle, the heat sink is brought into contact with the thermal stack to cool the workpiece through conduction. This dynamic design is in line with the manufacturing and design considerations noted in Sections 3.2 and 3.3.

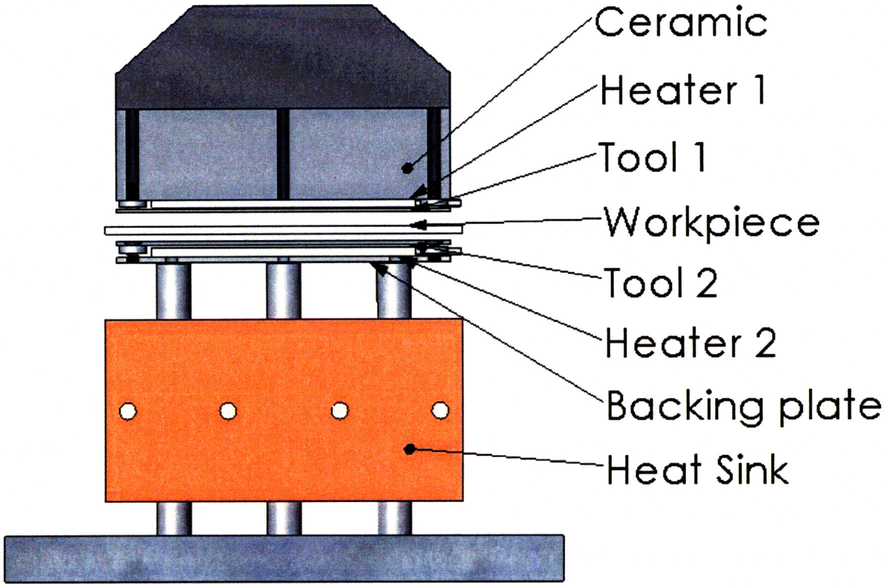

Figure 5-1: Thermal Stack

Because the heat sink is designed to be moveable, it cannot be used to support the thermal stack. Whatever support structure is used instead must still allow the heat sink to contact the thermal stack for conductive cooling. Figure 5-2 shows several possible heat sink and supporting material configurations.

The configuration in design (a) would support a thermal stack (simplified in the figures to simply a workpiece) on a beam fixed at the ends. This allows good contact with the heat sink, but bending of the beam in that fixed-fixed configuration would be a significant issue. Design (b) supports a workpiece on two edges, which poses an even worse bending problem than in design a). Note that for both a) and b), the support could be on the edges of the 25mm direction instead of the 75mm length, which would significantly reduce the bending, but supporting along the 25mm direction limits access to the heat sink for water cooling fixtures to be attached. Design (c) uses supports directly underneath the workpiece, running through the heat sink. This limits bending while still allowing area for contact between the heat sink and the bottom of the workpiece. If the supports are made of ceramic, the heat flow through the supports to the frame is also minimized. Design (c) also provides open access to the heat sink for actuation and cooling passages. For these reasons, design (c) was chosen as the best support configuration.

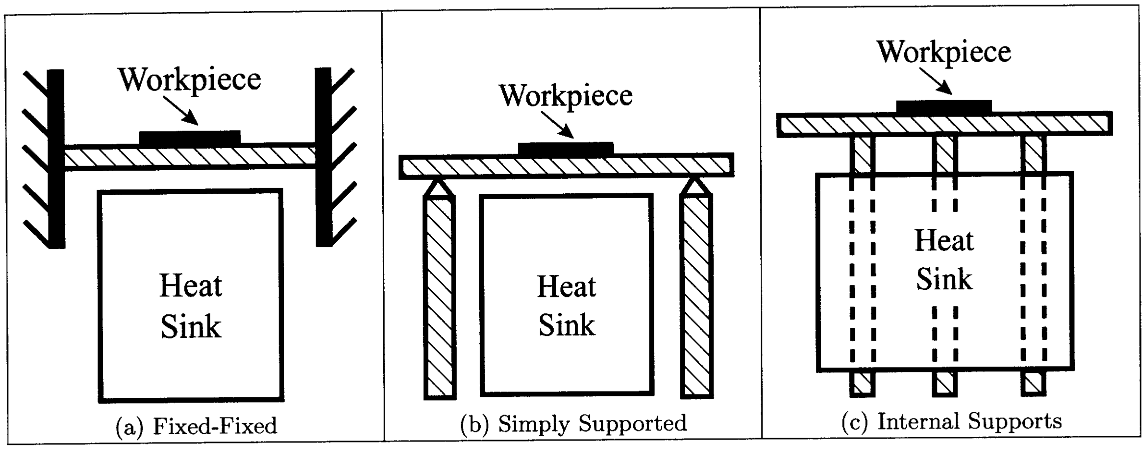

Figure 5-2: Possible Heat Sink Support Configurations

The size of the heat sink and the water cooling passages in the heat sink also needs to be designed. The thermal load created during the heating portion of the embossing cycle was calculated in Equation 3.1 to be 5545J. The heat sink should be able to absorb at least this much energy, and preferably more, so that if for some reason the cooling water failed the heat sink could absorb the heat from one or more full embossing cycles. For the purpose of volume estimation, the heat sink is limited to a five degree Celsius rise in temperature when absorbing the 5545J energy from one embossing cycle.

$$Thermal\ Energy\ in\ Stack = Thermal\ Energy\ Absorbed\ by\ Heat\ Sink = 5545J$$

$$5545J = \rho_{heat\,sink} V_{heat\,sink} C_{p_{heat\,sink}} \Delta T$$

$$V_{heat\,sink} = \frac{5545}{8960 * 385 * 5} = 321.5\ (cm^3)$$

The width and length of the heat sink should be at least 2.5 cm by 7.5 cm, to cover all of the available contact area between the heat sink and the bottom of the thermal stack. A convenient, compact form factor is 10.0 cm by 7.5 cm by 5.0 cm (roughly 4” by 3” by 2”), which gives a volume of 375 cm^3 with a safety factor of 1.17 above the required 321.5 cm^3.

Two other design decisions for the heat sink are the diameter and number of cooling water passages. The number of cooling water passages was based on convenience - three

Given constants:	
tube length l	0.06 m
Temperature 1	22 ºC
Temperature 2	80 ºC
h	3000 W/mK

(a)

Diameter (m)	Area of 4 Passages (m^2)	Convection (W)
0.005	0.0038	656
0.010	0.0075	1312
0.015	0.0113	1968
0.020	0.0151	2624
0.025	0.0188	3280

(b)

Table 5.1: Calculation of Diameter of Heat Sink Cooling Passages

vertical clearance holes were already needed for the three ceramic support pins, which divide the heat sink into four regions available for horizontal passages. A cooling water passage was placed in each region, for a total of four water cooling passages.

The diameter of the cooling water passages can be figured from Newton's Law of Cooling, and should be large enough to provide the cooling power required for the heat sink (calculated in Equation 3.2 as 154 Watts). Assuming constant cooling water temperature, horizontal circular cylinders, and considering convection effects only, Table 5.1 gives the constants used and the cooling power calculated for varying diameters. This table shows that even at a diameter as small as 0.005 m (which is about the smallest diameter that can easily be machined), there is plenty of excess cooling power. Excess cooling power is not a problem (since it does not cause more expense or more complications), so the tubes should just be drilled a convenient size. Pipe fittings generally come as small as 1/8" , which requires a drill bit size of 21/64." Water tubing also comes commonly at these sizes, so a tube diameter of 0.328" was chosen. This corresponds to a tube diameter of 0.008m, which gives a cooling power of 1050W (an order of magnitude greater than the required cooling power of 154W).

5.2.3 Analysis of Heating

It is important to make sure that the heating and cooling systems have enough power, given the configuration of the thermal stack, to meet functional requirements such as cycle time given in Table 3.3. The heating portion of the embossing cycle was modeled with the

Component	**Thickness (mm)**	**Width (mm)**	**Length (mm)**	**Quantity**	**Material**
Workpiece	2	25	75	1	acrylic
Tool	2	35	95	2	aluminum
Heater	2.5	25	75	2	aluminum nitrate ceramic
Backing plate	2	35	95	1	steel

(a) Geometry of Components for FEA Heating Analysis

CosmosWorks Settings	
Initial Temperature	20ºC all components
Boundary Conditions	No heat transfer through top and bottom surfaces of thermal stack
Heater Power Generation	700 Watts per heater
Thermostat Settings	Heaters on if below 143ºC - off if above 145ºC
Simulation Step Time	0.5 sec
Simulation Total Time	35 sec
Probe Location 1	Center of top face of workpiece
Probe Location 2	Center of bottom face of workpiece

(b) Settings for FEA Heating Analysis

Table 5.2: Parameters of Heating FEA Components

components and settings given in Table 5.2 using CosmosWorks transient thermal analysis in Solidworks. Figure 5-3 shows these components modeled in Solidworks.

The results of the analysis were plotted in Figure 5-4 as the temperature at two points (Probe Location 1 and Probe Location 2) against time. This plot shows that it takes approximately 35 seconds for the workpiece to be heated from room temperature to an embossing temperature of 140ºC. This is an ideal minimum time, and does not take into account the effect of contact resistance between the components in the thermal stack. This analysis also does not take into account heat losses from the edges of the components, which is assumed to be negligible. This estimate of 35 seconds for the heating portion of the cycle is actually conservative, however, because in a manufacturing setting each cycle would only be from demolding temperature to embossing temperature - a difference of 80ºC to 140ºC instead of 20ºC to 140ºC. Figure 5-5 illustrates the temperature distribution in the thermal stack 10.2 seconds into heating, showing that as expected the edges of the workpiece are the last things to come to temperature.

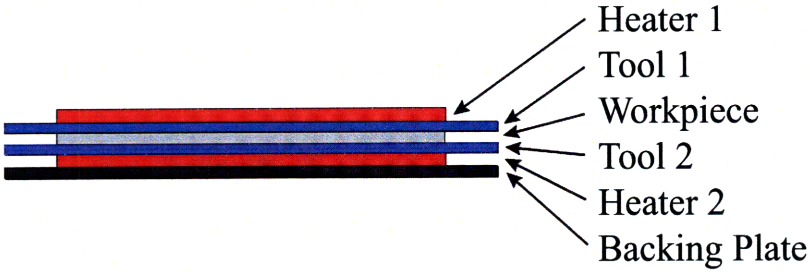
Heater 1
Tool 1
Workpiece
Tool 2
Heater 2
Backing Plate

Figure 5-3: CAD Model used for Heating Analysis

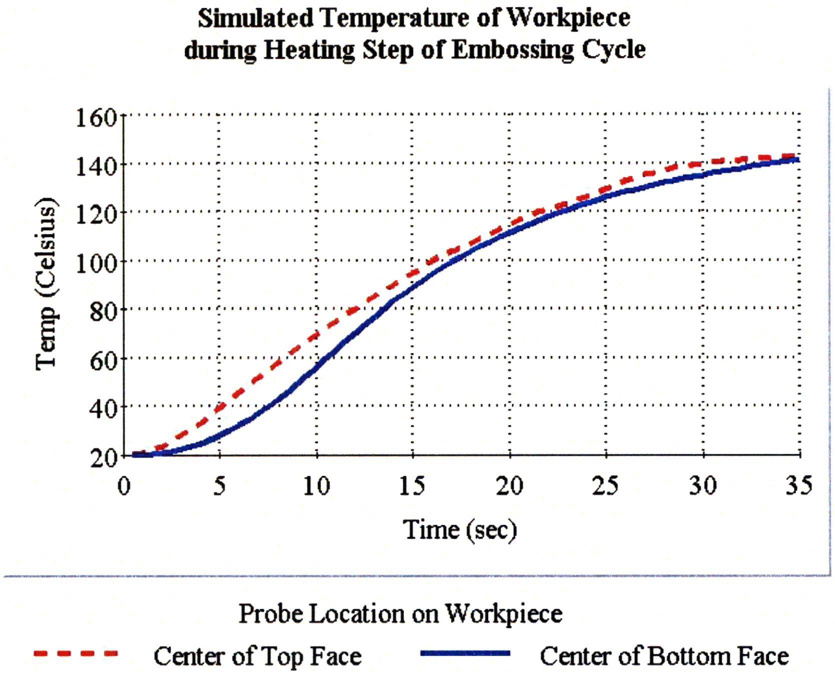

Figure 5-4: Results of FEA Heating Analysis showing a minimum of 35 seconds needed to reach embossing temperature

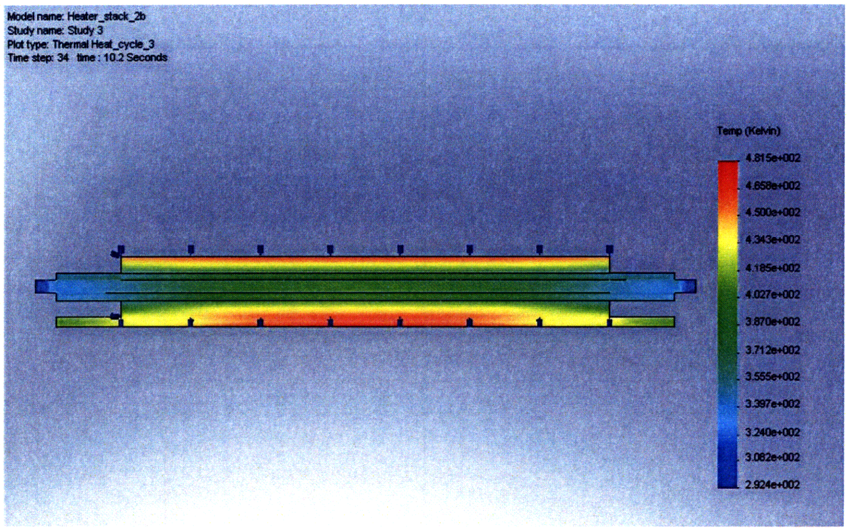
Model name: Heater_stack_2b
Study name: Study 3
Plot type: Thermal Heat_cycle_3
Time step: 34 time : 10.2 Seconds
Temp (Kelvin)
4.815e+002
4.658e+002
4.500e+002
4.343e+002
4.185e+002
4.027e+002
3.870e+002
3.712e+002
3.555e+002
3.397e+002
3.240e+002
3.082e+002
2.924e+002

Figure 5-5: FEA Plot of Thermal Stack During Heating

5.2.4 Analysis of Cooling

In the cooling portion of the embossing cycle, a heat sink with chilled water circulating through internal passages is brought into contact with the bottom of the same thermal stack analyzed in the previous section. The components and settings given in Table 5.3 were modeled using CosmosWorks transient thermal analysis in Solidworks. Figure 5-6 shows these components modeled in Solidworks.

The results of the cooling analysis were plotted in Figure 5-7 as the temperature at two points (Probe Location 1 and Probe Location 2) against time. This plot shows that it takes approximately 45 seconds for the workpiece to be cooled from an embossing temperature of 140C to a demolding temperature of 80C. This is an ideal minimum time, and does not take into account the effect of contact resistance between the components in the thermal stack. This analysis also does not take into account heat losses from the edges of the components, which is assumed to be negligible. The chilled water flowing through the channels in the heat sink is assumed to be kept at a constant temperature by the water chiller. Figure 5-8 illustrates the temperature distribution in the thermal stack 30 seconds into heating, showing that as expected the top edge of the workpiece is the last thing to cool.

Taken together, Figures 5-4 and 5-7 show that a minimum of 85 seconds will be necessary for a full embossing cycle. The actual cycle time is expected to be longer than 85 seconds, but no longer than the 120 second cycle time goal stated in Table 3.3.

Component	Thickness (mm)	Width (mm)	Length (mm)	Quantity	Material
Workpiece	2	25	75	1	acrylic
Tool	2	35	95	2	aluminum
Heater	2.5	25	75	2	aluminum nitrate ceramic
Backing plate	2	35	95	1	steel
Heat Sink	66	56	106	1	copper

(a) Geometry of Components for FEA Cooling Analysis

CosmosWorks Settings	
Initial temperature	5ºC heat sink
	140ºC all other components
Boundary Conditions	Water channels in heat sink isothermal at 5ºC
	No heat transfer through top surface of thermal stack
Thermostat Settings	Heaters on if below 143ºC - off if above 145ºC
Step Time	1s - temp
Total Time	50s - temp
Probe Location 1	Center of top face of workpiece
Probe Location 2	Center of bottom face of workpiece

(b) Settings for FEA Cooling Analysis

Table 5.3: Parameters of Cooling FEA Components

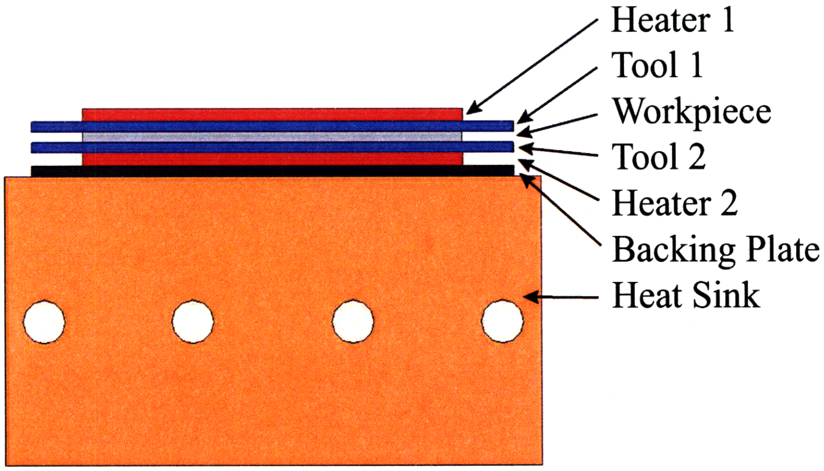

Figure 5-6: CAD Model used for Cooling Analysis

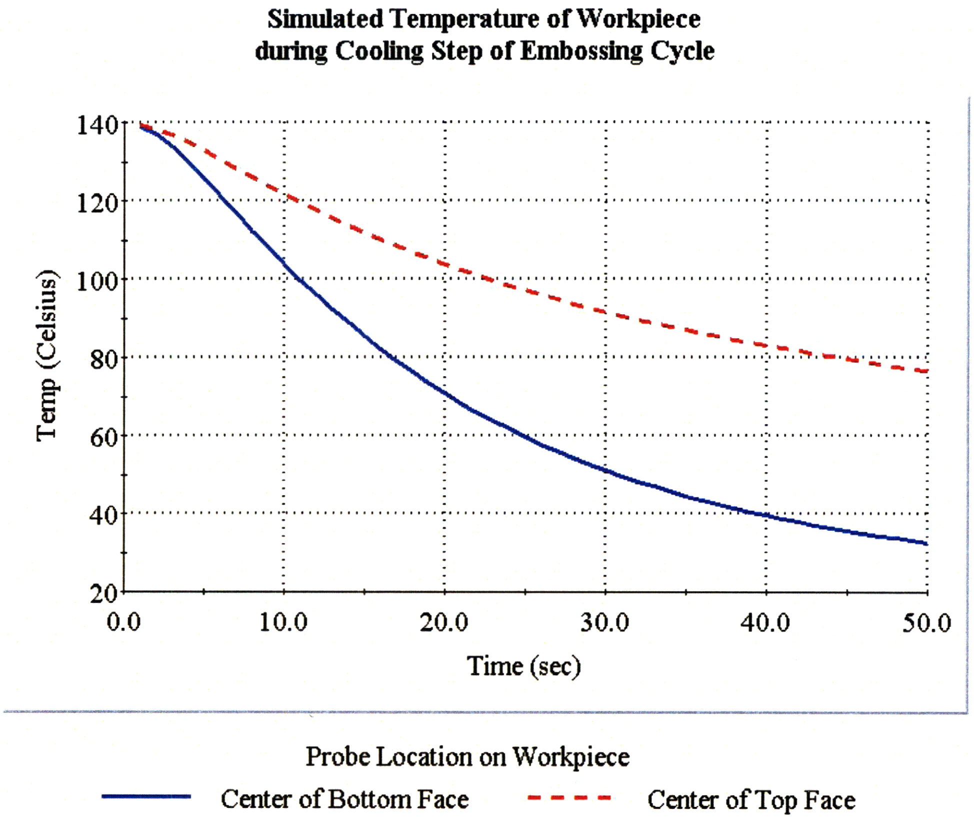

Figure 5-7: Results of FEA Cooling Analysis showing a minimum of 50 seconds needed to reach demolding temperature

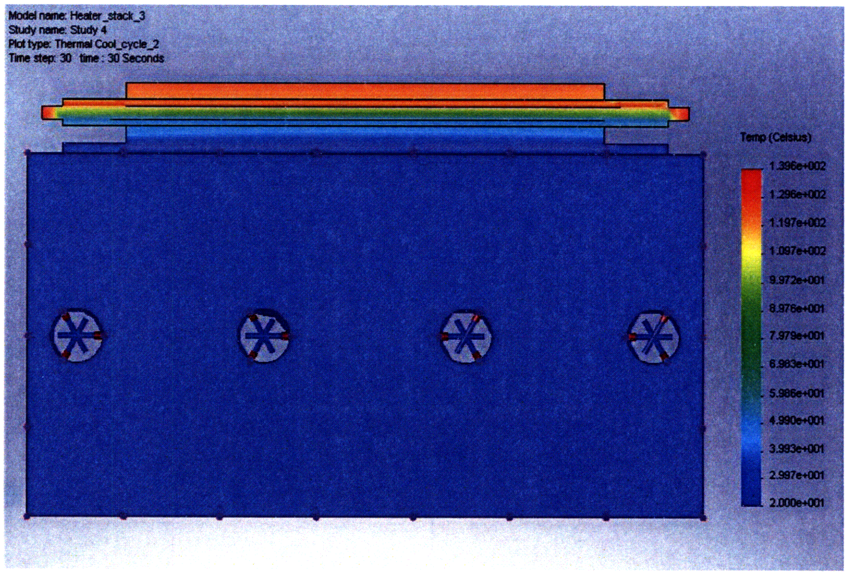
Model name: Heater_stack_3
Study name: Study 4
Plot type: Thermal Cool_cycle_2
Time step: 30 time : 30 Seconds
Temp (Celsius)
1.396e+002
1.296e+002
1.197e+002
1.097e+002
9.972e+001
8.976e+001
7.979e+001
6.983e+001
5.986e+001
4.990e+001
3.993e+001
2.997e+001
2.000e+001

Figure 5-8: FEA Plot of Thermal Stack During Cooling

5.3 Structural and Force Application Design

In addition to heating and cooling, force application is the other major step in the hot embossing cycle. According to Table 3.3, a maximum force capacity of 9375N is required over an area of 2mm5 by 75mm, and a pneumatic cylinder was chosen as the best concept for achieving that (Table 4.6). The following section discusses the selection of a pneumatic cylinder, the design of the frame and support components to support the force applied to the workpiece, and the modeling of the equipment for feedback control of the force applied.

5.3.1 Pneumatic Cylinder Design

There are many companies that supply hydraulic and pneumatic cylinders for force application, but two of the largest which have product lines in the right range for this application are Air Cylinders Direct and Mead Fluid Dynamics. Given required parameters of 2200 lbf over an area of 1" by 3" (which roughly equates to 750psi), and an inlet air pressure supply of 80-100psi, sales representatives from both companies recommended a cylinder with a 6" bore. A Mead Fluid Dynamics pneumatic cylinder model DM600 was the product finally purchased, based on technical specifications, pricing and availability of technical support. A cylinder with a 3" stroke was originally specified, but this was changed to a 1" stroke. Three inches of travel added to the expense and the physical size of the cylinder, yet was not needed for functionality.

5.3.2 Load cell design

A load cell is needed to provide feedback for controlling the force applied to the workpiece. There are two main ways to measure the forming force: mount a load cell in line with the cylinder and the thermal stack, or instrument the machine frame to measure strain. Instrumenting the frame requires careful recalibration for any change in test setup, and is particularly tricky for a C-frame (as opposed to a gantry style) with rather low loads. It is important to know precisely the force applied, so the load cell was designed to be in line with both the cylinder and the thermal stack. The maximum capacity of the cylinder was designed to be around 2500 lbf (just slightly over the 2200 lbf in the function requirements in Table 3.3). Standard load cells based on strain gage technology can come in "S" configurations, or tall skinny shapes. However pancake configurations are better for this application, because a thinner profile keeps the force path short and the equipment as compact as possible. LoadStar sensors makes load cells based on capacitance sensors rather than strain gages in a compact pancake configuration, with several other attractive features. Their line of load cells requires no programming, a simple calibration, and has digital integrated electronics with a standard USB output and USB power input. Also, each sensor can measure both compression and tension which is rare.

5.3.3 Support design

The force applied to the workpiece during embossing must be supported by the hot embossing equipment frame; there must be a load path through the equipment. The pneumatic cylinder will be bolted to the frame, and apply force through a load cell to the thermal stack. All of the elements in the thermal stack are designed to withstand this embossing force and be in the load path (see Section 5.2.1). The trickier problem is how to support the thermal stack.

The ceramic pins in design (d) of Figure 5-2 insulate and prevent heat from travelling through the frame, and allow the heat sink to slide up into contact with the thermal stack. There is a design trade off to be made in the number and size of the ceramic pins. Multiple pins spaced closely together minimize bending, but fewer pins farther apart maximize area for contact with the heat sink, which allows faster cooling and shortens cycle time. Two possible configurations for ceramic pins are shown in Figure 5-9. Although design (a) has more open area for contact with the heat sink, the 1/8" ceramic pins are more fragile than the 3/8" pins. It would also be difficult to align all six pins in parallel, and any misalignment would likely result in a fractured pin or in jamming when actuating the heat sink. Design (b) was chosen as a more robust design.

The ceramic pins are in contact with a backing plate which supports the bottom heater. This backing plate must not allow a bending moment or point forces to be applied to the heater, which is ceramic and very brittle. Rough guidelines of at least 18 μm surface roughness and 0.002" (50.8 micrometers) flatness across the length of the 75mm heater were suggested in conversations with a Watlow company representative. This means that the backing plate between the lower heater and the supporting ceramic pins must be designed to well within these constraints. The thickness and material used for the backing plate are the critical design choices. A simple bending analysis was used to find the maximum bending that would occur under the maximum uniform load for a given thickness of plate.

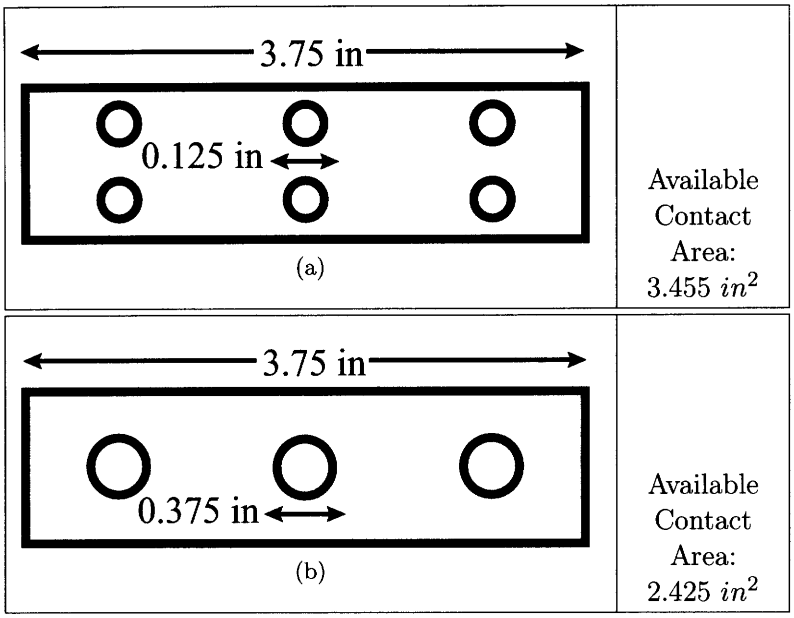
3.75 in
0.125 in
(a)
Available Contact Area: 3.455 in^2
3.75 in
0.375 in
(b)
Available Contact Area: 2.425 in^2

Figure 5-9: Possible Ceramic Pin Configurations

The thickness should be minimized in order to reduce thermal mass and shorten cycle time.

Table 5.4 gives the constants used in the bending analysis. Table 5.5 shows that the maximum predicted deflection will occur between pins, not from a pin to a free edge. Therefore, the between-pin case is used as the limiting case. Table 5.6 considers the limiting between-pin case for both aluminum and steel, and plots the maximum deflection of the backing plate as a function of backing plate stiffness. This table shows that for aluminum, a thickness of approximately 2.5 millimeters is needed to keep the maximum deflection under 10 micrometers, whereas steel only requires around 1.75 millimeters of thickness for the same deflection. Aluminum has a better thermal conductivity than steel (see Table A.1), so the question is whether having a thinner backing plate is worth the poorer thermal response. Table 5.7 compares the thermal mass of backing plates made of steel and aluminum, each thick enough to keep bending to 15 micrometers. The table shows that the thinner backing plate of steel and a thicker plate of aluminum have comparable thermal masses, although steel actually has a slightly higher thermal mass. Even though an aluminum backing plate seems slightly better, steel was chosen in the interest of keeping all components in the thermal stack as thin as possible.

Finally, it is useful to have an upper limit estimate of the bending in the case that the fixed-fixed beam assumption is incorrect, and that the section of backing plate between

Given constants:	
Young's modulus E	2 e 11 Pa
width b	0.0254 m
thickness h	0.003175 m
applied load w	9375 N
Moment of Inertia I	6.7746 e -11

Table 5.4: Bending Analysis Constants

Possible Limiting Case	**Case 1: Between Pins**	**Case 2: From Pin to Free Edge**
Boundary Conditions	Fixed-Fixed with Uniform Loading	Fixed-Free with Uniform Loading
Equation for Max. Deflection	$y = wl^4/384EI$	$y = wl^4/8EI$
Length l	0.032 m	0.012m
Max. Deflection	1.8894 microns	1.7935 microns
	0.0744 thous	0.0706 thous

Table 5.5: Determining Bending Limiting Case: Pin-to-Pin or Pin-to-Free

supporting pins has true boundary conditions closer to simply supported. Table 5.8shows that even in this worst-case scenario, for a three millimeter thick steel backing plate the maximum deflection is still under 10 micrometers, which is well within the acceptable range of about 50 micrometers.

In addition to the backing plate bending, another mode of failure of the support structure might be buckling of the ceramic pins under the applied load. To check that buckling will not occur, the constants given in Table 5.9 are used to calculate the critical load under which the pins will buckle, assuming long column buckling and that the boundary conditions are fixed-fixed for the ends of the pins. The worst case boundary condition would be pinned-pinned, so that case is also checked. Table 5.10 shows that the anticipated safety factor is 13.8, and that even under the worst case boundary conditions there is still a safety factor of 3.4 before the ceramic pins will buckle.

5.4 Control System Design

The essential parameters to control during the embossing cycle are the force applied, the temperature of the workpiece, and the duration of each step. Helpful but optional parameters to control include the position of the tool and the temperature of the cooling water.

Maximum deflection of a fixed-fixed beam under a constant load:
$y = wl^4/384EI$

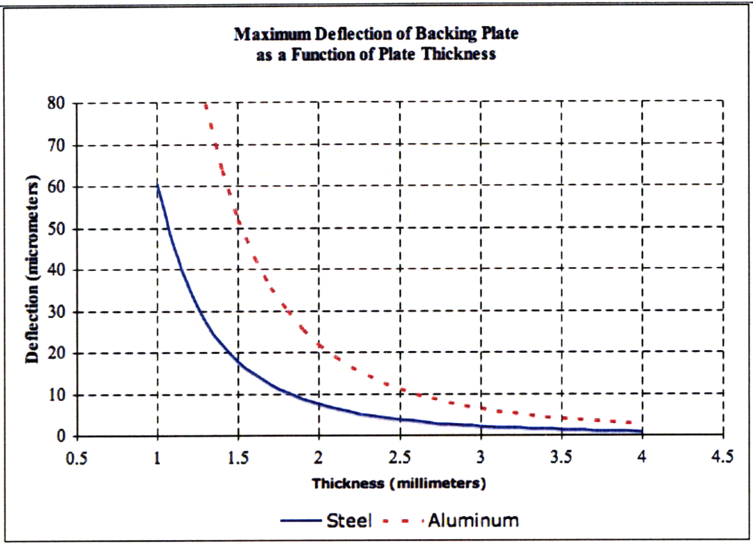

Table 5.6: Maximum Deflection of Backing Plate vs. Thickness for Aluminum and Steel

	Steel Backing Plate	**Aluminum Backing Plate**
Thickness needed to keep bending under 10 micrometers (see Table 5.6)	1.6 mm	2.3 mm
Thermal Mass	1012 J	929 J

Table 5.7: Comparison of Thermal Mass of Aluminum and Steel Backing Plates

Possible Worst Case	Case: Simply Supported
Boundary Conditions	Simply Supported with Uniform Loading
Equation for Max. Deflection	$y = 5wl^4/384EI$
Material	steel
Thickness	.003175 m
Length l	0.032 m
Max. Deflection	9.4471 microns
	0.3719 thousandths

Table 5.8: Determining Worst Case Bending of Simply Supported Beam

Given constants:	
Young's modulus E	6.69 e 10 Pa
diameter d	0.01 m
length l	0.1 m
applied load w	9375 N
Moment of Inertia I	4.909 e -10

Table 5.9: Bending Analysis Constants

Boundary Conditions	Fixed-Fixed Pin Ends	Pinned-Pinned Pin Ends
Governing Equation	$F = 4 * \pi^2 * E * I/l^2$	$F = \pi^2 * E * I/l^2$
Critical Force	129645 N	32411 N
Safety Factor under maximum load	13.8	3.4

Table 5.10: Critical Force for Buckling

For this first iteration of a hot embossing system, a position sensor will not be included because it is more important to control the force applied to the workpiece than to control the displacement. The temperature of the cooling water will be considered part of a system separate from the embossing equipment, and the temperature will be maintained by regulation internal to the chiller.

For convenience, the embossing system is broken into four categories: overall architecture, heating, cooling, and force application. Figure 5-10 diagrams the layout of the components in these subsystems. The overall architecture is made up of a laptop (for portability) running LabView (a commonly used control software) that connects via USB to the embossing system. This fulfills the requirements for connectivity given in Table 3.3. The rest of the equipment will connect to a USB hub, either directly or through a data acquisition card (DAQ). The DAQ will be used for collecting data and for sending signals to the equipment. The control loops for each subsystem - heating, cooling, and force application - will be kept separate from each other and external to the computer wherever possible. Making separate control loops for each subsystem not solely reliant on the computer does several things: it protects against failure in one loop causing failure in the entire equipment, it reduces the load on the computer because the computer only needs to send set points, and it helps protect against catastrophic failure in case of the computer freezing.

The heating subsystem of the embossing equipment consists of two identical sets of four components - a heater, controller, relay, and power supply. The temperature of the heaters are measured with internal thermocouples, and the temperature data are fed into both the DAQ for data collection and the heater controller as feedback. The controllers use the thermocouple to regulate the temperature of the heater to a set point sent from the laptop controlling software. Having the top and bottom heaters and controllers separate and identical allows independent manipulation of the heater temperatures if necessary, follows the modular manufacturing design philosophy, and makes replacing parts easier. Note that the actual temperature of the workpiece will not be known, because it isn't feasible to insert a thermocouple into each workpiece. The temperature of both the top and bottom heater will be known, so these can act as a proxy for the actual workpiece temperature (perhaps an average of the two).

The cooling subsystem consists of the heat sink, two solenoid activators, power supplies and relays for the solenoids, and the tubing to connect to the chiller. The chiller and its internal temperature regulation are considered a separate system, and are not controlled from the overall architecture. This leaves a very trivial control problem - the solenoids just need to be activated and deactivated at the proper time points with a signal sent from the laptop through the DAQ.

The force application subsystem consists of the pneumatic cylinder, three way valve, valve controller, power supply, and load cell. The load cell provides feedback into the valve controller and also feeds into the DAQ for data collection. The valve controller is a simple proportional controller which matches the feedback from the load cell to a given set point from laptop.

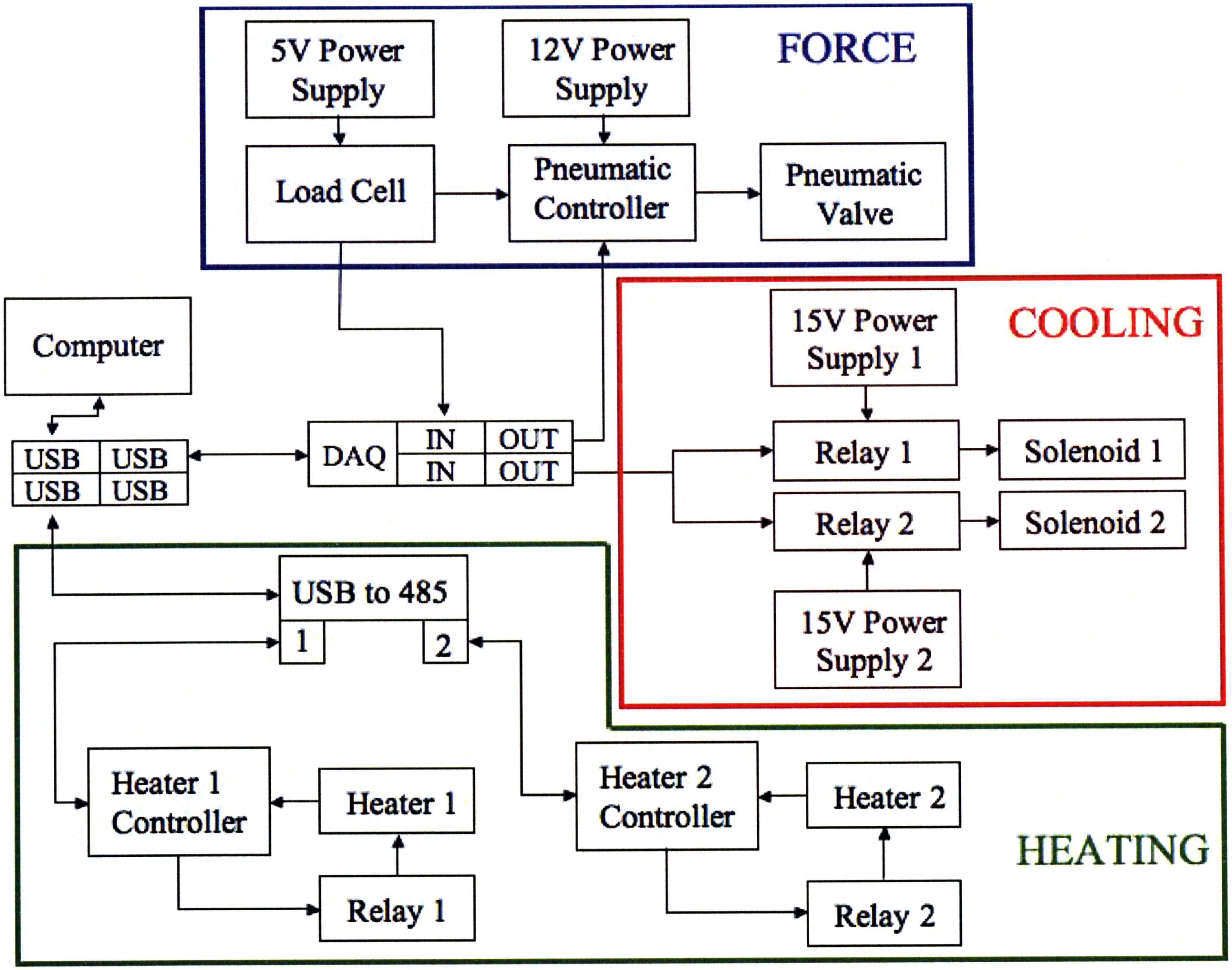
FORCE
5V Power Supply
12V Power Supply
Load Cell
Pneumatic Controller
Pneumatic Valve
COOLING
15V Power Supply 1
Computer
USB
USB
USB
USB
DAQ
IN
IN
OUT
OUT
Relay 1
Solenoid 1
Relay 2
Solenoid 2
15V Power Supply 2
USB to 485
1
2
Heater 1 Controller
Heater 1
Relay 1
Heater 2 Controller
Heater 2
Relay 2
HEATING

Figure 5-10: Control System Layout (see Section 6.5 for part numbers)

Chapter 6

Fabrication

The overall CAD model of the hot embossing equipment is given in Figure 6-1. The description of each component is given in the following chapter.

6.1 Structural Components

The frame of the hot embossing equipment (Figure 6-3) was bought prefabricated from Mead Fluid Dynamics rather than custom built because it saved many hours of labor and ensured good parallelism in the construction. The frame is model AP-600, designed for a 6" bore pneumatic cylinder, intended as a press frame, and fabricated with steel welded construction. Figure 6-2 shows the dimensions of the frame (image courtesy of www.meadfluiddynamics.com). The frame is slightly modified by drilling four holes in the

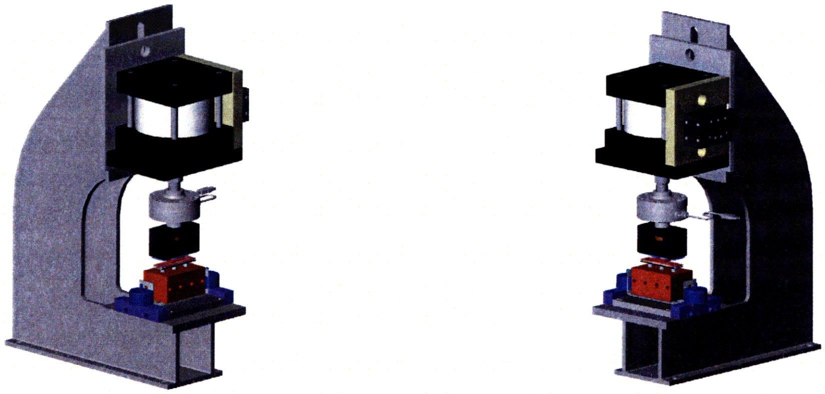

Figure 6-1: Overall CAD model

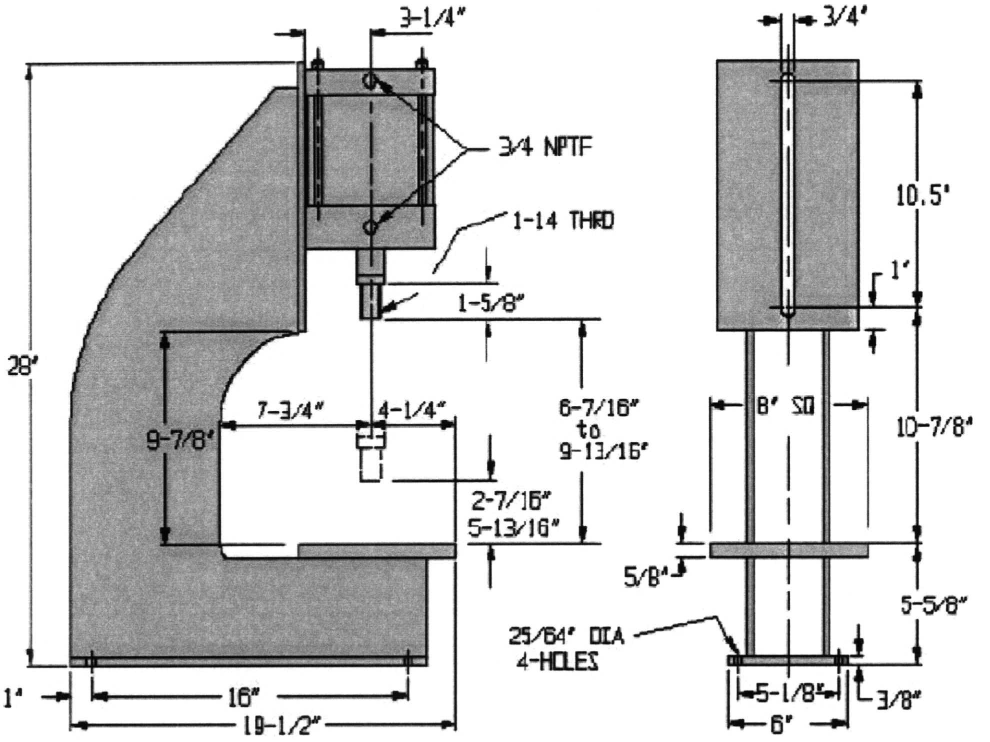

Figure 6-2: Press Frame

base plate to allow attachment of other structural elements. If a custom frame had been designed, it probably could have been made more compact, but it was worth the compromise to choose the prefabricated frame.

The pneumatic cylinder chosen did not have the same attachment configuration as the frame, so a cylinder adapter plate was machined from steel to mate the cylinder with the frame (Figure 6-3). The drawing for this adapter plate is given in Appendix C, Figure C-1. The pneumatic valve is intended to be mounted as close to the cylinder as possible, so an adapter plate was used to screw into the hole pattern on the valve and bolt through the through-holes on the face of the cylinder. Because this is not a critical structural piece, it is made of scrap polymer with holes marked and drilled in place. There is no drawing for this adapter plate.

The next piece of structure in the equipment is the base plate, which attaches to the frame through the four drilled holes. This base plate holds the ceramic pins, which support the rest of the thermal stack. The drawing for the base plate is given in Appendix C, Figure C-2. The ceramic pins are slightly varying diameters, and they need to be tightly fitted into

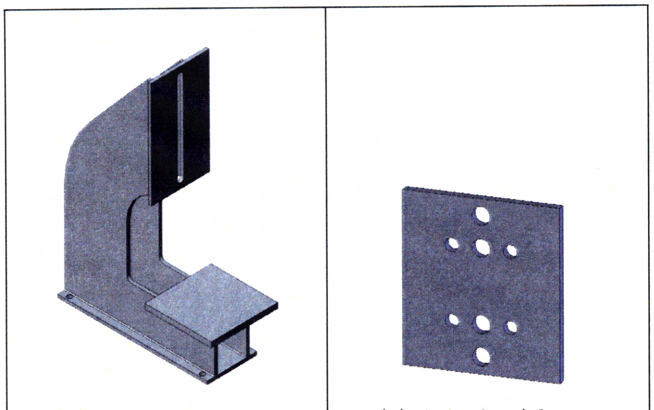

(a) Frame (b) Cylinder Adapter

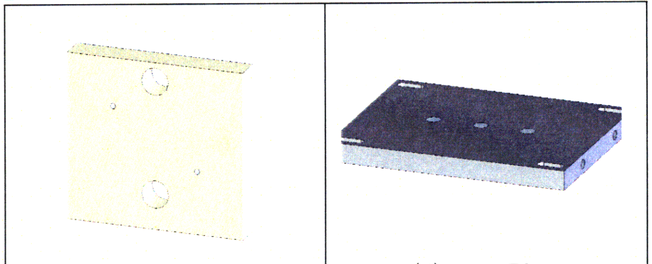

(c) Valve Adapter (d) Base Plate

Figure 6-3: Structural Components

the base plate, so the holes in the base plate are reamed to the closest reamer size. The blueprint includes optional 1/8" holes, which were not used, for a design which uses dowel pins to help secure the ceramic pins.

6.2 Thermal Stack Components

The steel backing plate on top of the pins (Figure 6-4) is the plate designed in section 5.3.3. In accordance with those design decisions, it was machined from 1/8" ground steel. (The ground steel is necessary to provide a flat surface against the ceramic heaters to prevent cracking). The three holes along the centerline were reamed to fit the dowel pins and attach to the ceramic pins, while the four corner holes were tapped for attachment to the bottom heater fixturing plate. The blueprint for this plate can be found in Appendix C, Figure C-3.

The two heaters used in the design are Ultamic 600 heaters by Waltow, provided through FM Keefe, part #CER-1-01-00007, 75mm x 25mm x 2.5mm. Each heater uses a heater controller also provided by Watlow model SD6C-HCUE-AARG 1/16 DIN temperature controllers, with the 485 communications option and an additional optional relay. Each heater also needs an AC solid state relay between the controllers and the wall power, which are

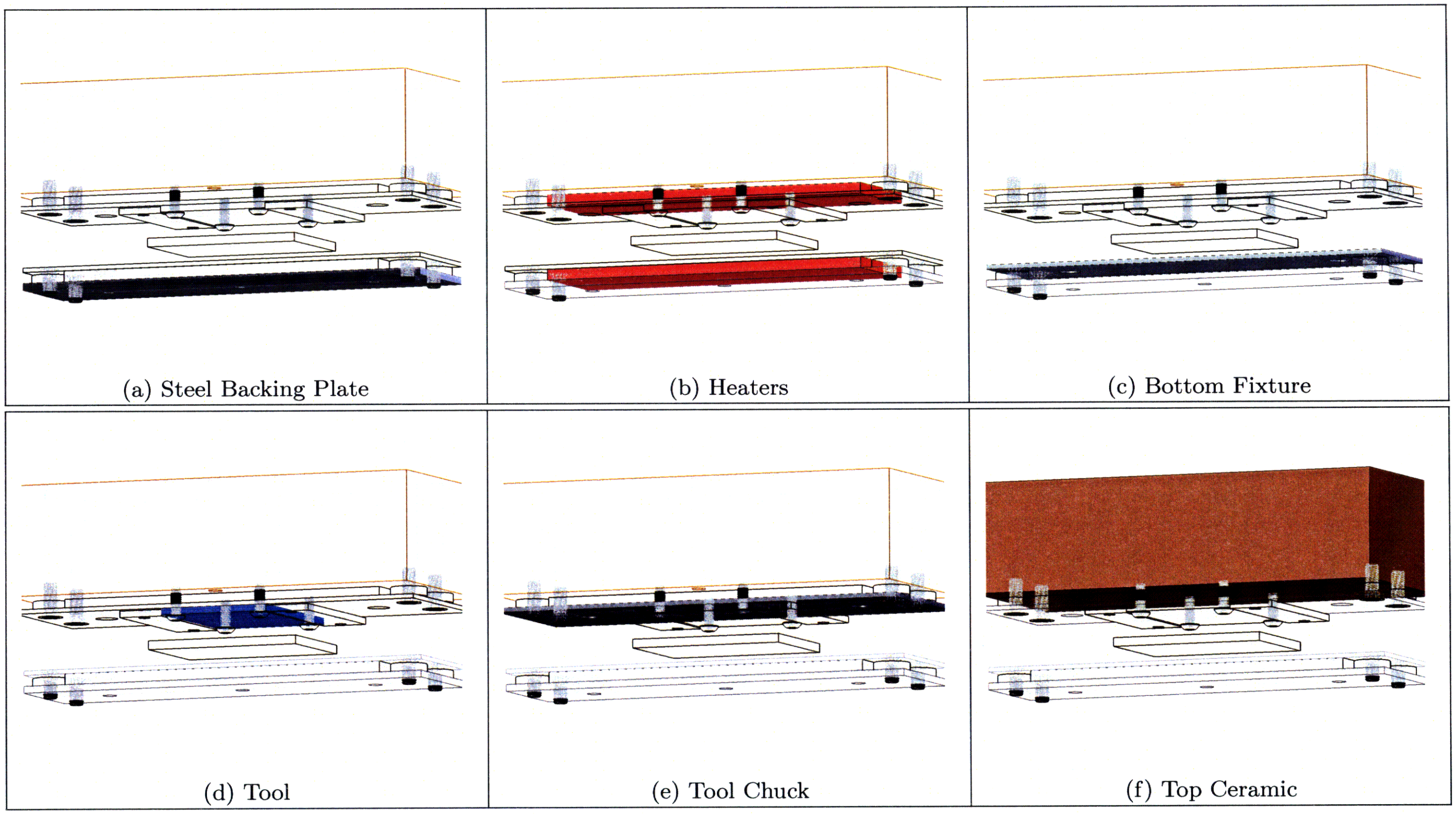

(a) Steel Backing Plate

(b) Heaters

(c) Bottom Fixture

(d) Tool

(e) Tool Chuck

(f) Top Ceramic

Figure 6-4: Thermal Stack Components

model RS1A23D25 Carlo Gavazzi relays.

The bottom fixture plate is in the thermal stack to clamp the bottom heater in place (the heaters can not be drilled into for screws or fixturing) and to provide an optically flat surface to emboss against. This bottom fixture plate is made from aluminum, polished on the top surface (Figure 6-4).

Above the workpiece, the next element is the tool (Figure 6-5). For all of the production runs discussed in the Results Chapter, a tool fabricated by David Henann from bulk metallic glass (BMG) is used [22]. This tool is patterned with a simple micromixer pattern which is useful for testing and characterizing the embossing process. Tools can also be made of micromachined steel or aluminum.

Above the tool is the tool chuck (Figure 6-4), which is made of aluminum and has mounting holes for the tool and optional demolding tabs. This tool chuck also serves to clamp the top heater in place. Behind the top heater, the last element in the thermal stack is the ceramic backing. This ceramic piece insulates the heater and thermal elements from the load cell and pneumatic cylinder above, and provides a flat surface against the top heater. The drawing for the ceramic piece can be found in Appendix C, Figure C-4.

The assembled thermal stack is shown in Figure 6-6.

6.3 Force Components

The pneumatic cylinder used for force application (Figure 6-7) in the hot embossing equipment is a Mead Fluid Dynamics DM-600 x 1" stroke FH-CB model cylinder. This model has a 6" bore, and a capacity of 2262 lbf at 80 psi supply pressure, or 2827 lbf at 100 psi supply pressure. The valve used is an LSC-V25c High Speed Proportional Valve from Enfield technologies, with the recommended LS-C10 Analog Motion Control valve controller.

The load cell chosen was an iLoad Pro Analog™ Integrated Load Cell, from LoadStar Sensors. The first load cell chosen was +/- 5,000 lbf capacity, and the replacement load cell is the +/- 500 lbf variety. Both were ordered with the tension adapter which allows for loading and measurement in the tensile direction. A 5V DC power supply was ordered with the load cell to meet its power requirements.

The force adapter is a machined aluminum piece which transitions between the load cell mounting threads and the ceramic backing piece from the thermal stack. The drawing

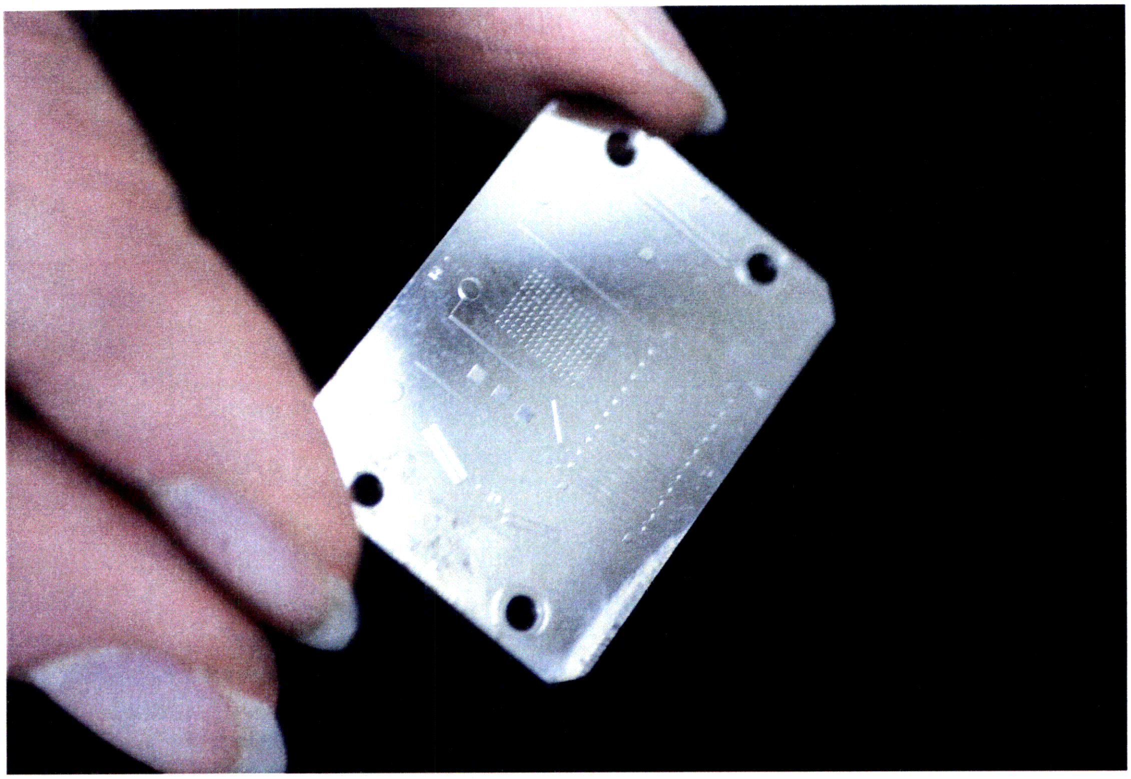

(a) BMG Tool

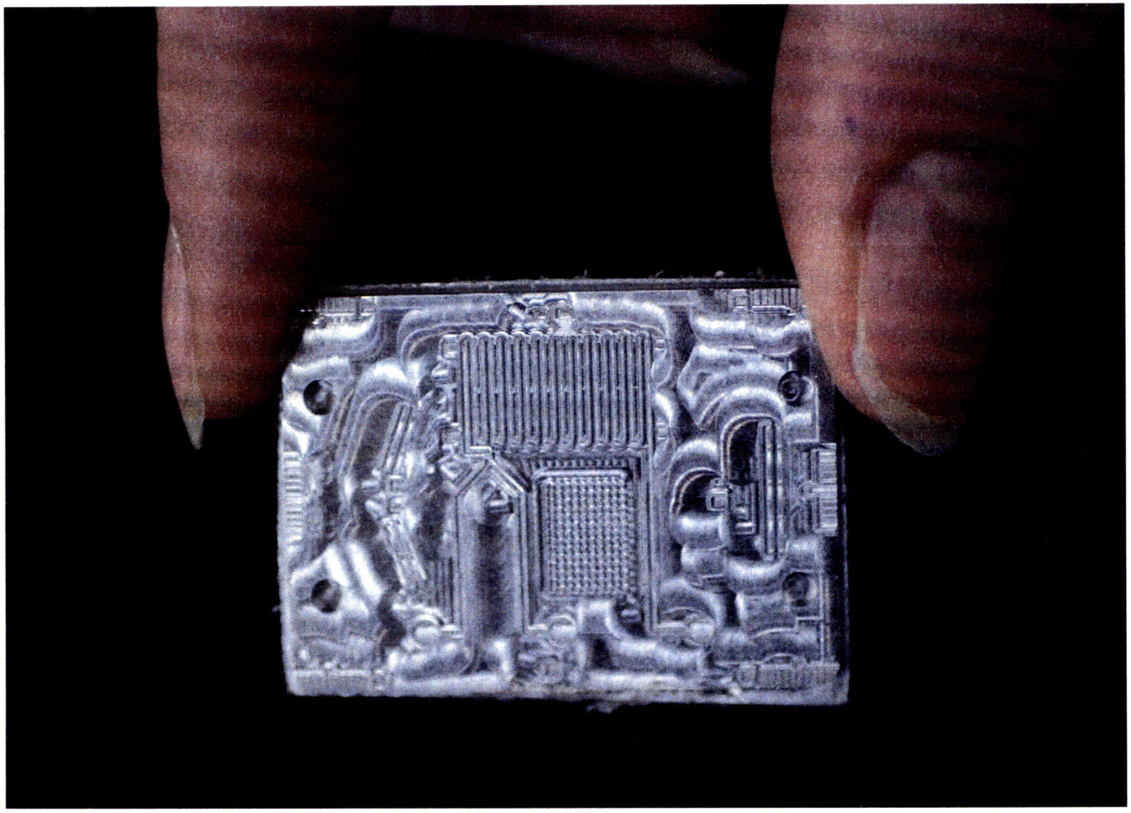

(b) Alternate Micromachined Aluminum Tool

Figure 6-5: Embossing Tools

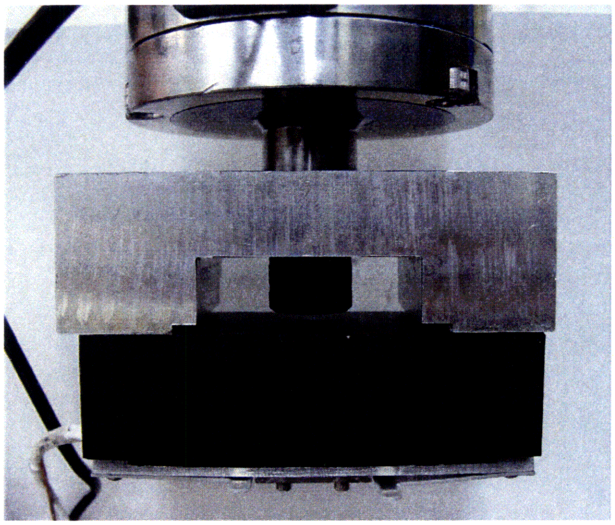

Figure 6-6: Actual Thermal Stack

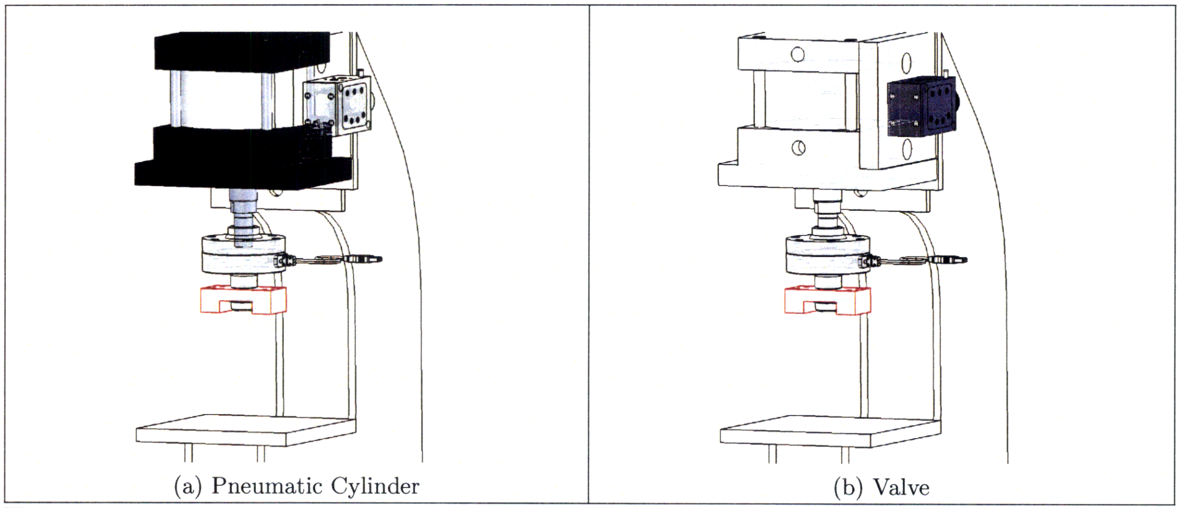

(a) Pneumatic Cylinder

(b) Valve

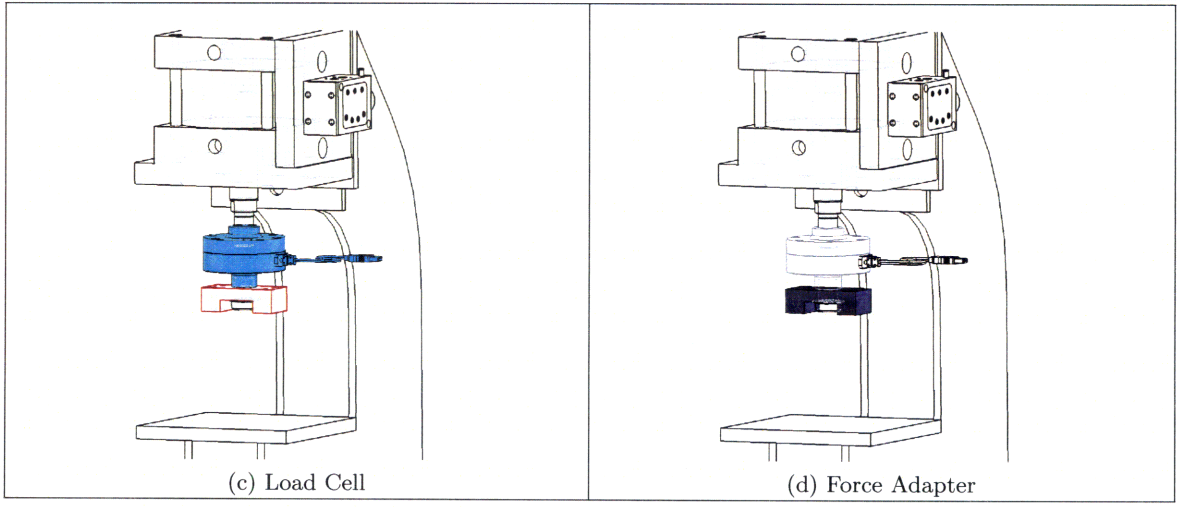

(c) Load Cell

(d) Force Adapter

Figure 6-7: Force Components

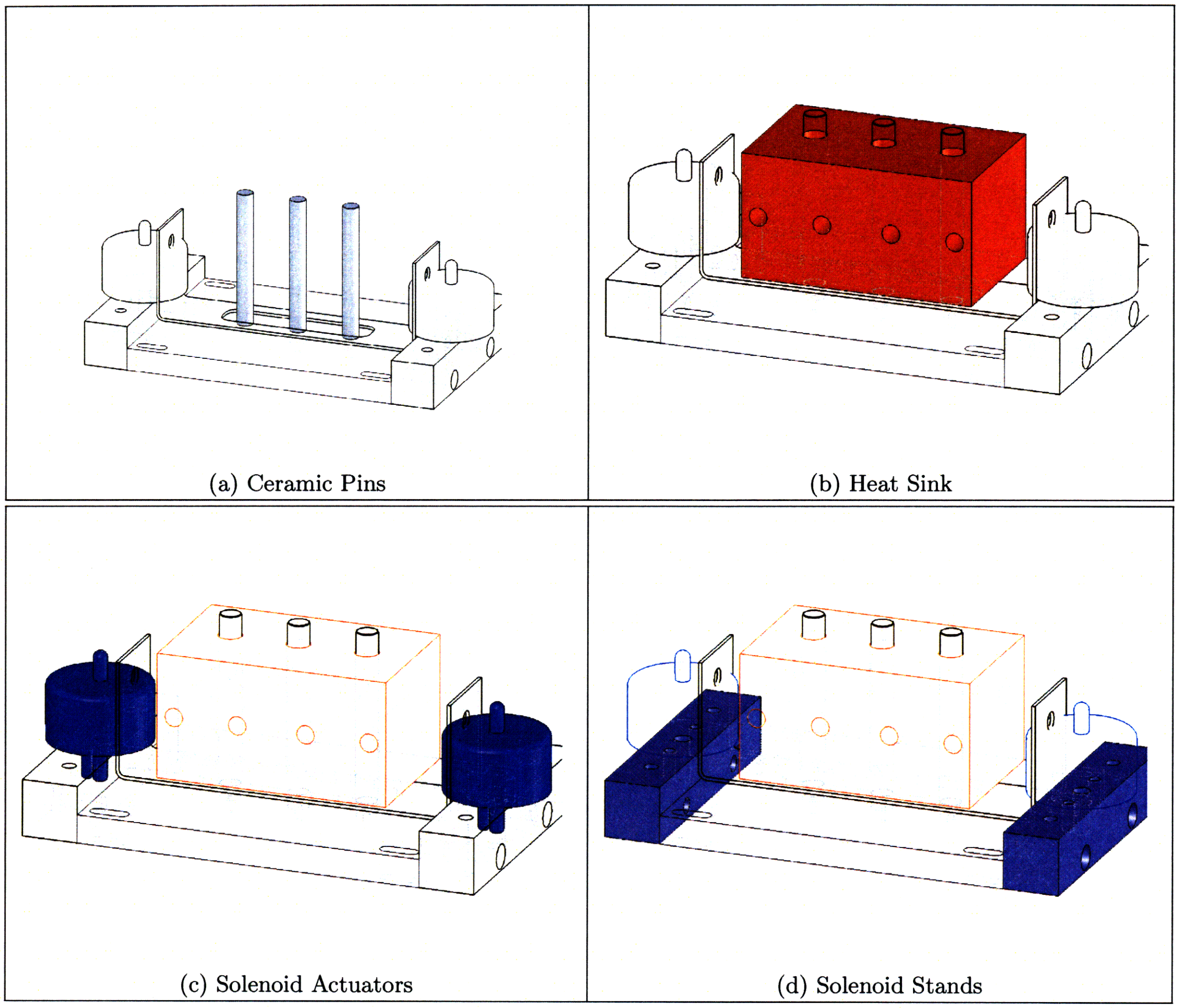
(a) Ceramic Pins

(b) Heat Sink

(c) Solenoid Actuators

(d) Solenoid Stands

Figure 6-8: Cooling Components

for this piece is given in Appendix C, Figure C-5. This piece serves to spread the force as evenly as possible over the thermal stack, rather than being a point load from the pneumatic cylinder rod.

6.4 Cooling Components

The ceramic pins (Figure 6-8) are ultra-high temperature machinable glass-mica ceramic, ordered from McMaster, 3" long and 3/8" in diameter. The pins are drilled with 1/8" carbide bits to accept 1/8" dowel pins for attachment to the steel backing plate on top of the pins. The heat sink is machined from a block of copper roughly sized at 2" x 2.5" x 4" (Figure 6-8), and fly cut and polished on the top surface to provide good contact with the bottom

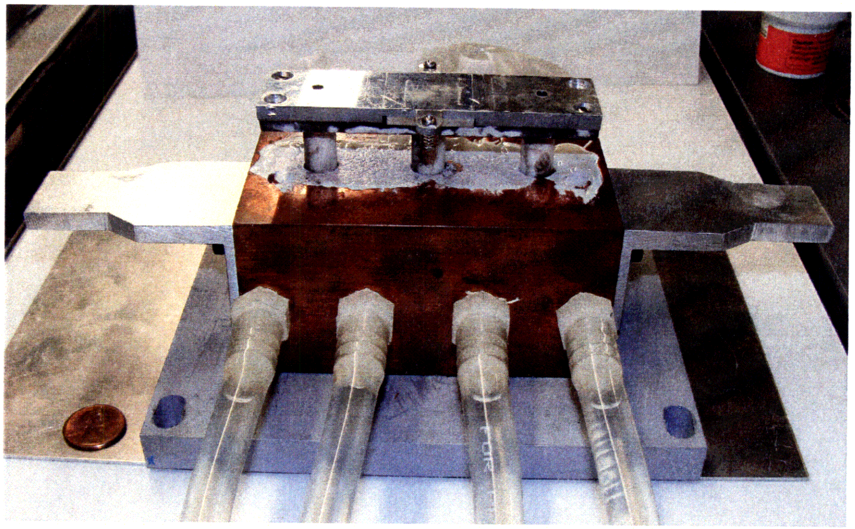

Figure 6-9: Actual Cooling Components

of the thermal stack. The drawing for the heat sink can be found in Appendix C, Figure C-6). The actuator solenoids are Ledex Linear Low-Profile 5EC solenoids part #129415-025, which are mounted on custom aluminum holders to actuate the heat sink, (Figure 6-8). The power supplies that power the solenoids are 45W, 15VDC power supplies from Wolf Automation. The tubing and fittings that bring water through the heat sink are not shown, but the tubing is clear PVC (3/8" ID, 1/2" OD) with standard barbed 3/8" nylon tubing fittings into 1/4" pipe threads in the heat sink.

The assembled cooling components are shown in Figure 6-9.

6.5 Control System Elements

All of the electronic and control system elements are housed in a standard 19" DIN rack. A D-Link DUB-H7 8-port USB hub is used to collect all signals and output them on one USB cable to the laptop. A National Instruments NI USB-6009 Low-Cost Multipurpose DAQ board is used to send and acquire signals between the laptop and the embossing equipment. The Watlow heater controllers communicate using Modbus communications protocol; an EasySync USA dual port industrial USB-RS422/RS485 converter translates signals between the USB hub and the 485 heater communication ports. National Instrument's LabView software is used to program the control software for the hot embossing equipment. (MatLab was considered as the control software of choice, but a myriad of problems prevented seamless communication between MatLab and the Modbus heater controller protocol, and between MatLab and the NI DAQ board.)

6.6 Assembly

All of these components were designed with ease of manufacture low thermal mass of the thermal elements in mind. They were not however designed for assembly, and the bolts (particularly in the thermal stack) are difficult to access and require assembly in a very particular order. Future improvements would include bolts with side access where possible, instead of bolting through the faces of the pieces and trying to maneuver in the small space where the workpiece is inserted. There should also be a better way of adjusting the cylinder on the frame, because as designed it requires two people - one to hold the cylinder in position, and one to tighten the bolts.

The finished equipment is shown in Figure 6-10.

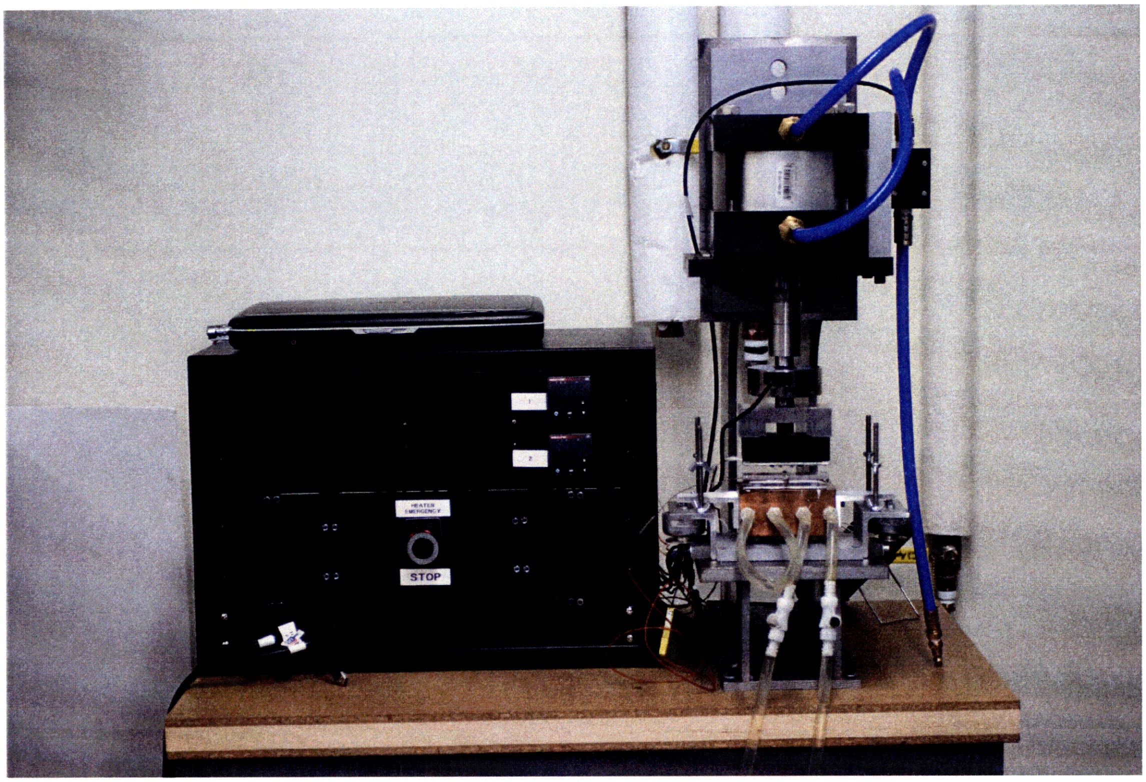
HEATER EMERGENCY
STOP

(a) Front View

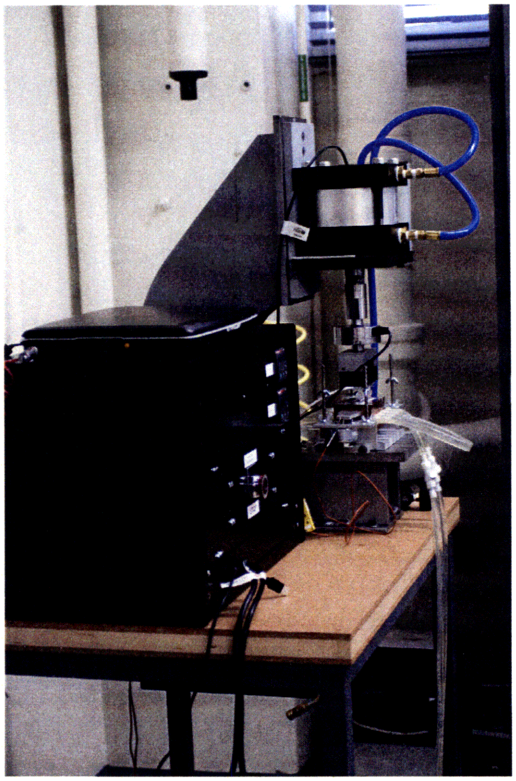

(b) Side View

Figure 6-10: Fabricated Hot Embossing Equipment

Chapter 7

Results and Discussion

To test the completed fabricated equipment, runs of parts were manufactured and then measured. During the manufacture of each part, data was collected through the LabView software control program. Data was collected once every second from six places: the time stamp from the laptop, the stage of execution in the embossing cycle from the LabView control program, the temperature of the top heater from the heater controller, the temperature of the bottom heater, the force setpoint being sent to the valve controller, and the force measured from the load cell. Note that the force setpoint being sent to the valve controller was measured by looping a signal wire coming out of the DAQ output port back into a DAQ input port. Also note that the valve controller received the load cell signal directly (without going through the laptop), meaning that the load cell wires were only run into the DAQ input ports for recording purposes. The two temperatures recorded from the heaters are a proxy for the temperature of the workpiece, because it is not possible to embed a thermocouple into every part formed.

7.1 Microfactory Project

During the summer of 2008, a group of students and faculty involved with the Singapore-MIT Alliance collaborated on a project to create a microfluidic factory, dubbed "µFac" (a shortened form of micro-factory). The goal of this project was to use the polymer manufacturing knowledge of each student to put together a manufacturing assembly line and create microfluidic devices in volumes of at least 100 with a target Takt time of five minutes [19]. This author was a part of this project, and contributed the hot embossing machine to the manufacturing line. The test device chosen for this project was a micromixer pattern on a 25mm by 25mm chip. Although the design workpiece area for the hot embossing equipment was originally 75mm by 25mm, in order to participate in this project some modifications (including slightly different mounting holes in the thermal stack elements, demolding tabs, and a smaller load cell) were made to accommodate the 25x25mm workpiece.

7.2 Iterations A, B, and C

The results in this chapter will be drawn from three runs of parts: PMMA Run A, B, and C. The first full run of parts after the early testing stage is referred to as "PMMA Run A." Parts from this run were produced from blanks created by the laser cutter out of sheet PMMA (polymethylmethacrylate). The laser cutter was used to cut the outline of the blank, input and output holes for functionality of the microfluidic device, an etched letter to denote the part run, and etched sequential numbers to keep track of parts within the run. The data on temperature, force, and channel dimensions from this run is presented in later sections. A sampling of parts from this run were bonded to a cover plate and functionally tested (also as a part of the µFac project, with the help of Eehern Wong) [19]. This functional testing showed that the main source of failure was blocked channels at the input and output port locations. To correct for this, the laser cutter file was modified so that the locations of the input and output ports on the blanks would be directly on top of the embossed channel. The run of parts produced with these slightly modified blanks is referred to as "PMMA Run B." Again, the data from this run is presented later. Functional testing of this run of parts showed that the issue of bonding blocking the input/output ports had been resolved. The next run of parts focused on improving the force control during the embossing cycle. For PMMA Run C, the same blanks were used as for Run B, but a new load cell was used and only one heater provided the heating. A laser cut blank is shown in Figure 7-1, a typical embossed part is shown in Figure 7-2, and a typical embossed part still in the material handling frame is shown in Figure 7-3.

7.3 Temperature Control

The temperature during the embossing cycle was controlled with Watlow heater controllers using thermocouples embedded in the ceramic heaters as feedback. During the testing phase,

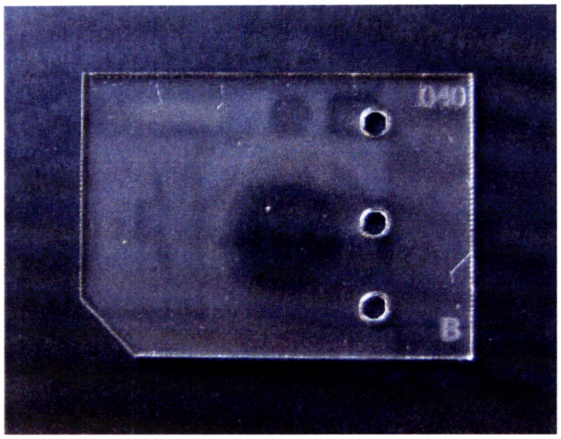

Figure 7-1: Part Blank

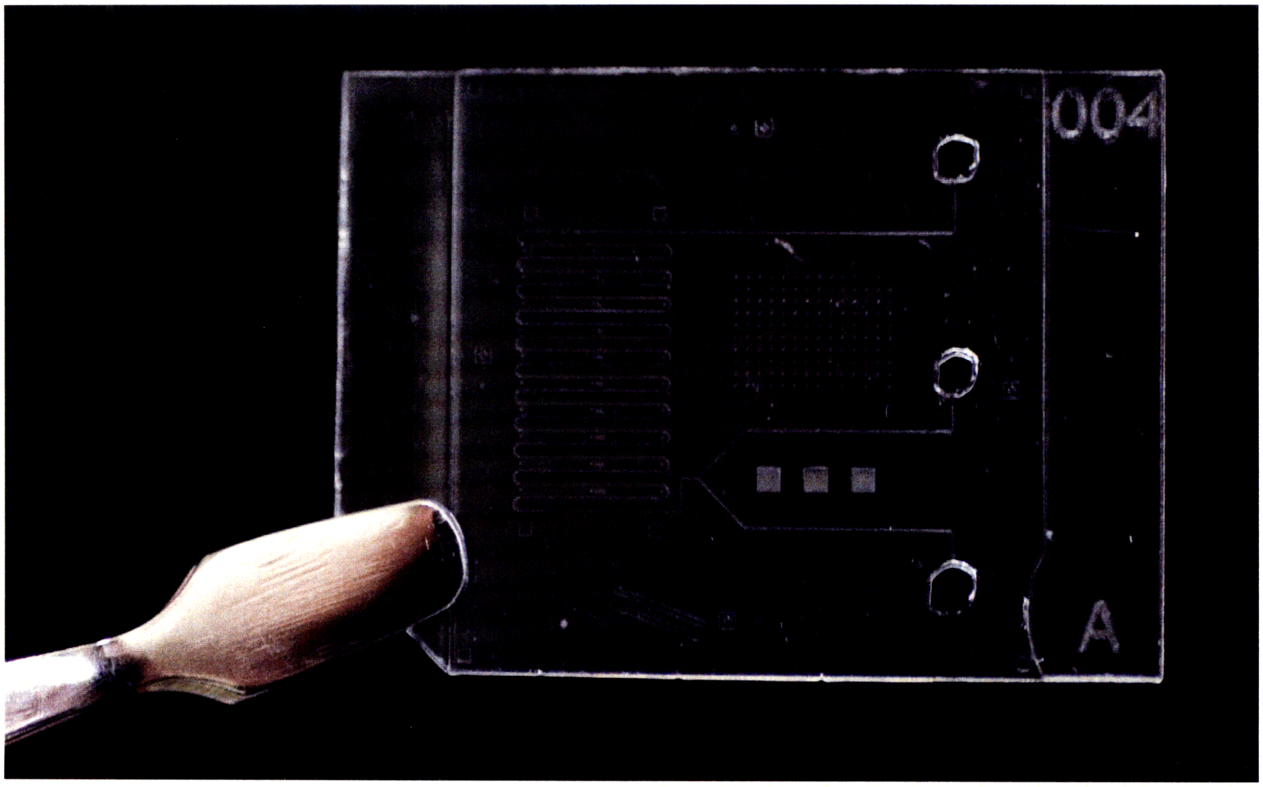

Figure 7-2: Embossed Part

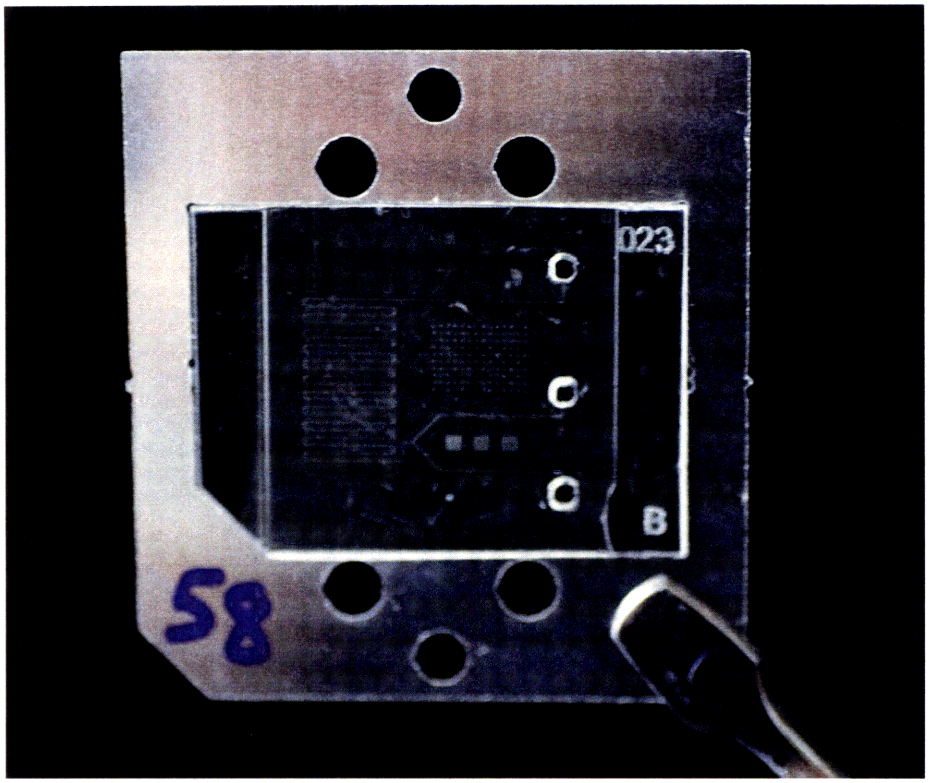

Figure 7-3: Embossed Part with Frame

the power setting of the heaters was restricted out of caution. At full 100% power, when in the "on" position, all current available is allowed to flow through the heaters. If heater power is set to a percentage of full power, when in the "on" position the heater controller cycles between "on" and "off" with a frequency proportional to the percentage of full power requested. This affects the transient initial phase of heating, but not the steady state behaviour. Figure 7-4 shows the increasing initial slope of heater temperature as heater power is increased from 40% of full power to 60% of full power. During part runs A, B, and C, the heater power was unrestricted (100%).

The data collected during each embossing cycle does not show the actual temperature of the workpiece, but only the temperatures of the top and bottom heaters. The workpiece is assumed to be approximately halfway between those values, but that assumption can also be experimentally verified. Figure 7-5 shows the temperature of the heaters during an embossing cycle plotted with the temperature of the workpiece, measured with a thermocouple embedded in the workpiece. The settings for this cycle were 50 seconds of heating at a setpoint of 150C, followed by 60 seconds of cooling with the heaters turned off. The

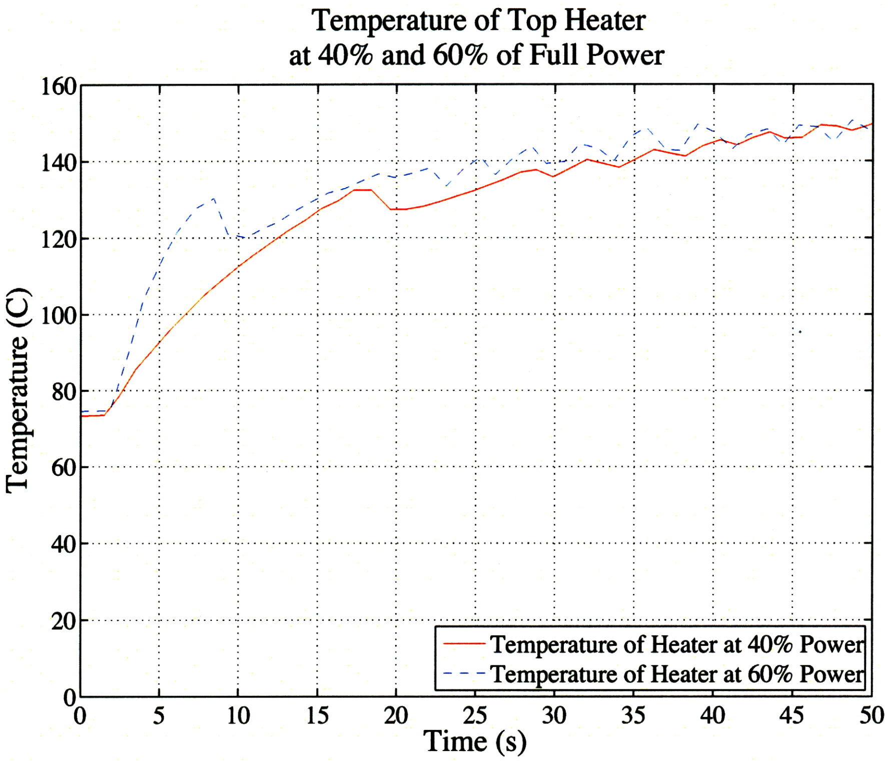

Figure 7-4: Heating Response at Varying Heater Powers

workpiece does not show appreciable heating during time 0-18 seconds, because the tool is moving downwards and the top heater is not in contact with the workpiece. Just before the 20-second mark, the tool makes contact and applies force to the thermal stack. At this point the heaters cool as they come into contact with a workpiece at room temperature, and the workpiece begins to heat up. At 51 seconds, the cooling phase begins. The top heater has just reached the setpoint of 150C, while the bottom heater never reached the setpoint. This is still acceptable because the temperatures of the top heater, bottom heater, and workpiece are all well above the workpiece glass transition temperature. During the cooling phase, the temperature of the workpiece remains roughly halfway between the upper and lower heater temperatures. After 60 seconds of cooling (110 seconds into the embossing cycle) the workpiece has reached a suitable temperature for demolding. The slight uptick in workpiece temperature at the end of the cycle occurs when the demolding step is reached. As the pneumatic cylinder retracts, the workpiece sticks to the heated tool and is carried away from the cooling heat sink until it hits the demolding tabs.

The temperature data collected from PMMA Run A is shown in Figure 7-6 - the tem-

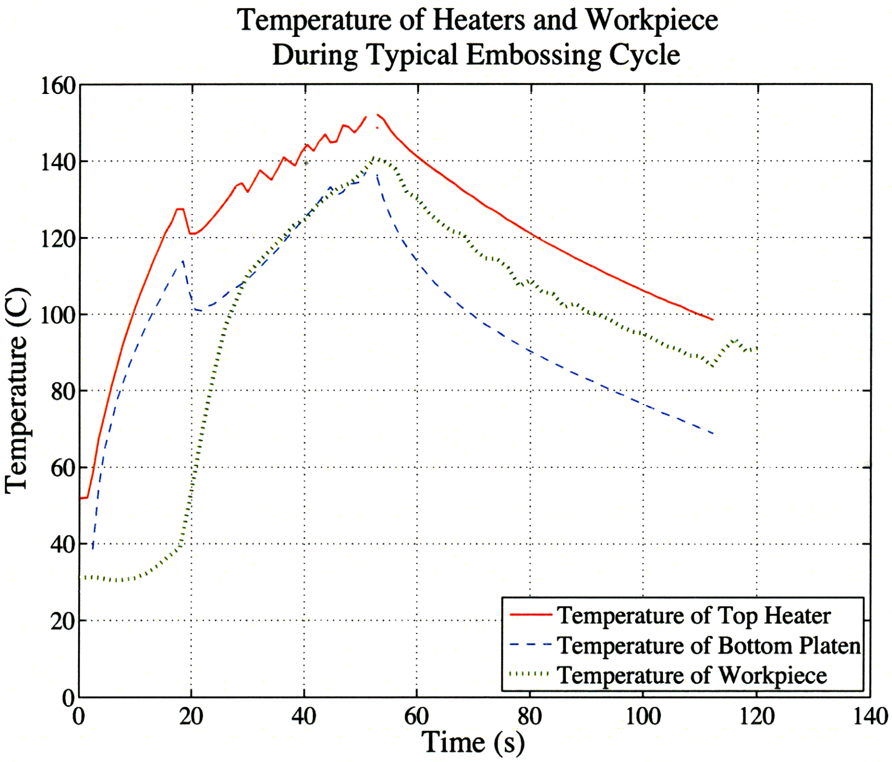

Figure 7-5: Temperature of Heaters and the Workpiece during Embossing Cycle

perature profiles of 18 consecutive parts are plotted on the same graph. The settings for this cycle were 50 seconds of heating at a setpoint of 150C, followed by 60 seconds of cooling with the heaters set at the demolding temperature of 38C. The temperature of the bottom heater is not available for this run, because the first version of the LabView control software only recorded the top heater temperature. This figure shows that the initial heating ramp has a consistent slope, but the ramp profile varies depending on the starting temperature. The starting temperature is based on the demolding temperature of the previous part, and the amount of time that elapses between unloading the previous part and loading the next part. This material handling time is variable because it is done by hand, and not automated. The longer it takes to load the next part, the cooler the starting point for the next run. However, no matter the starting point, all the runs reach a consistent temperature of 150C before the cooling step.

For PMMA Run B, the LabView control software was modified to collect the temperature of the bottom heater as well. The temperature profiles from PMMA Run B are shown in Figure 7-7. The settings for this run were the same as for PMMA Run A: 50 seconds of

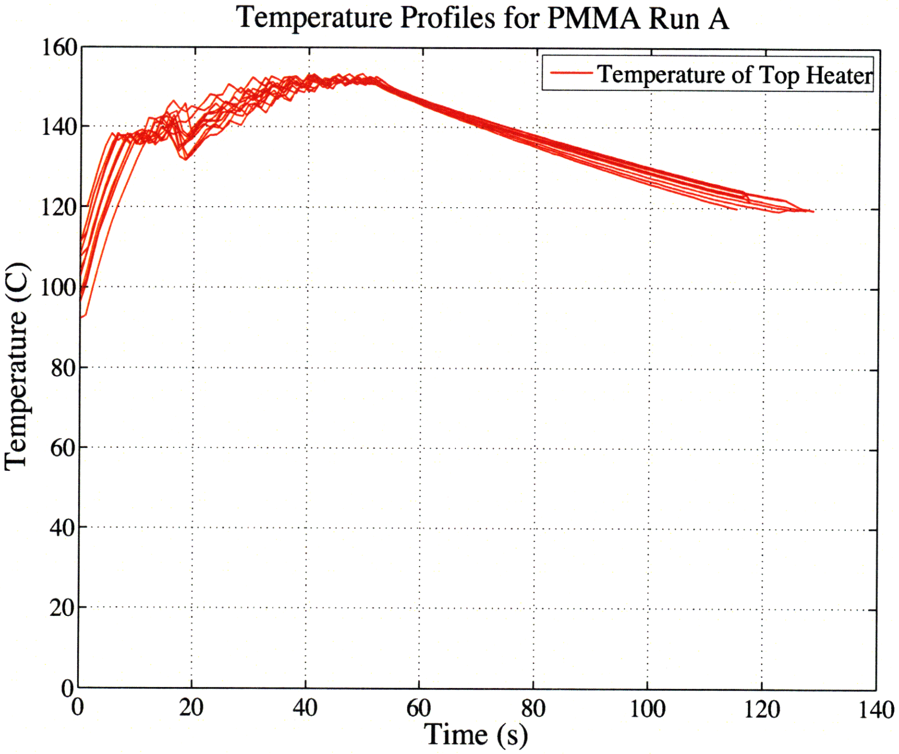

Figure 7-6: Temperature Profiles for PMMA Run A

heating at 150C, then 60 seconds of cooling with the heaters set at the demolding temperature of 38C. The dip that occurs when the pneumatic cylinder contacts and applies force to the thermal stack can be seen around the 20 second mark. The cooling rate of the top heater is not as fast as it was for the embossing cycle shown in Figure 7-5, and this may be because the bottom heater was kept at 38C instead of being turned completely off.

Between Run B and Run C, the load cell in the embossing equipment was changed. Problems related to this and other factors (discussed in force control, Section 7.4) caused the bottom heater to shatter. Because the heater is one of the most expensive components of the equipment, to avoid breaking another one PMMA Run C was completed with only the top heater, and a thermocouple embedded in the bottom platen for recording purposes. To compensate for the lack of a bottom heater, the setpoint for the top heater for PMMA Run C was higher than for A and B. The cycle time for this run was also longer than A and B, because the higher setpoint means that more heat must be removed from the thermal stack. The settings for PMMA Run C were 50 seconds of heating at a setpoint of 170C, followed by 120 seconds of cooling. Figure 7-8 plots the temperature profiles of

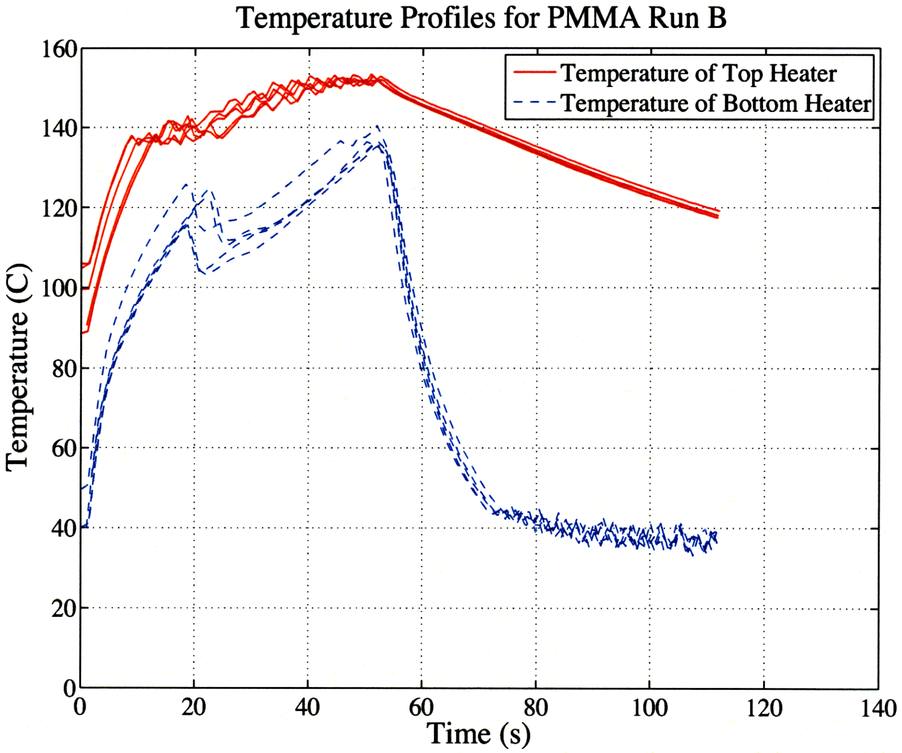

Figure 7-7: Temperature Profiles for PMMA Run B

22 consecutive parts from PMMA Run C. A conscious effort was made during this run to make the loading and unloading times consistent from part to part, so there is less variation in starting temperature for this run than for runs A and B (about a 15 degree spread in initial temperature as opposed to about a 25 degree spread), although some variation from operator error was unavoidable.

7.4 Force control

During each embossing cycle, voltage data is gathered from the load cell in the embossing equipment and voltage data is collected from the setpoint voltage being sent out of the DAQ to the valve controller. For PMMA run A with the first version of the LabView control software, this data was collected 1000 times per second. The calibration curves sent with the load cell were used to transform the voltage data into force data for graphing. The setpoint for the 18 cycles shown in Figure 7-9 is 468 Newtons of compression (compression is shown as a negative value), which would create 0.75 MPa of pressure on a 25mm by 25mm area. This figure shows that the force control is terrible - the actual force generated on the

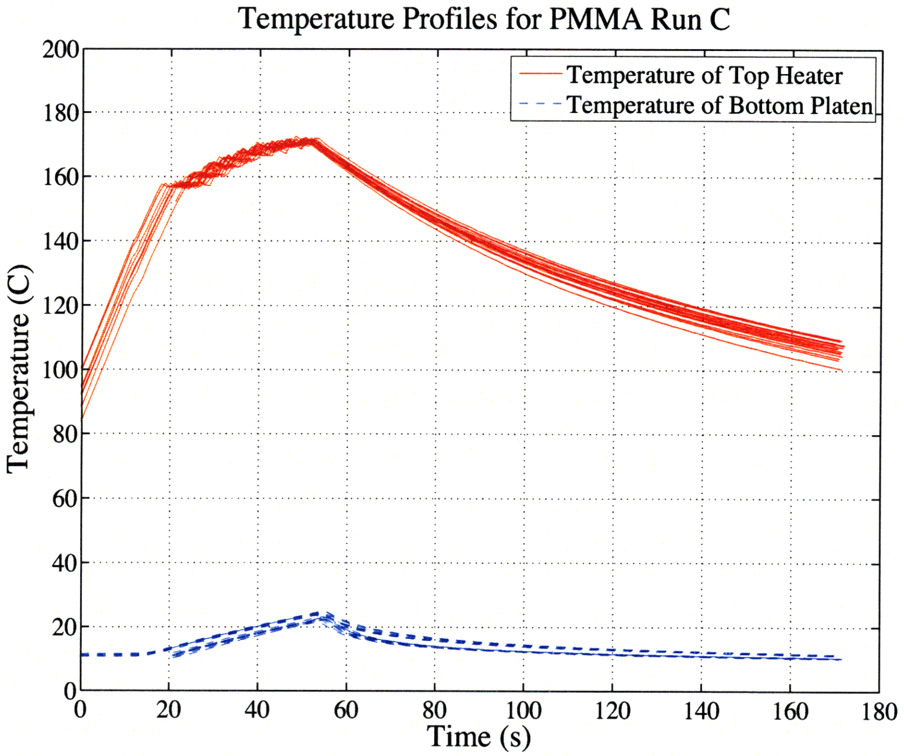

Figure 7-8: Temperature Profiles for PMMA Run C

workpiece does not conform at all to the setpoint. The data is also very noisy. A part of the noise in the load cell signal may be because the changes in voltage are very small for those forces with the large range of the load cell. But that does not explain why the setpoint voltage varies so much - at this point, the source of that noise is unknown. The current configuration with the new load cell has low levels of noise.

There was no change in processing conditions between PMMA Run A and Run B (still a setpoint of -468 N), but the LabView control software was updated to collect data only once per second. The force control graphs shown in Figure 7-10 are no better, in fact slightly worse than Run A regarding adherence to the setpoint. However the profiles of the force up to about a time of 80 seconds look remarkably consistent. A quick calculation shows that the load cell's capacity (+/- 5,000 lbf = +/- 22,241 N) is mismatched for the desired load (105 lbf = 468 N). The voltage change between the setpoint (468 N) and the point at which the valve seems to respond and lower the force (about 2,000 N) is only 0.172 V, which is 3.4% of the 0-5V range of the load cell. It is possible that the behaviour shown is caused by equipment operating at the limits of its capacity, coupled with a very low loop gain through

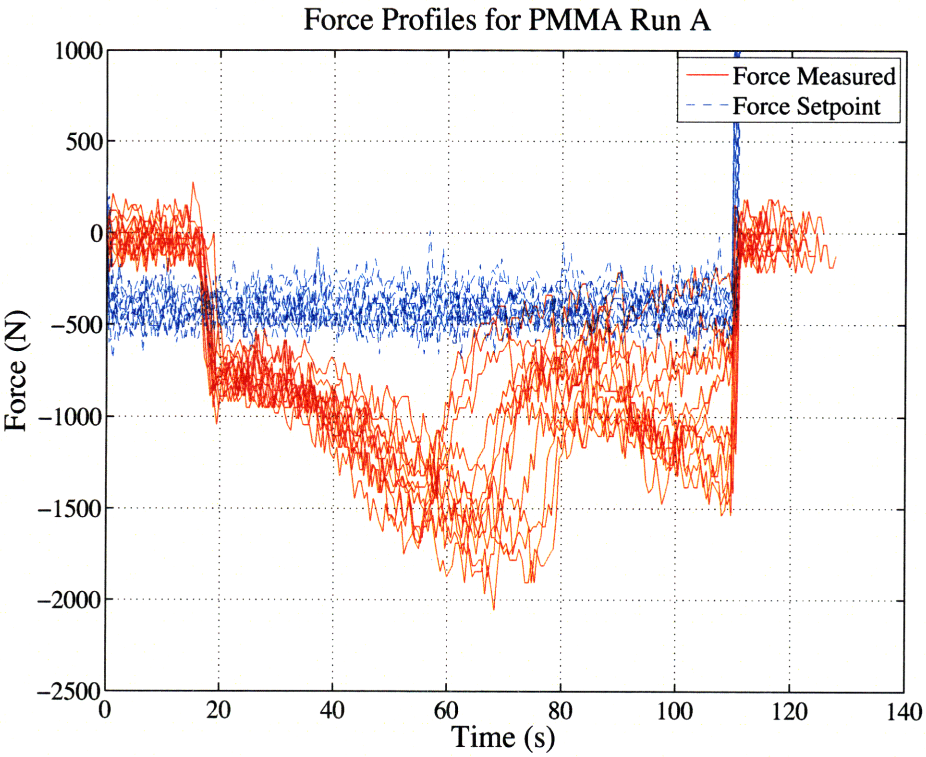

Figure 7-9: Force Profiles for PMMA Run A, Using a +/- 5000 lbf Load Cell

the proportional valve controller.

To test this hypothesis, the +/- 5,000 lbf load cell was replaced with a +/- 500 lbf load cell from the same manufacturer, and the gain was increased using an adjustable pot in the analog proportional valve controller. When this new setup was tested, the result was oscillation (shown in Figure 7-11). Up to the point of contact there is no load, then suddenly the force overshoots the setpoint upon contact with the stiff workpiece material - so the cylinder retracts slightly, loses contact and reads no load. This pattern causes a limit cycle in the system that would continue indefinitely. In the case of this system, the oscillation had the unfortunate consequence of shattering the bottom ceramic heater and the ceramic pins (Figure 7-12). To avoid breaking another expensive heater while still working on understanding the force control dynamics, the bottom heater was not replaced.

Common fixes for contact oscillation include making the system less stiff, using displacement control instead of force control during contact, or using a more sophisticated control system than a simple proportional control. In this hot embossing machine, the stiffness of the system could be changed by heating the plastic to make it softer, but heating the

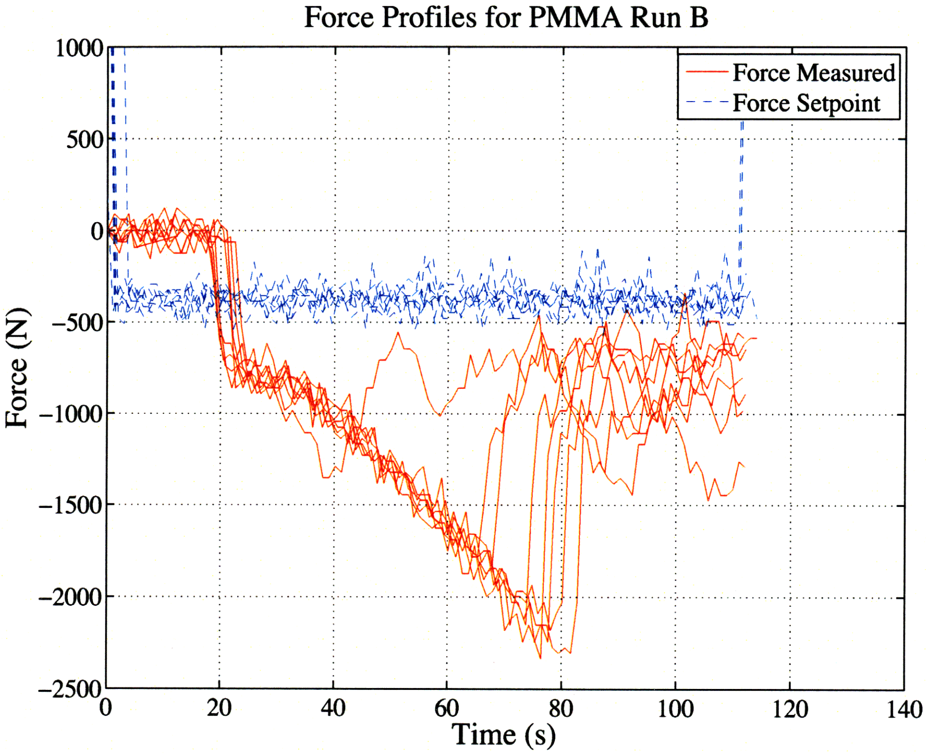

Figure 7-10: Force Profiles for PMMA Run B

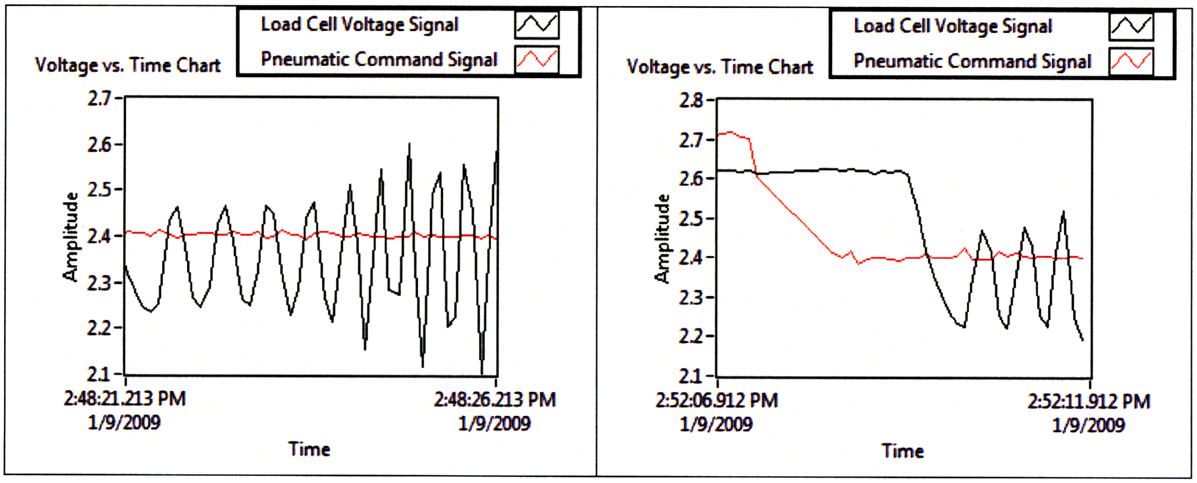

Figure 7-11: Force Profiles with Incorrect Gain Setting, Showing Oscillation

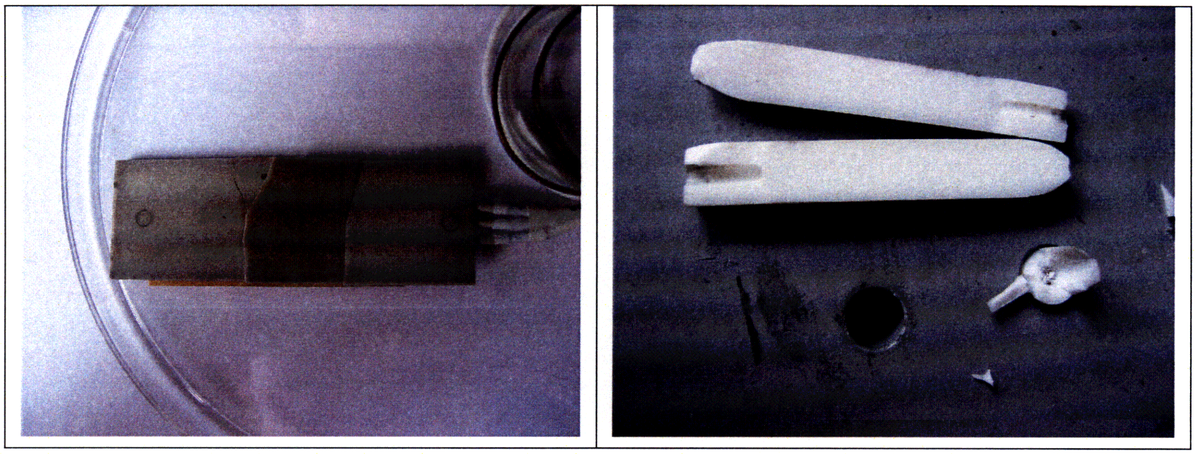

Figure 7-12: Broken Ceramic

plastic to make it softer is difficult without a bottom heater in the embossing system. The workpiece could be preheated, but this is hard to implement without automated material handling. The material needs to be pre-heated enough to compensate for cooling as it is carried from the heating station to the embossing machine, but too much softening deforms the blank by drooping and makes it very difficult to insert the blank into the embossing fixture. The stiffness of the system of the system could also be changed by adding a springy material in the thermal stack, but this would increase the thermal mass and the cycle time. It would also mean that the force being applied to the workpiece would be ambiguous as measured through the load cell. (See Section 7.4.1 for an exploration of how these changes would affect the system.)

The ideal fix would be to use displacement control during contact, but this iteration of embossing equipment was not designed with displacement sensing (which is intended for the next generation). Using a more sophisticated control system would also require moving the control system from outside hardware in the proportional controller to a control system implemented through LabView software, which is a large step also reserved for the next generation.

For the current configuration the solution to the contact limit cycle was to simply turn down the proportional gain until the system became stable. Figure 7-13 shows the force data collected over 22 parts in PMMA Run C, with the new load cell with low gain. The setpoint for this run was -968 N, which corresponds to a 1.5 MPa pressure applied to the workpiece. The low gain causes transient overshoot at the beginning of the cycle at about

Parameter	Value
Step Input	1
Gain	.01
Air Spring	1000 N/m
Mass	5 kg
Damper	100 $N/(m/s)$
Hard Stop Upper Bound	.01 m
Contact Stiffness at Upper Bound	1.55e+02 N/m
Contact Damping at Upper Bound	75 or 300 $N/(m/s)$

Table 7.1: Simulink Parameters

the 10 second mark when the cylinder comes into contact with the thermal stack, because the system is slow to respond (as seen in Sub-Figure a). To try and correct this, a smaller setpoint of -200 N was used until the cylinder made contact. The smaller setpoint (and lower error) meant that the cylinder traveled slower as it came into contact with the thermal stack, so the overshoot was smaller. However (as seen in Sub-Figure b) the change from -200 N setpoint to -968 N setpoint still caused the same magnitude of overshoot.

It is possible that a shaped setpoint, such as an S-curve, could alleviate the transient overshoot. However that would not affect the steady-state behaviour. The steady state behaviour is better than seen during Runs A and B (only varying 600 N off of the setpoint, instead of varying as much as 2000 N off of the setpoint) but it is still not acceptable. And more oddly, the profiles are not consistent. This could be because of the low gain, or it could be because of unanticipated dynamics in the valve.

7.4.1 Simulink Model of Force Control System

To understand the response of the system under force feedback proportional control, the pneumatic cylinder and workpiece were modeled in MatLab's Simulink environment. The simulated system is shown in Figure 7-14. Under the conditions given in Table 7.1, the response of the system is seen in Figure 7-15. This response is highly dependent on the stiffness and damping of the workpiece (in the Simulink model this is the hard stop). If the damping is modified, as seen in Figure 7-15, the system can be well-behaved.

There are several possible solutions for the spike in force on contact that causes the oscillation. One, as shown in Figure 7-15, would be to change the damping of the workpiece - but the damping is a function of the workpiece material properties. Other solutions might

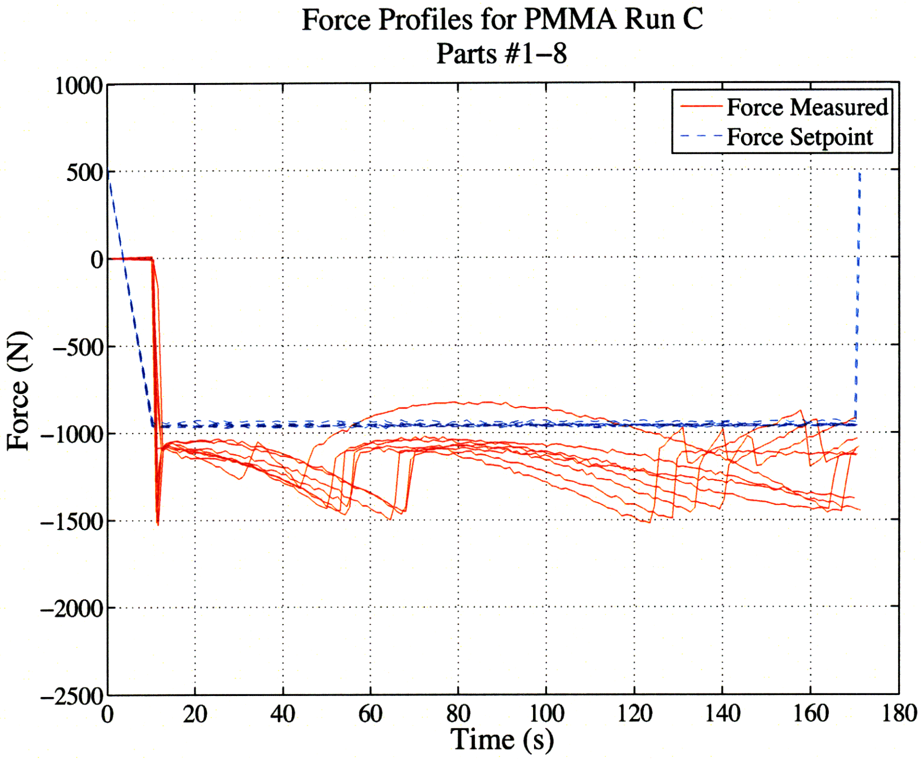

(a) Force Profiles for PMMA Run C Parts 1-8

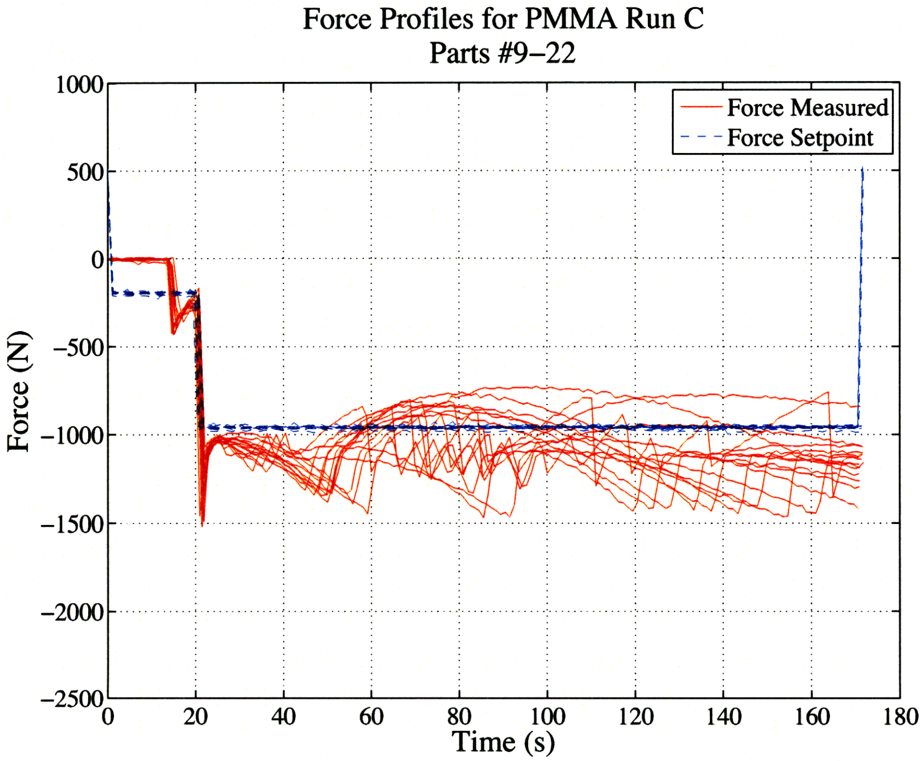

(b) Force Profiles for PMMA Run C Parts 9-22

Figure 7-13: Force Profiles for PMMA Run C

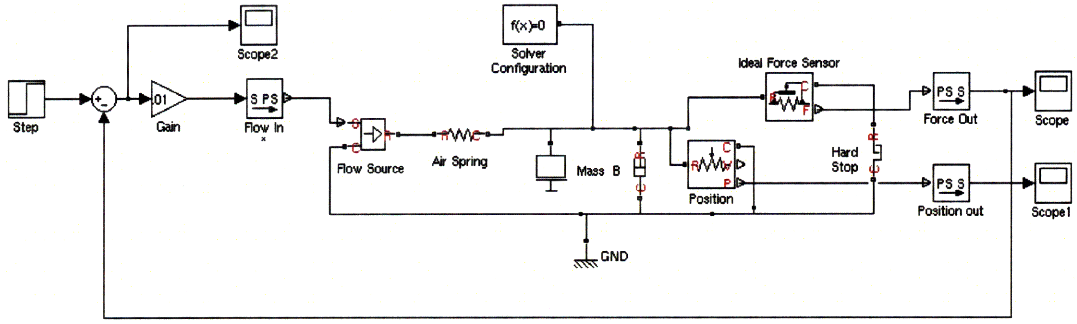
Step
Scope2
Gain
Flow In
f(x)=0
Solver
Configuration
Flow Source
Air Spring
Mass B
Ideal Force Sensor
Position
Hard
Stop
PS S
Force Out
Position out
Scope
Scope1
GND

Figure 7-14: Simulink Model of Embossing System in Force Feedback

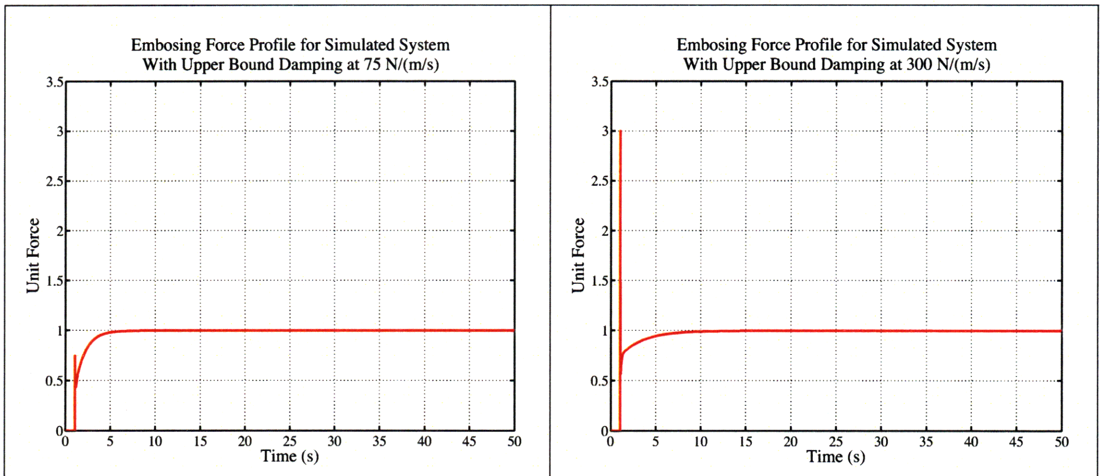
Embosing Force Profile for Simulated System
With Upper Bound Damping at 75 N/(m/s)

Embosing Force Profile for Simulated System
With Upper Bound Damping at 300 N/(m/s)

(a) Force Profile with Damping at 75 N/(m/s)

(b) Force Profile with Damping at 300 N/(m/s)

Figure 7-15: Simulink Force Response Graph

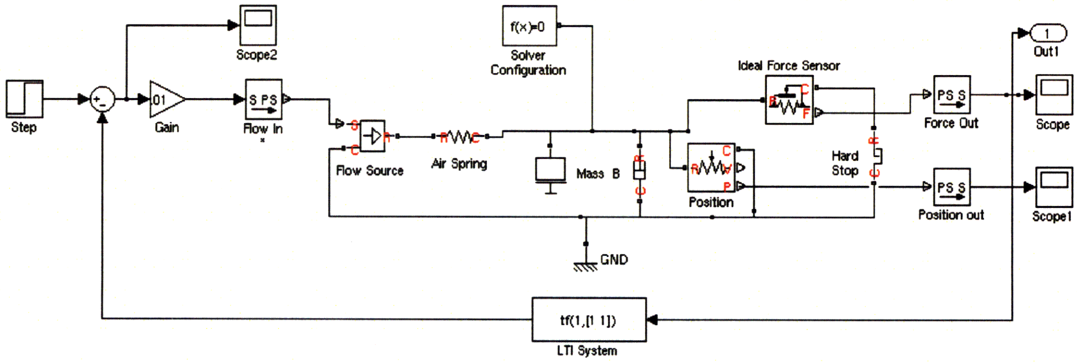
Step
Scope2
Gain
Flow In
f(x)=0
Solver
Configuration
Flow Source
Air Spring
Mass B
Ideal Force Sensor
Position
Hard
Stop
Out1
PS S
Force Out
Position out
Scope
Scope1
GND
tf(1,[1 1])
LTI System

Figure 7-16: Simulink Model of Embossing System in Force Feedback with Filter

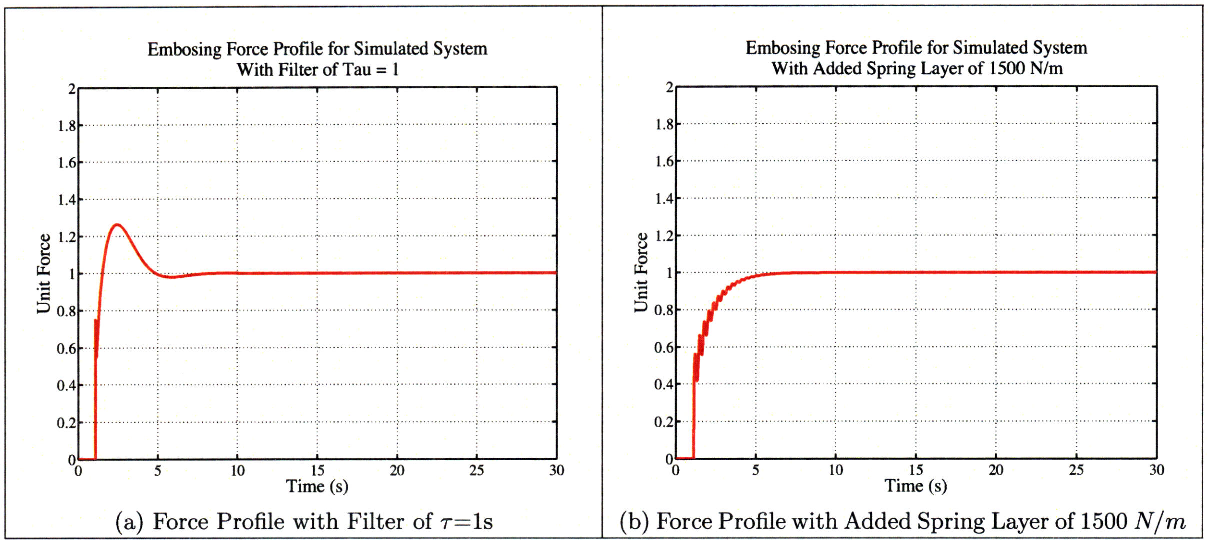

(a) Force Profile with Filter of τ=1s

(b) Force Profile with Added Spring Layer of 1500 N/m

Figure 7-17: Simulink Force Response Graph with Filter or with Added Spring Layer

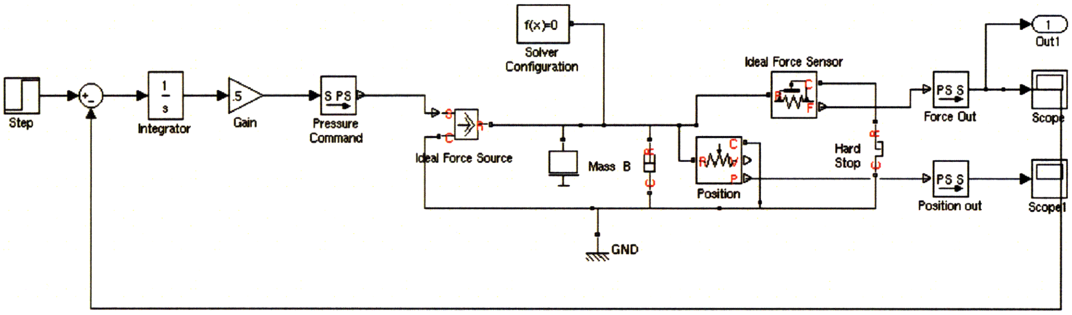
f(x)=0
Solver Configuration
1
Out1
Ideal Force Sensor
Step
Integrator
Gain
Pressure Command
S PS
Ideal Force Source
Mass B
Position
Hard Stop
PS S
Force Out
Scope
PS S
Position out
Scope1
GND

Figure 7-18: Simulink Model of Embossing System with Pressure Source

be to add a filter in the control system to reduce the response to the spike (Figure 7-16) to prevent the tool from leaving contact with the workpiece, or to add a spring layer into the stack as shown in Figure 7-17 (although adding a spring layer would increase the thermal mass). Yet another solution might be to use a pressure control source instead of a flow control source, which is shown in Figure 7-18. The response of a system with a pressure control valve instead of a flow control valve is shown in Figure 7-19.

After running these simulations, an air pressure regulator was added in front of the pneumatic valve and cylinder to limit the pressure available to the system. The air pressure was set to a value calculated using the area of the cylinder to predict the pressure needed for the force setpoint. Then the valve was commanded to full open during the embossing cycle, essentially making an open-loop system. The force response profiles for three consecutive

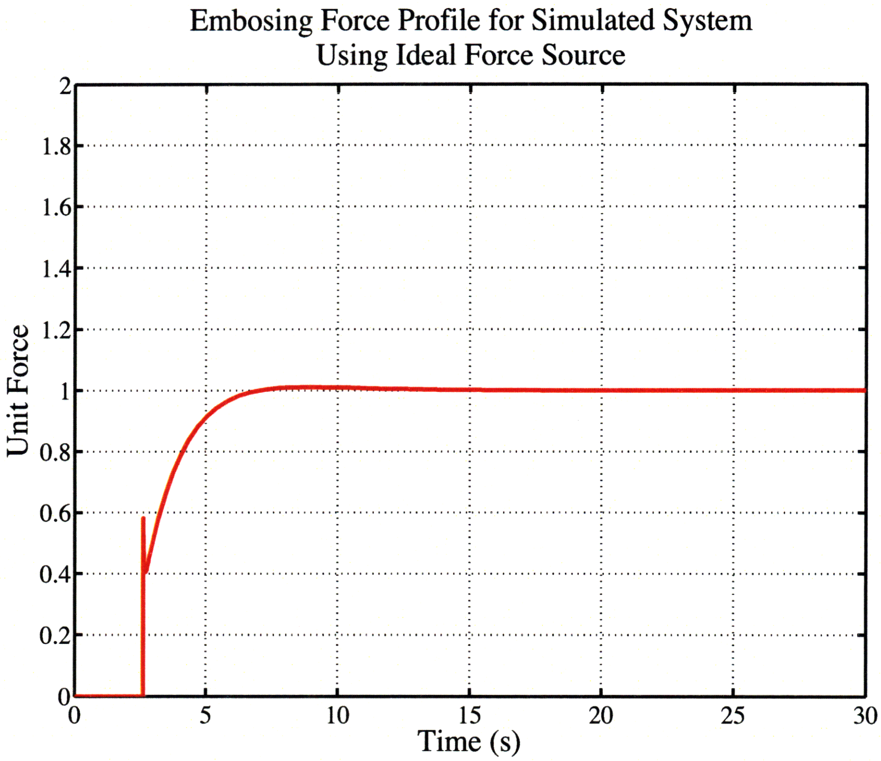

Figure 7-19: Simulink Force Response Graph with Pressure Control Valve

parts run with this open-loop pressure limited system is shown in Figure 7-20. This confirms that the current valve and control system is only making things worse - the system performance is better in an open-loop configuration. This also confirms that a pressure control valve is a better choice for the next generation of hot embossing equipment.

7.5 Channel Variability Analysis

The temperature and force data collected during PMMA Runs A, B, and C show how the equipment was behaving, but from a manufacturing point of view the accuracy (or variability) of those factors aren't the true measure of the process - for production equipment, what matters is the quality of the parts produced. The 18 parts shown in the Run A plots and the 22 parts from the PMMA Run C plots were measured with a Zygo NewView 5000 optical profilometer to determine the dimensions of the embossed channels. Parts from Run B were not measured, because the processing parameters and equipment were not changed (only the location of the input-output ports).

The measurement system was characterized first to determine the variability inherent in

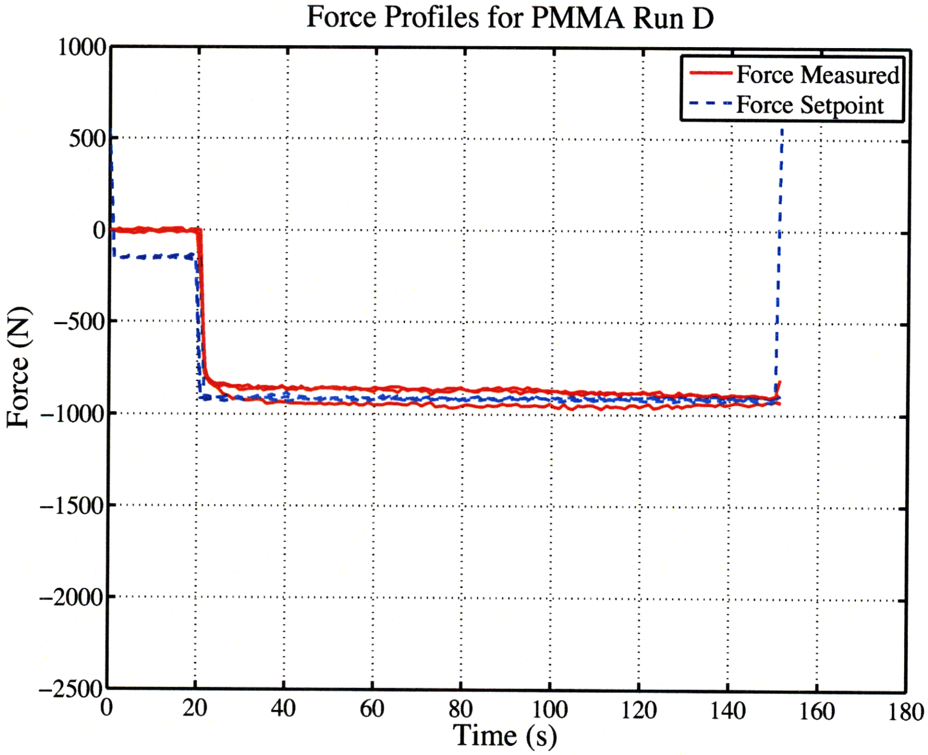

Figure 7-20: Force Profiles for PMMA Run C

the measurements. One channel on one part was scanned 10 times by the Zygo profilometer to determine the Zygo variability. Then the same channel on the same part was scanned 10 times while being taken in and out of the instrument after every scan, to characterize the variation in the fixturing. These scans were analyzed using a MatLab script by Aaron Mazzeo that extracts the height and width of the channel [29]. The width is always expected to have more variation, because the profilometer does not capture vertical walls, leaving gaps in the data when trying to determine width. Table 7.2 shows that the minimum variation we can expect in our measurements is about 0.2 micrometers. The standard deviation in the width dimension is actually less than the deviation in the height direction, which is unexpected, but all of the standard deviation are sub-micron.

All parts in this section were measured at three sites, shown in Figure 7-21. The tool used to produce all the parts is a bulk metallic glass (BMG) tool provided by David Henann with a micromixer design with two inputs and two outputs [22]. The three sites to measure were chosen as a channel from the left-most mixing loop, the center channel, and a channel from the right-most mixing loop.

PMMA Run A	Height (microns)		Width (microns)	
	Mean	Std. Dev.	Mean	Std. Dev
10 Scan Repeatability	38.8	0.0649	54.218	0.0200
10 Scan Repeatability with Part Reloading	38.89	0.195	54.243	0.0658

Table 7.2: Variability of Measurement System

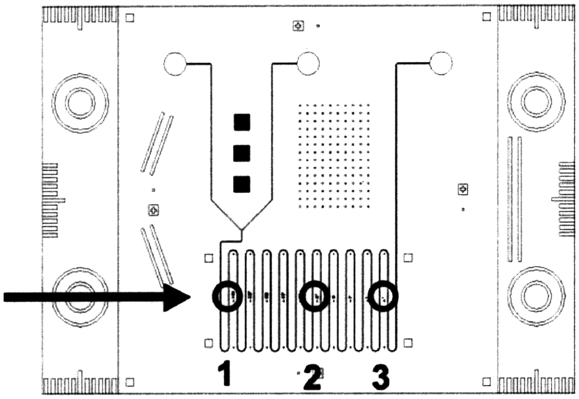

Figure 7-21: Measurement Sites on Micromixer Pattern

These sites were first measured on the actual tool to determine the true height and width. Table 7.3 shows the actual heights and width of the BMG tool at the three locations. The designed height was 40 micrometers, and the designed width was 50 micrometers.

Using a MatLab script created by Aaron Mazzeo [29], 18 parts from PMMA Run A were analyzed at those three sites and plotted on run charts for height and width of the channel at each site. Figures 7-22, 7-23, and 7-24 show the data from the analysis. Note that the height of part 6 was found to be significantly lower than the heights for rest of the run, for all three channels measured. It is highly probable that this part represents an outlier, and that some abnormality or operator error occurred during the embossing process, so this

	Height (μm)	Width (μm)
	Mean	Mean
BMG Site 2 - Channel 10	39.72	52.306
BMG Site 4 - Channel 5	39.65	51.948
BMG Site 3 - Channel 1	39.78	53.971

Table 7.3: Actual Measurement of BMG Tool used for all PMMA Runs

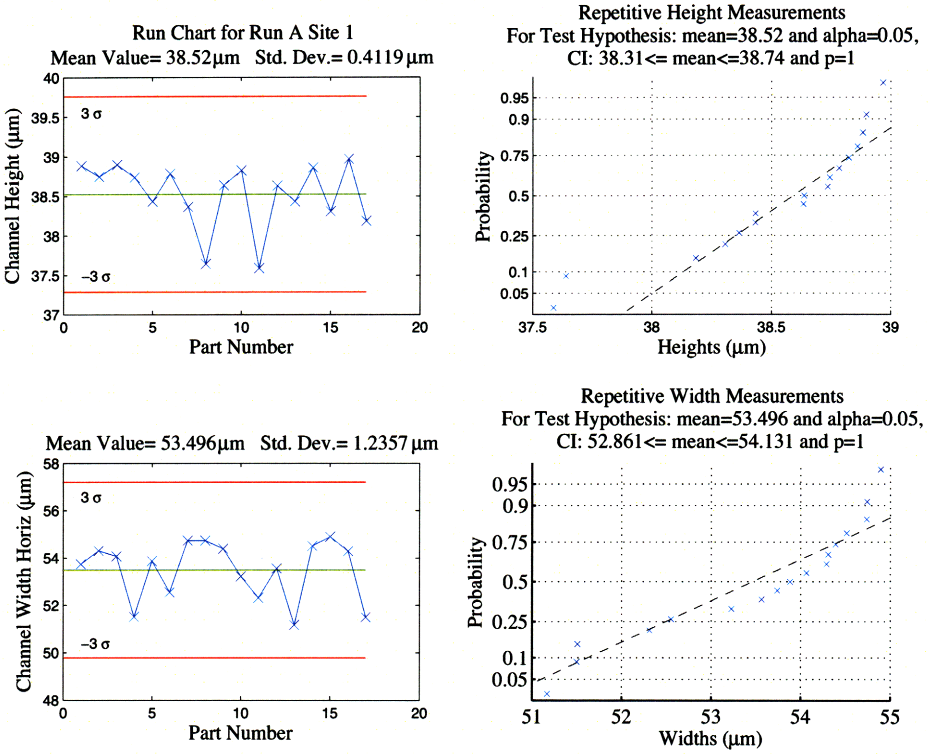

Figure 7-22: Run A Site 1 Height and Width

part is not included on the run charts or in the statistical analysis. There are other possible outliers (for instance the height of the last part of Run A Site 2 shown in Figure 7-23) but to be conservative those data points were included in the statistical analysis. The original data and run charts for all parts are included in Appendix B, and Table 7.4 reports the statistical data both with and without the outlying data points.

The same analysis was performed on 22 parts from PMMA Run C. Figures 7-25, 7-26, and 7-27 show the run charts and normal plots of the Run C measurements. There are again possible outliers in Figure 7-26 (for instance parts 8 and 12), but the standard deviation is already below 0.1 μm (nearly equal to the measurement variation), and it is possible those outliers are measurement artifacts. To be conservative, those possible outlying data points were included in the statistical analysis. However the data showed a clear outlier in the height of part 17 for Run C Site 3 and for the height of part 15 of Run C Site 1; these data points were assumed to be caused by some abnormality or operator error, and were removed from the run chart and from the data set for statistical purposes. The original data and run charts for all parts are included in Appendix B, and Table 7.5 summarizes the statistical

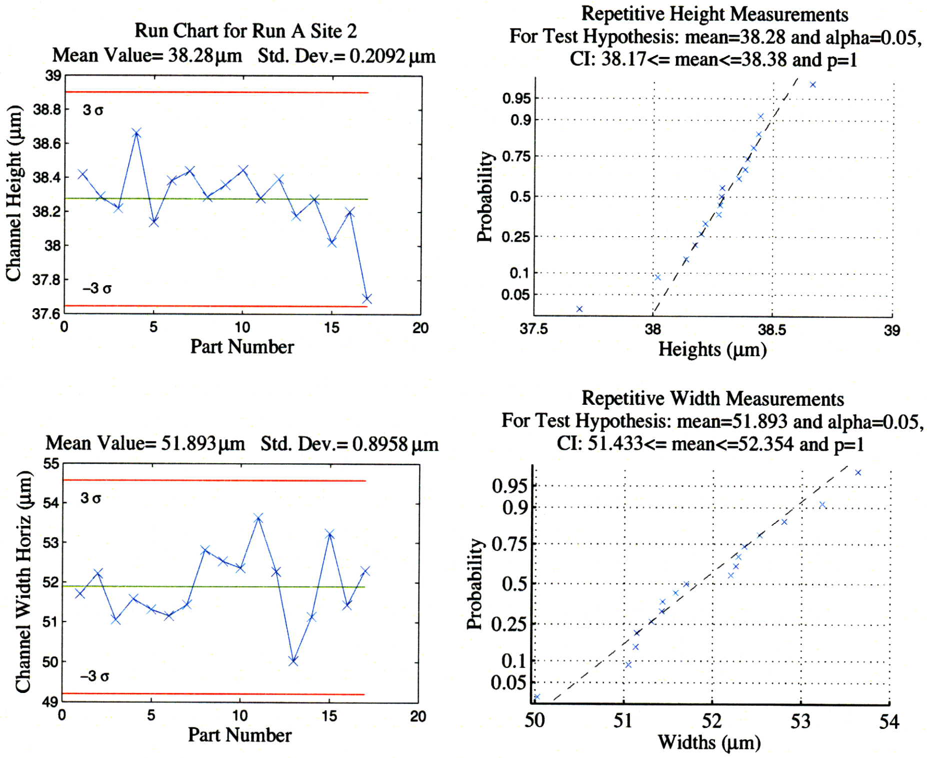

Figure 7-23: Run A Site 2 Height and Width

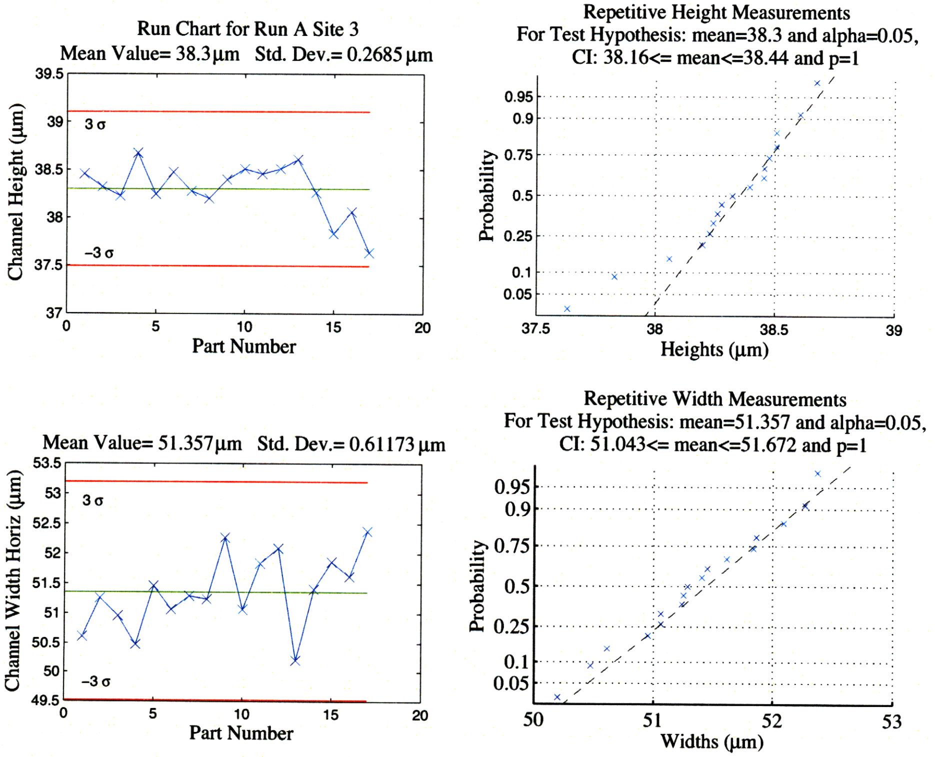

Figure 7-24: Run A Site 3 Height and Width

	Height (µm)		Width (µm)	
	Mean	Std. Dev.	Mean	Std. Dev
Site 1	38.44	0.538	53.56	1.227
Site 1 Without Outlier	38.52	0.411	53.50	1.236
Site 2	38.24	0.241	51.90	0.869
Site 2 Without Outlier	38.28	0.209	51.89	0.896
Site 3	38.24	0.375	51.37	0.595
Site 3 Without Outlier	38.30	0.269	51.36	0.612

Table 7.4: Summary of PMMA Run A Height and Width Data

	Height (µm)		Width (µm)	
	Mean	Std. Dev.	Mean	Std. Dev
Site 1	39.10	0.070	49.10	0.321
Site 1 Without Outlier	39.11	0.044	49.10	0.329
Site 2	39.05	0.056	49.70	0.479
Site 3	39.40	0.307	50.35	1.491
Site 3 Without Outlier	39.34	0.067	50.24	1.424

Table 7.5: Summary of PMMA Run C Height and Width Data

data both with and without the outlying data point.

The data that the charts and figures use are included in Appendix B. Figure 7-28 compares the actual height and width measurements of the tool (at three channel locations) with the average and standard deviation of measurements across PMMA Run A and PMMA Run C at the same locations. (One sigma error bars are included on part measurements.) This figure shows that despite extremely poor force control in Run A, and only one heater for Run C, the parts produced are remarkably consistent - acceptable parts can be produced under a wide range of conditions (at least at these feature dimensions). The height measurements of the parts are always slightly shorter than the tool height, which could be caused by under-filling in the polymer (as observed by Wang [33]).

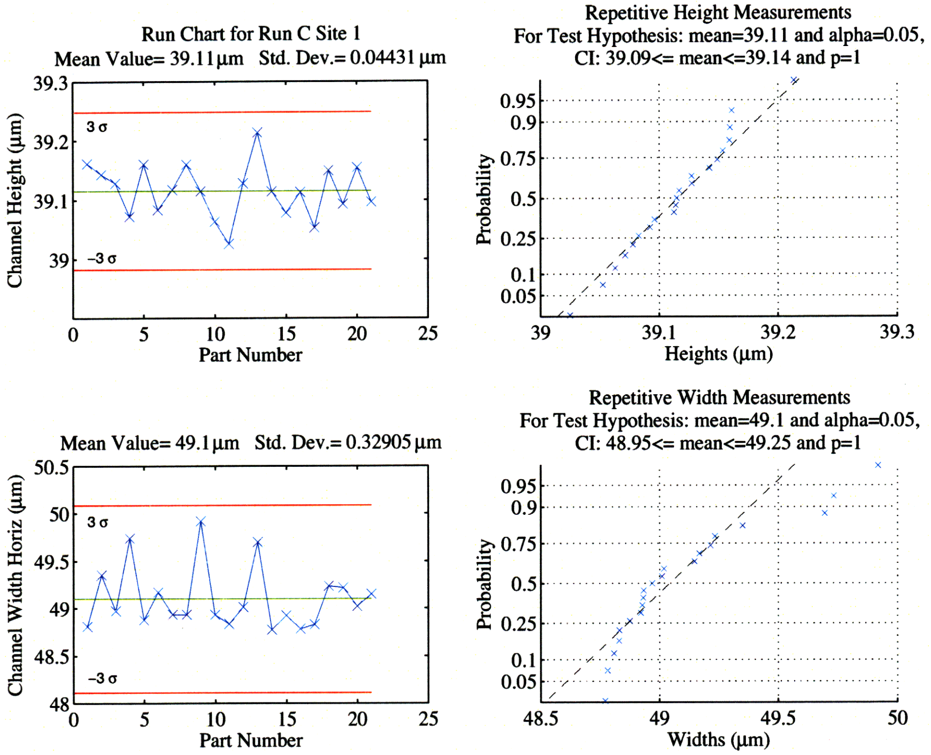

Figure 7-25: Run C Site 1 Height and Width

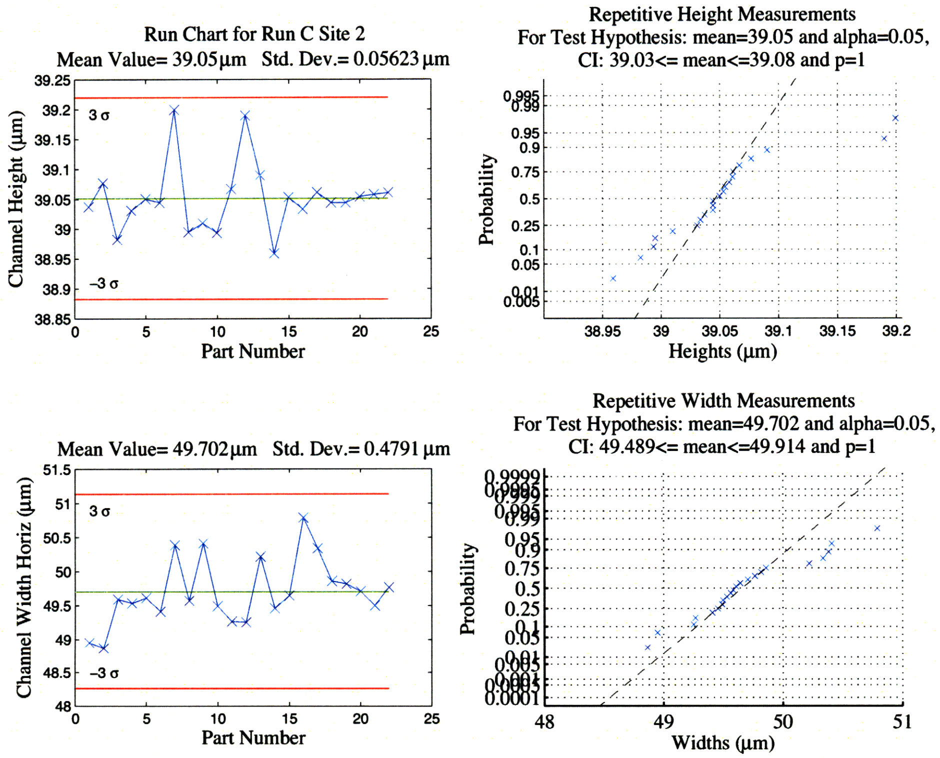

Figure 7-26: Run C Site 2 Height and Width

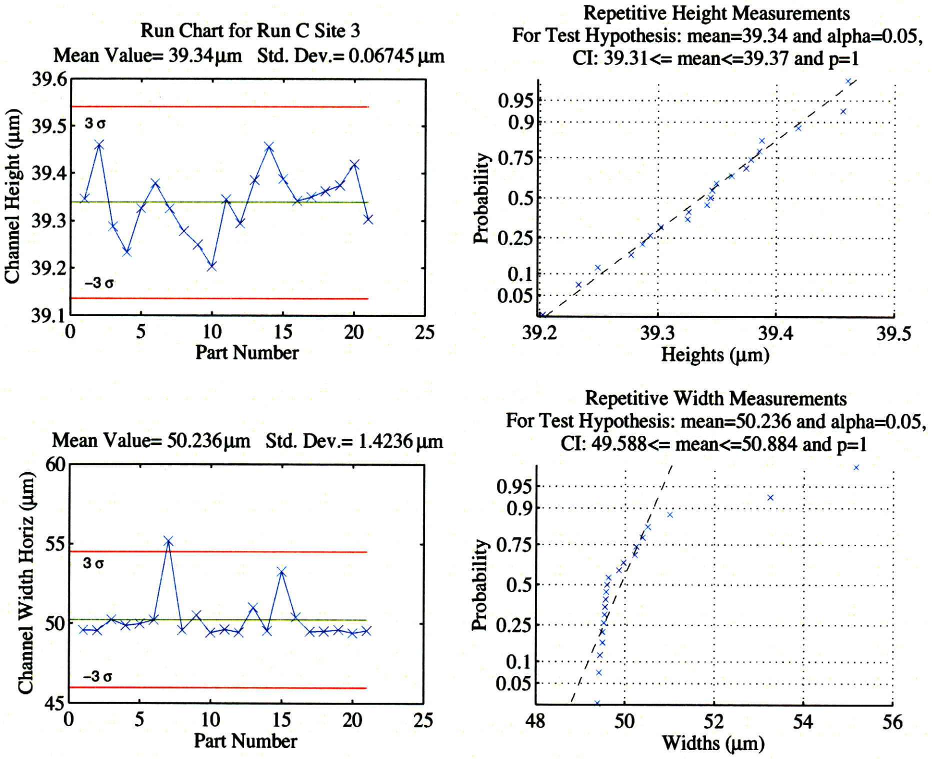

Figure 7-27: Run C Site 3 Height and Width

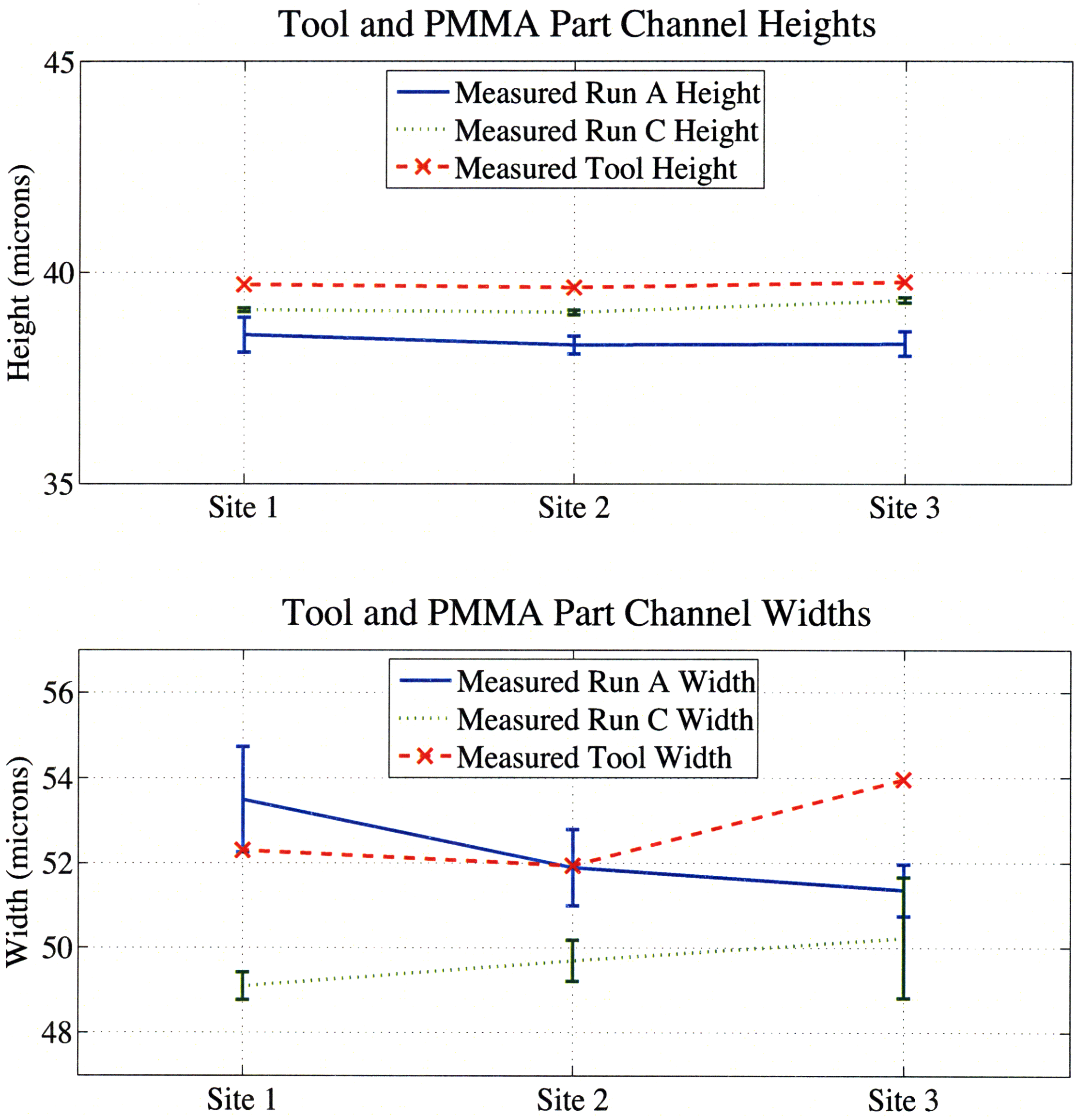

Figure 7-28: Comparison of Tool Dimensions with Average PMMA Part Run Dimensions

Chapter 8

Conclusions

Over the course of this project, equipment for hot embossing in a manufacturing environment was designed, built, and tested. The capital cost for this equipment has been decreased by an order of magnitude (from about \$80k for the previous generation of research embossing equipment, or \$250k and up for commercial hot embossing equipment) to only \$8k. The physical size of the equipment has been reduced from several meters cubed to a benchtop model only 0.2m by 0.75m by 0.75m. The cycle time for each part has been reduced from 5-15 minutes down to 2 minutes. The variability of feature dimensions has been proven to be sub-micron, under a variety of less-than-ideal conditions. These advances have been made through careful decisions to minimize cost and reduce thermal mass, and through innovations in design (most notably using Watlow Ultamic ceramic heaters for heating and a moveable heat sink). The equipment met all of the functional requirements listed in Table 3.3 except for the accuracy in force control. The flaws in the design have been identified, and improvements will be integrated into the next generation. The goal of this project was to have production equipment for microfluidic devices, and in that was a success.

8.1 Future Work

In a next generation of hot embossing equipment, there are several areas to address. The first is the force control, which can be addressed using a pressure control valve rather than a flow control valve and by adding displacement feedback control as well as force feedback control. Pressure control directly relates to force (with an area factor), while flow control adds an integration term, so from a control system perspective pressure control would be preferable. Also, decreasing pressure in the cylinder by venting would not cause the tool to retract, so contact oscillation would not be a problem.

The temperature controllers can be tuned for more optimal performance during the embossing cycle. The material handling should also be addressed - automating the loading and unloading of parts would decrease the variation in the initial starting temperature, and is necessary for a truly production environment. Although the moving heat sink did serve the purpose of reducing wasted heat, the ceramic pins are not very robust and easily break with any misalignment. Using either ceramic-capped steel pins, or a different arrangement of structural support for the thermal stack would make the structure of the equipment more robust. Finally, the equipment can be tested with smaller feature sizes to determine the limits of the capability of the machine, or with a patterned tool on both the top and bottom sides to extend the design to double-sided parts.

Appendix A

Material Properties

Material	**k (W/m-K)**	**C_p (J/kg-C)**	**ρ (kg/m^3)**
PMMA	0.2	1500	1190
Nickel	60.2	460	8880
Copper	385	385	8960
AlN	80	819	3300
Steel	50	486	7830
Aluminum	210	900	2700

Table A.1: Material Properties

Appendix B

Part Height and Width Measurements

Filename	Ave Height	Width Horiz	Width Dist
PMMA Run A Site 1			
pmma092308_005_2	38.883252	53.740259	53.774383
pmma092308_007_2	38.744605	54.312369	54.340709
pmma092308_008_2	38.896935	54.065367	54.107145
pmma092308_012_2	38.735965	51.510389	51.516064
pmma092308_014_2	38.43299	53.88301	53.887045
pmma092308_015_2	36.999588	54.603195	54.603449
pmma092308_020_2	38.783011	52.553428	52.559189
pmma092308_022_2	38.364424	54.743671	54.763925
pmma092308_023_2	37.641123	54.743925	54.867058
pmma092308_024_2	38.636823	54.392607	54.396475
pmma092308_025_2	38.824621	53.227067	53.231771
pmma092308_026_2	37.588002	52.313158	52.340078
pmma092308_027_2	38.63322	53.566182	53.56995
pmma092308_029_2	38.432913	51.173728	51.176591
pmma092308_033_2	38.86091	54.517331	54.548263

Filename	Ave Height	Width Horiz	Width Dist
pmma092308_034_2	38.3054	54.896493	54.899338
pmma092308_035_2	38.967768	54.292517	54.31935
pmma092308_036_2	38.184228	51.502231	51.547825
PMMA Run A Site 2			
Filename	Ave Height	Width Horiz	Width Dist
pmma092308_005_4	38.417587	51.706337	51.785389
pmma092308_007_4	38.288895	52.211235	52.308868
pmma092308_008_4	38.219286	51.05871	51.101168
pmma092308_012_4	38.663562	51.584573	51.593954
pmma092308_014_4	38.13918	51.313708	51.340044
pmma092308_015_4	37.72543	51.979569	51.993858
pmma092308_020_4	38.382873	51.150004	51.161059
pmma092308_022_4	38.43896	51.442773	51.503989
pmma092308_023_4	38.286348	52.807331	52.856279
pmma092308_024_4	38.357428	52.529801	52.554583
pmma092308_025_4	38.445698	52.357838	52.401619
pmma092308_026_4	38.280148	53.633509	53.656085
pmma092308_027_4	38.392854	52.263603	52.288727
pmma092308_029_4	38.176022	50.032257	50.044202
pmma092308_033_4	38.274419	51.138081	51.182009
pmma092308_034_4	38.020576	53.232868	53.317474
pmma092308_035_4	38.201187	51.432954	51.473457
pmma092308_036_4	37.693014	52.290834	52.322462
PMMA Run A Site 3			
Filename	Ave Height	Width Horiz	Width Dist
pmma092308_005_3	38.455629	50.614002	50.614502

Filename	Ave Height	Width Horiz	Width Dist
pmma092308_007_3	38.323918	51.254242	51.263688
pmma092308_008_3	38.226777	50.957543	50.959584
pmma092308_012_3	38.673947	50.477527	50.478654
pmma092308_014_3	38.243215	51.456111	51.456345
pmma092308_015_3	37.155039	51.540146	51.545658
pmma092308_020_3	38.47691	51.064001	51.065883
pmma092308_022_3	38.277718	51.289555	51.297069
pmma092308_023_3	38.198685	51.238941	51.239426
pmma092308_024_3b	38.395852	52.269584	52.281185
pmma092308_025_3	38.508327	51.065291	51.06845
pmma092308_026_3	38.455276	51.839864	51.842069
pmma092308_027_3	38.506823	52.088742	52.09076
pmma092308_029_3b	38.606793	50.2004	50.2012
pmma092308_033_3	38.261157	51.406894	51.408426
pmma092308_034_3	37.830134	51.862824	51.862964
pmma092308_035_3	38.059412	51.616005	51.616942
pmma092308_036_3	37.633199	52.370904	52.372113

Table B.1: PMMA Run A Sites 1, 2, 3 Height and Width Data

Filename	Ave Height	Width Horiz	Width Dist
Repeatability with No Part Movement			
pmma092308_007_rep2_1	38.77427	54.184324	54.21472
pmma092308_007_rep2_10	38.746871	54.206797	54.236695
pmma092308_007_rep2_2	38.816507	54.218347	54.25204
pmma092308_007_rep2_3	38.6613	54.239912	54.271218
pmma092308_007_rep2_4	38.834788	54.214678	54.245799
pmma092308_007_rep2_5	38.772221	54.206771	54.238575
pmma092308_007_rep2_6	38.816225	54.234625	54.265468
pmma092308_007_rep2_7	38.839592	54.195175	54.227137

Filename	Ave Height	Width Horiz	Width Dist
pmma092308_007_rep2_8	38.904586	54.23722	54.268955
pmma092308_007_rep2_9	38.816828	54.242126	54.274523
Repeatability with Part			
Re-fixtured after every Scan			
Filename	Ave Height	Width Horiz	Width Dist
pmma092308_007_mov2_1	38.900536	54.26037	54.278494
pmma092308_007_mov2_10	38.842887	54.2687	54.292626
pmma092308_007_mov2_2	39.120632	54.211712	54.243721
pmma092308_007_mov2_3	38.777558	54.226846	54.255522
pmma092308_007_mov2_4	38.894427	54.246142	54.277337
pmma092308_007_mov2_5	39.320482	54.146019	54.157764
pmma092308_007_mov2_6	38.86549	54.205816	54.225038
pmma092308_007_mov2_7	38.760742	54.185515	54.219209
pmma092308_007_mov2_8	38.762042	54.295781	54.316743
pmma092308_007_mov2_9	38.65538	54.384064	54.404564

Table B.2: PMMA Run A Repeatability of Zygo

Filename	Ave Height	Width Horiz	Width Dist
PMMA Run C Site 1			
run_c_p10_n3_s2	39.161085	48.809303	48.809491
run_c_p11_n4_s2	39.142523	49.350633	49.350724
run_c_p12_n5_s2	39.127542	48.970703	48.970862
run_c_p13_n6_s2	39.071556	49.7349	49.735763
run_c_p14_n7_s2	39.159649	48.87672	48.876722
run_c_p15_n8_s2	39.082853	49.168848	49.168904
run_c_p19_n9_s2	39.116858	48.935395	48.935415
run_c_p20_n10_s2	39.159047	48.933109	48.93311

Filename	Ave Height	Width Horiz	Width Dist
run_c_p21_n11_s2	39.114813	49.920411	49.920467
run_c_p22_n12_s2	39.062961	48.928877	48.928968
run_c_p24_n13_s2	39.025052	48.832436	48.832454
run_c_p25_n14_s2	39.127417	49.01179	49.011958
run_c_p26_n15_s2	39.213207	49.696829	49.696867
run_c_p27_n16_s2	39.114173	48.772719	48.772731
run_c_p28_n17_s2	38.854778	49.056284	49.056335
run_c_p29_n18_s2	39.077918	48.92369	48.923699
run_c_p30_n19_s2	39.11266	48.783759	48.783766
run_c_p31_n20_s2	39.052667	48.831095	48.83119
run_c_p32_n21_s2	39.149065	49.235008	49.235072
run_c_p33_n22_s2	39.092524	49.215612	49.215678
run_c_p8_n1_s2	39.153632	49.020065	49.020118
run_c_p9_n2_s2	39.096331	49.148775	49.148947
PMMA Run C Site 2			
Filename	Ave Height	Width Horiz	Width Dist
run_c_p10_n3_s4	39.037247	48.9497	48.949823
run_c_p11_n4_s4	39.076965	48.866565	48.866708
run_c_p12_n5_s4	38.982516	49.586857	49.586857
run_c_p13_n6_s4	39.03067	49.533869	49.533966
run_c_p14_n7_s4	39.050089	49.610046	49.610055
run_c_p15_n8_s4	39.044272	49.411306	49.411498
run_c_p19_n9_s4	39.199661	50.385339	50.387611
run_c_p20_n10_s4	38.994916	49.565457	49.565478
run_c_p21_n11_s4	39.010015	50.410955	50.411001
run_c_p22_n12_s4	38.993853	49.492047	49.492939
run_c_p24_n13_s4	39.0668	49.2688	49.269199
run_c_p25_n14_s4	39.189965	49.254682	49.254797

Filename	Ave Height	Width Horiz	Width Dist
run_c_p26_n15_s4	39.090467	50.219477	50.219926
run_c_p27_n16_s4	38.959225	49.457346	49.457598
run_c_p28_n17_s4	39.053404	49.644389	49.64503
run_c_p29_n18_s4	39.033745	50.790422	50.79046
run_c_p30_n19_s4	39.061499	50.336125	50.336135
run_c_p31_n20_s4	39.044546	49.860541	49.860544
run_c_p32_n21_s4	39.044533	49.817947	49.817947
run_c_p33_n22_s4	39.054638	49.706996	49.707125
run_c_p8_n1_s4	39.058297	49.498668	49.498693
run_c_p9_n2_s4	39.060919	49.766719	49.766761
PMMA Run C Site 3			
Filename	Ave Height	Width Horiz	Width Dist
run_c_p10_n3_s3	39.346185	49.57412	49.574149
run_c_p11_n4_s3	39.46048	49.547691	49.547702
run_c_p12_n5_s3	39.287166	50.254055	50.25436
run_c_p13_n6_s3	39.233095	49.866847	49.86691
run_c_p14_n7_s3	39.326169	49.972255	49.972416
run_c_p15_n8_s3	39.378631	50.228891	50.228963
run_c_p19_n9_s3	39.325114	55.174292	55.20698
run_c_p20_n10_s3	39.277522	49.577977	49.57818
run_c_p21_n11_s3	39.249299	50.512361	50.512559
run_c_p22_n12_s3	39.202912	49.425518	49.426402
run_c_p24_n13_s3	39.34468	49.632324	49.632877
run_c_p25_n14_s3	39.293466	49.450487	49.450504
run_c_p26_n15_s3	39.385693	51.013048	51.014028
run_c_p27_n16_s3	39.456316	49.533252	49.533311
run_c_p28_n17_s3	39.387744	53.253967	53.302873
run_c_p29_n18_s3	39.341695	50.392649	50.392768

Filename	Ave Height	Width Horiz	Width Dist
run_c_p30_n19_s3	40.746901	52.773478	52.807297
run_c_p31_n20_s3	39.349527	49.499147	49.499196
run_c_p32_n21_s3	39.362575	49.502913	49.503647
run_c_p33_n22_s3	39.374516	49.600253	49.601547
run_c_p8_n1_s3	39.418602	49.39569	49.395744
run_c_p9_n2_s3	39.302806	49.55739	49.557817

Table B.3: PMMA Run C Sites 1, 2, 3 Height and Width Data

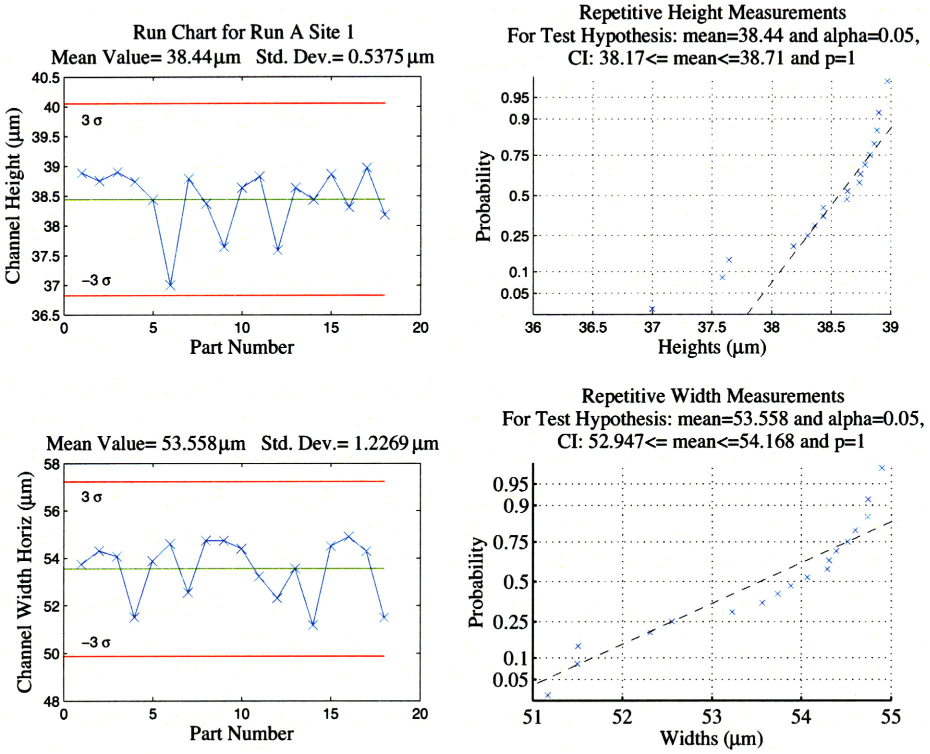

Figure B-1: Run A Site 1 Height and Width Including Outliers

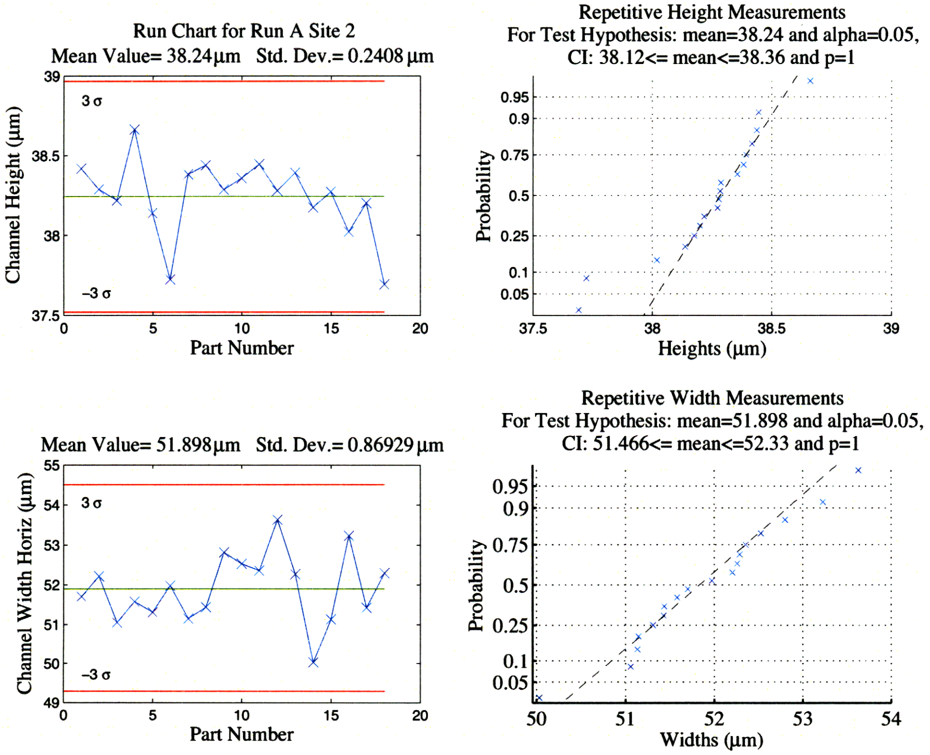

Figure B-2: Run A Site 2 Height and Width Including Outliers

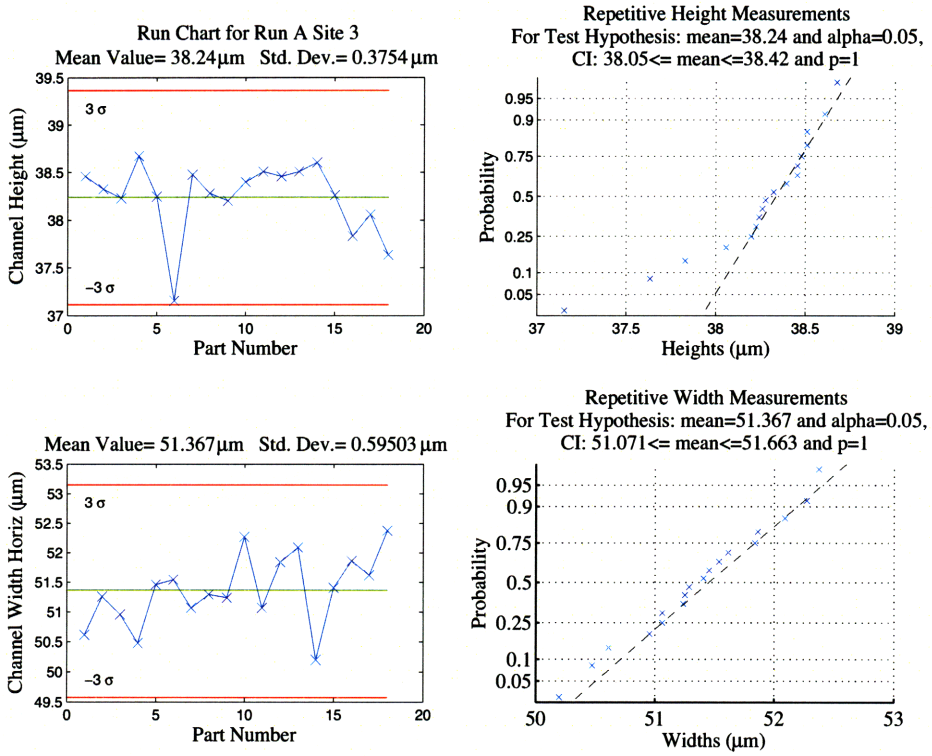

Figure B-3: Run A Site 3 Height and Width Including Outliers

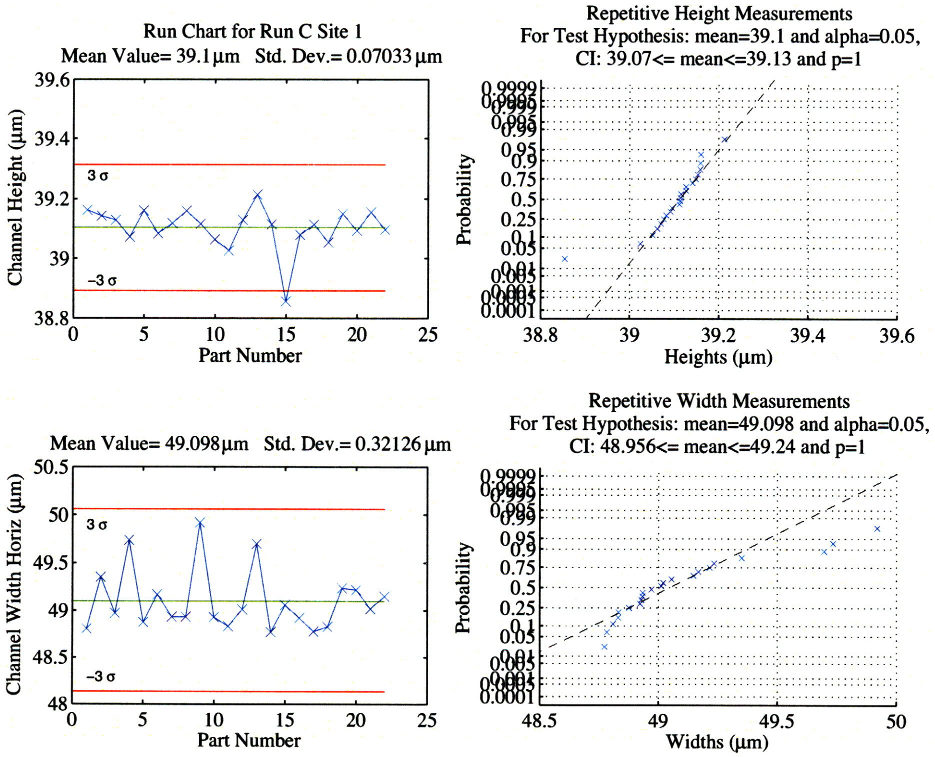

Figure B-4: Run C Site 1 Height and Width Including Outliers

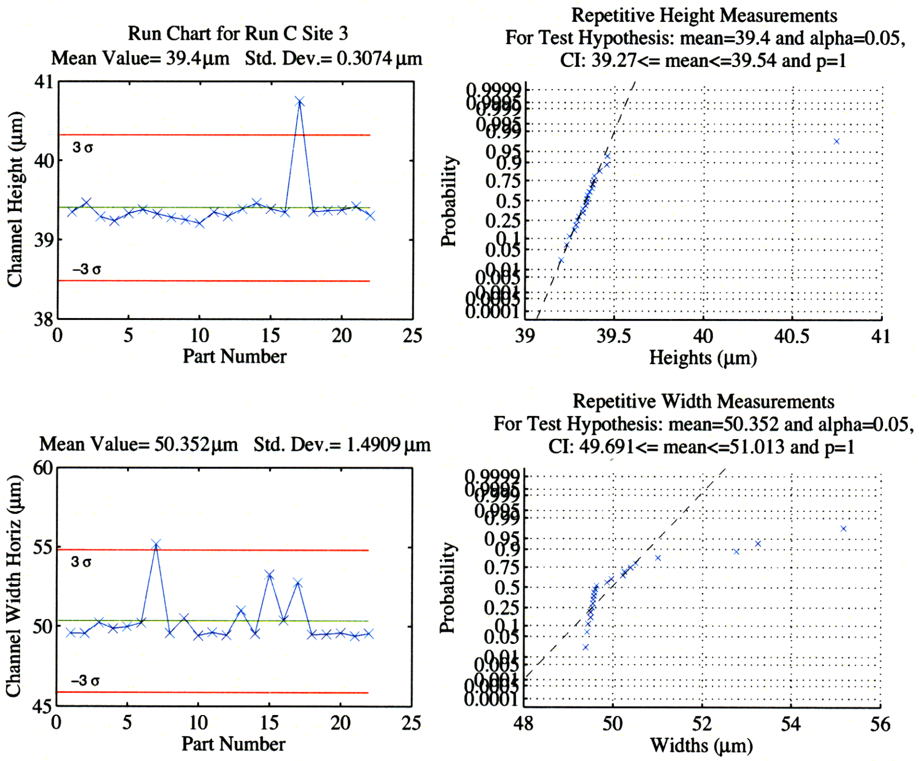

Figure B-5: Run C Site 3 Height and Width Including Outliers

Appendix C

Drawings

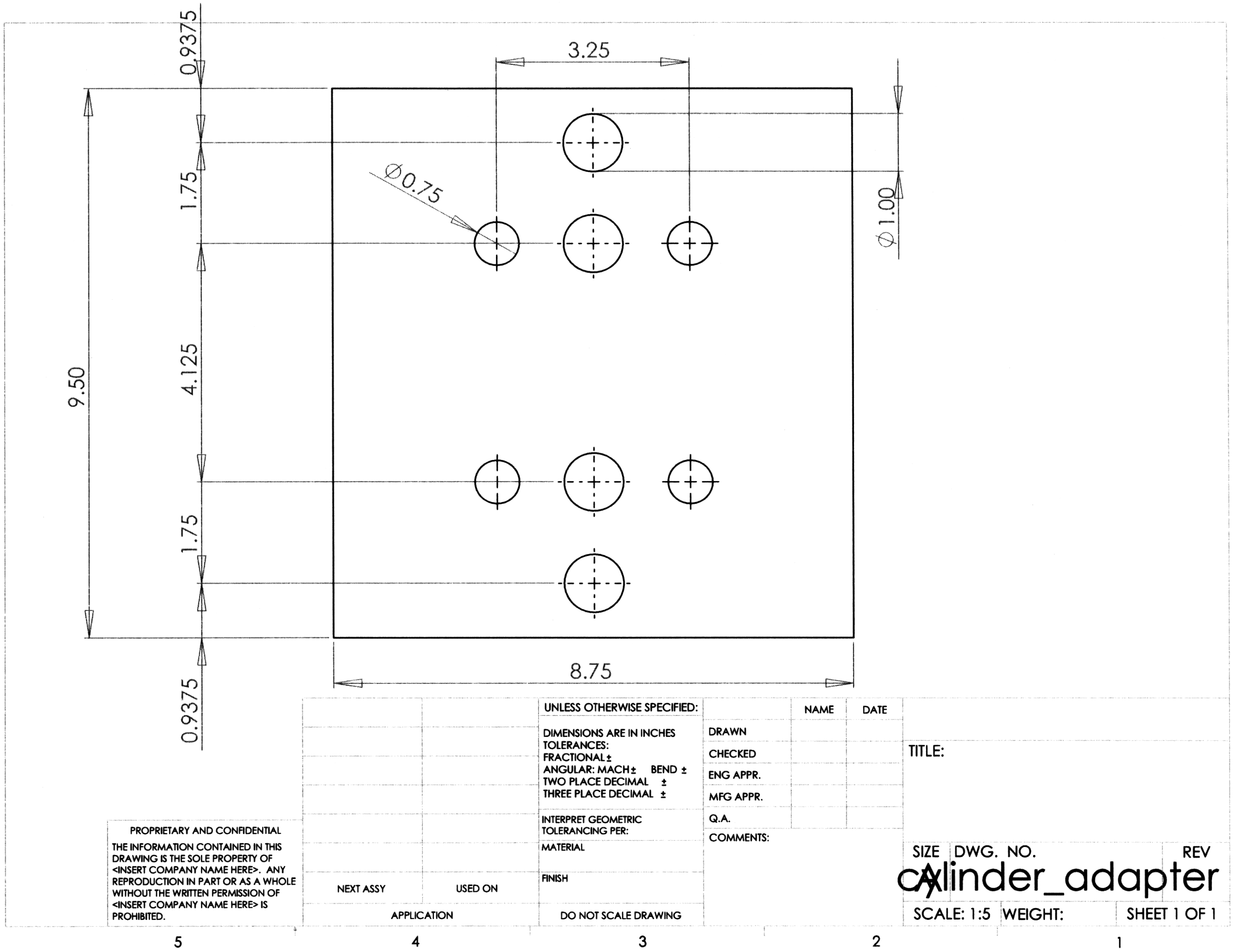
3.25
0.9375
1.75
4.125
1.75
0.9375
9.50
8.75
Ø0.75
Ø1.00
UNLESS OTHERWISE SPECIFIED:
DIMENSIONS ARE IN INCHES
TOLERANCES:
FRACTIONAL±
ANGULAR: MACH± BEND ±
TWO PLACE DECIMAL ±
THREE PLACE DECIMAL ±
INTERPRET GEOMETRIC TOLERANCING PER:
MATERIAL
FINISH
DO NOT SCALE DRAWING
NAME
DATE
DRAWN
CHECKED
ENG APPR.
MFG APPR.
Q.A.
COMMENTS:
TITLE:
SIZE
DWG. NO.
REV
A
cylinder_adapter
SCALE: 1:5
WEIGHT:
SHEET 1 OF 1
NEXT ASSY
USED ON
APPLICATION
PROPRIETARY AND CONFIDENTIAL
THE INFORMATION CONTAINED IN THIS DRAWING IS THE SOLE PROPERTY OF <INSERT COMPANY NAME HERE>. ANY REPRODUCTION IN PART OR AS A WHOLE WITHOUT THE WRITTEN PERMISSION OF <INSERT COMPANY NAME HERE> IS PROHIBITED.
5
4
3
2
1

Figure C-1: Solidworks Cylinder Adapter

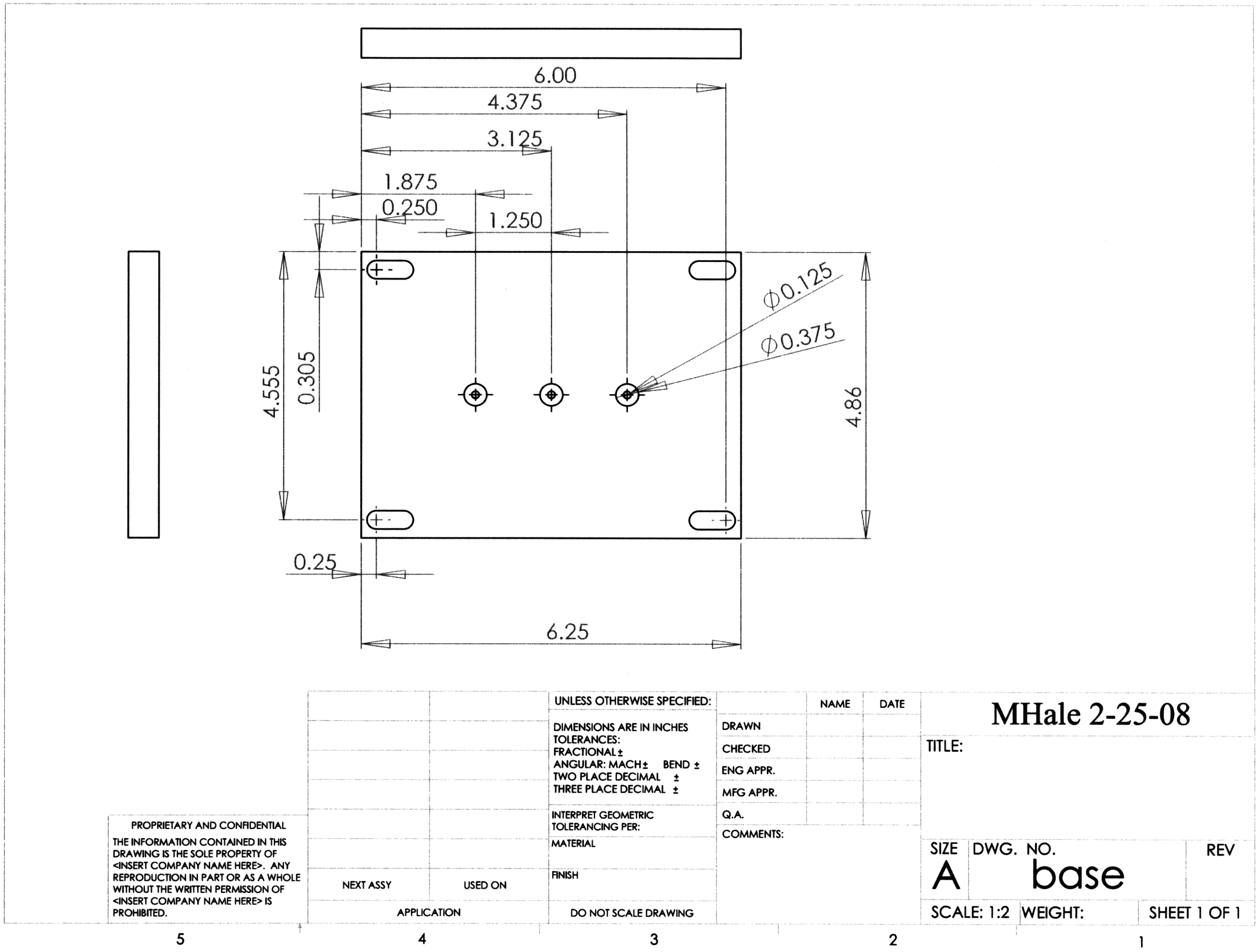
6.00
4.375
3.125
1.875
0.250
1.250
4.555
0.305
Φ0.125
Φ0.375
4.86
0.25
6.25
UNLESS OTHERWISE SPECIFIED:
DIMENSIONS ARE IN INCHES
TOLERANCES:
FRACTIONAL±
ANGULAR: MACH± BEND ±
TWO PLACE DECIMAL ±
THREE PLACE DECIMAL ±
INTERPRET GEOMETRIC TOLERANCING PER:
MATERIAL
FINISH
DO NOT SCALE DRAWING
NEXT ASSY
USED ON
APPLICATION
PROPRIETARY AND CONFIDENTIAL
THE INFORMATION CONTAINED IN THIS DRAWING IS THE SOLE PROPERTY OF <INSERT COMPANY NAME HERE>. ANY REPRODUCTION IN PART OR AS A WHOLE WITHOUT THE WRITTEN PERMISSION OF <INSERT COMPANY NAME HERE> IS PROHIBITED.
NAME
DATE
DRAWN
CHECKED
ENG APPR.
MFG APPR.
Q.A.
COMMENTS:
MHale 2-25-08
TITLE:
SIZE
A
DWG. NO.
base
REV
SCALE: 1:2
WEIGHT:
SHEET 1 OF 1
5
4
3
2
1

Figure C-2: Solidworks Base

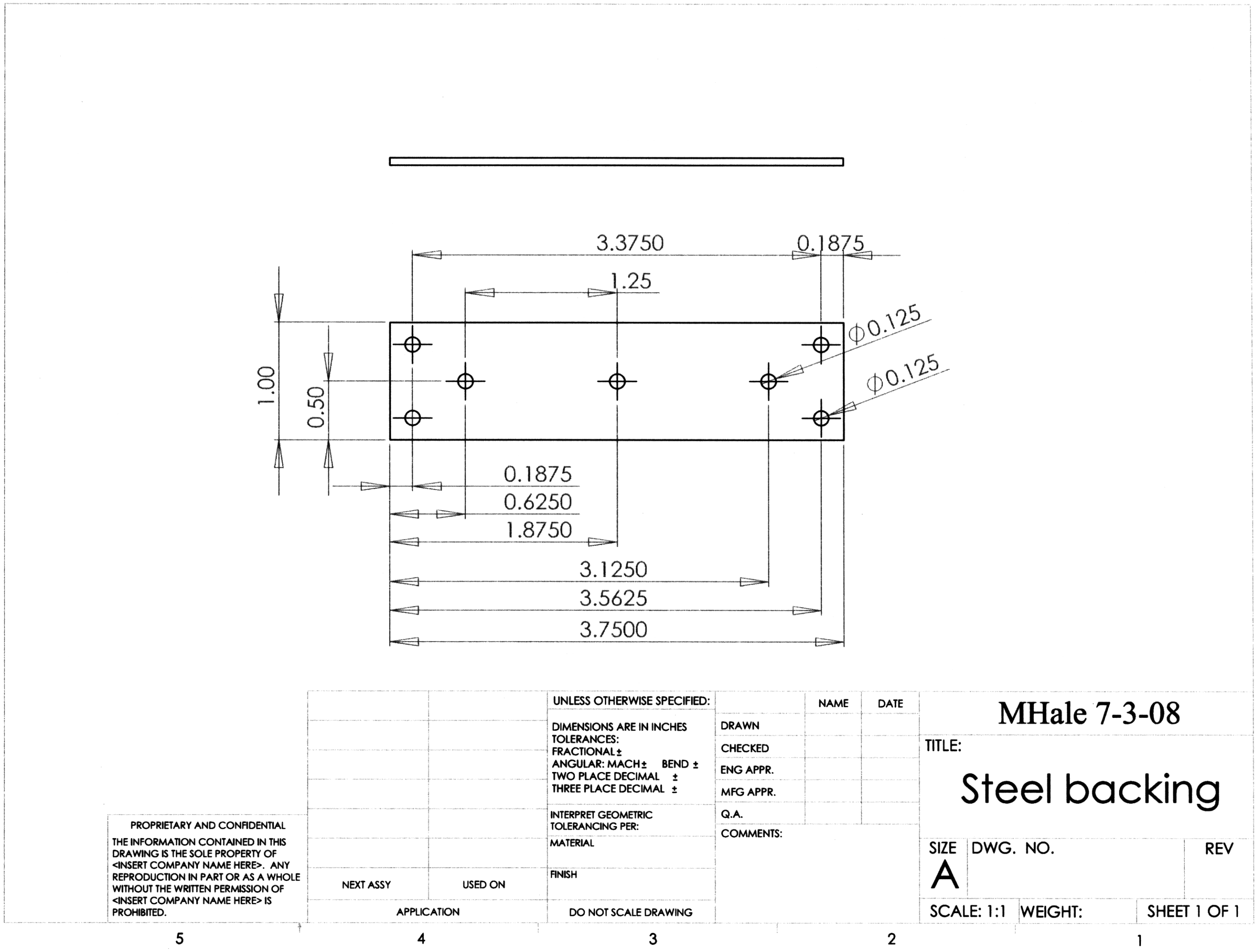
3.3750
0.1875
1.25
⌀0.125
⌀0.125
1.00
0.50
0.1875
0.6250
1.8750
3.1250
3.5625
3.7500
UNLESS OTHERWISE SPECIFIED:
DIMENSIONS ARE IN INCHES
TOLERANCES:
FRACTIONAL±
ANGULAR: MACH± BEND ±
TWO PLACE DECIMAL ±
THREE PLACE DECIMAL ±
INTERPRET GEOMETRIC TOLERANCING PER:
MATERIAL
FINISH
DO NOT SCALE DRAWING
NAME
DATE
DRAWN
CHECKED
ENG APPR.
MFG APPR.
Q.A.
COMMENTS:
MHale 7-3-08
TITLE:
Steel backing
SIZE
A
DWG. NO.
REV
SCALE: 1:1
WEIGHT:
SHEET 1 OF 1
PROPRIETARY AND CONFIDENTIAL
THE INFORMATION CONTAINED IN THIS DRAWING IS THE SOLE PROPERTY OF <INSERT COMPANY NAME HERE>. ANY REPRODUCTION IN PART OR AS A WHOLE WITHOUT THE WRITTEN PERMISSION OF <INSERT COMPANY NAME HERE> IS PROHIBITED.
NEXT ASSY
USED ON
APPLICATION
5
4
3
2
1

Figure C-3: Solidworks Steel Backing Plate

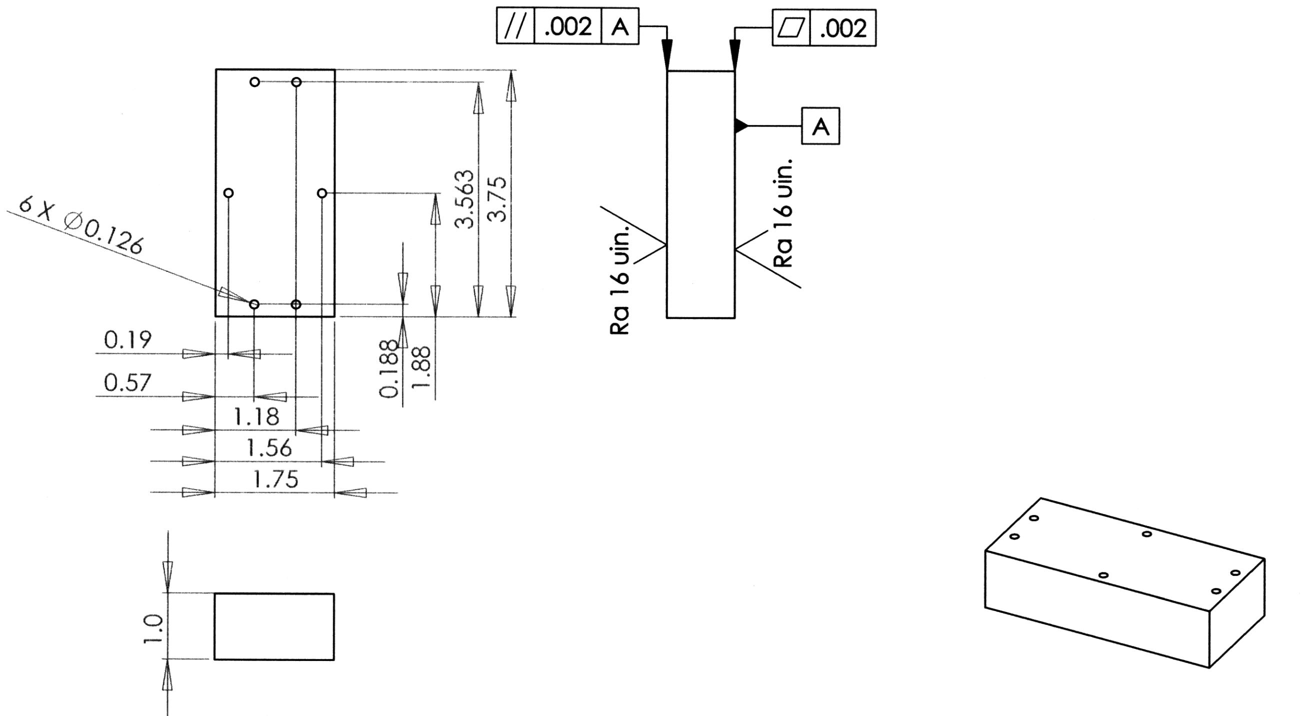

UNLESS OTHERWISE SPECIFIED:		NAME	DATE	TITLE:	
DIMENSIONS ARE IN INCHES TOLERANCES: .X = ±0.1 .XX = ± .01 .XXX = ±0.005 .XXXX = ±.0005 ANGLES = ±0.5° FRACTIONS = ±1/16	DRAWN	MH	1-18-08	Ceramic Embossing Backing	
	CHECKED				
	ENG APPR.			Melinda Hale 77 Mass Ave 35-135 Cambridge, MA 02139 halem@mit.edu 405-338-0103	
	MFG APPR.				
INTERPRET GEOMETRIC TOLERANCING PER:	Q.A.				
MATERIAL Rescor 914 Glass Ceramic	COMMENTS:			SIZE A DWG. NO. MH00021	REV 0
FINISH					
DO NOT SCALE DRAWING				SCALE: 1:2 WEIGHT:	SHEET 1 OF 1

NEXT ASSY	USED ON
APPLICATION	

PROPRIETARY AND CONFIDENTIAL

THE INFORMATION CONTAINED IN THIS DRAWING IS THE SOLE PROPERTY OF M.I.T LABORATORY FOR MANUFACTURING AND PRODUCTIVITY. ANY REPRODUCTION IN PART OR AS A WHOLE WITHOUT THE WRITTEN PERMISSION OF M.I.T LMP IS PROHIBITED.

5 4 3 2 1

Figure C-4: Solidworks Top Ceramic Spacer

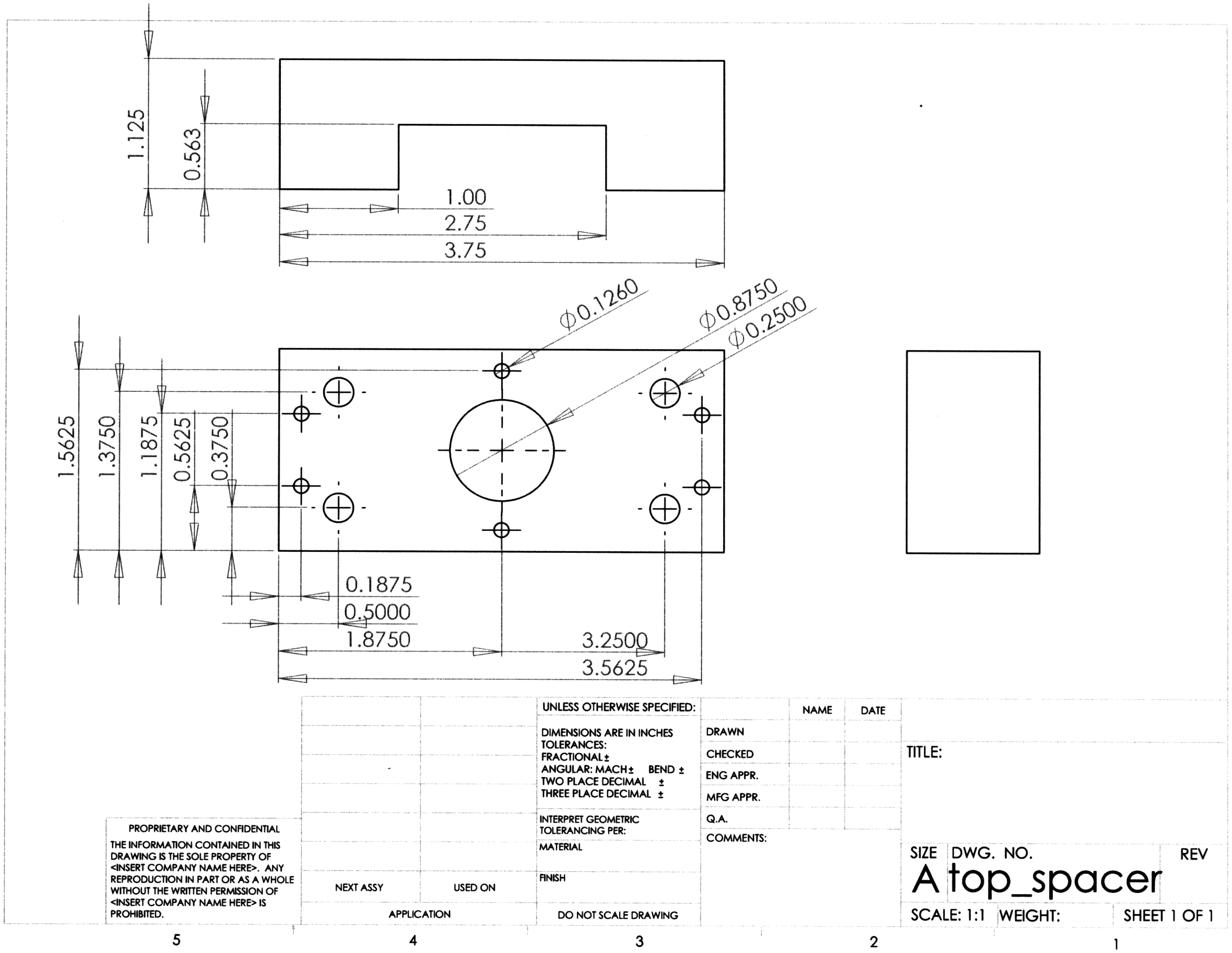
1.125
0.563
1.00
2.75
3.75
⌀0.1260
⌀0.8750
⌀0.2500
1.5625
1.3750
1.1875
0.5625
0.3750
0.1875
0.5000
1.8750
3.2500
3.5625
UNLESS OTHERWISE SPECIFIED:
DIMENSIONS ARE IN INCHES
TOLERANCES:
FRACTIONAL ±
ANGULAR: MACH ± BEND ±
TWO PLACE DECIMAL ±
THREE PLACE DECIMAL ±
INTERPRET GEOMETRIC TOLERANCING PER:
MATERIAL
FINISH
DO NOT SCALE DRAWING
NAME
DATE
DRAWN
CHECKED
ENG APPR.
MFG APPR.
Q.A.
COMMENTS:
TITLE:
SIZE
DWG. NO.
REV
A
top_spacer
SCALE: 1:1
WEIGHT:
SHEET 1 OF 1
PROPRIETARY AND CONFIDENTIAL
THE INFORMATION CONTAINED IN THIS DRAWING IS THE SOLE PROPERTY OF <INSERT COMPANY NAME HERE>. ANY REPRODUCTION IN PART OR AS A WHOLE WITHOUT THE WRITTEN PERMISSION OF <INSERT COMPANY NAME HERE> IS PROHIBITED.
NEXT ASSY
USED ON
APPLICATION
5
4
3
2
1

Figure C-5: Solidworks Force Adapter

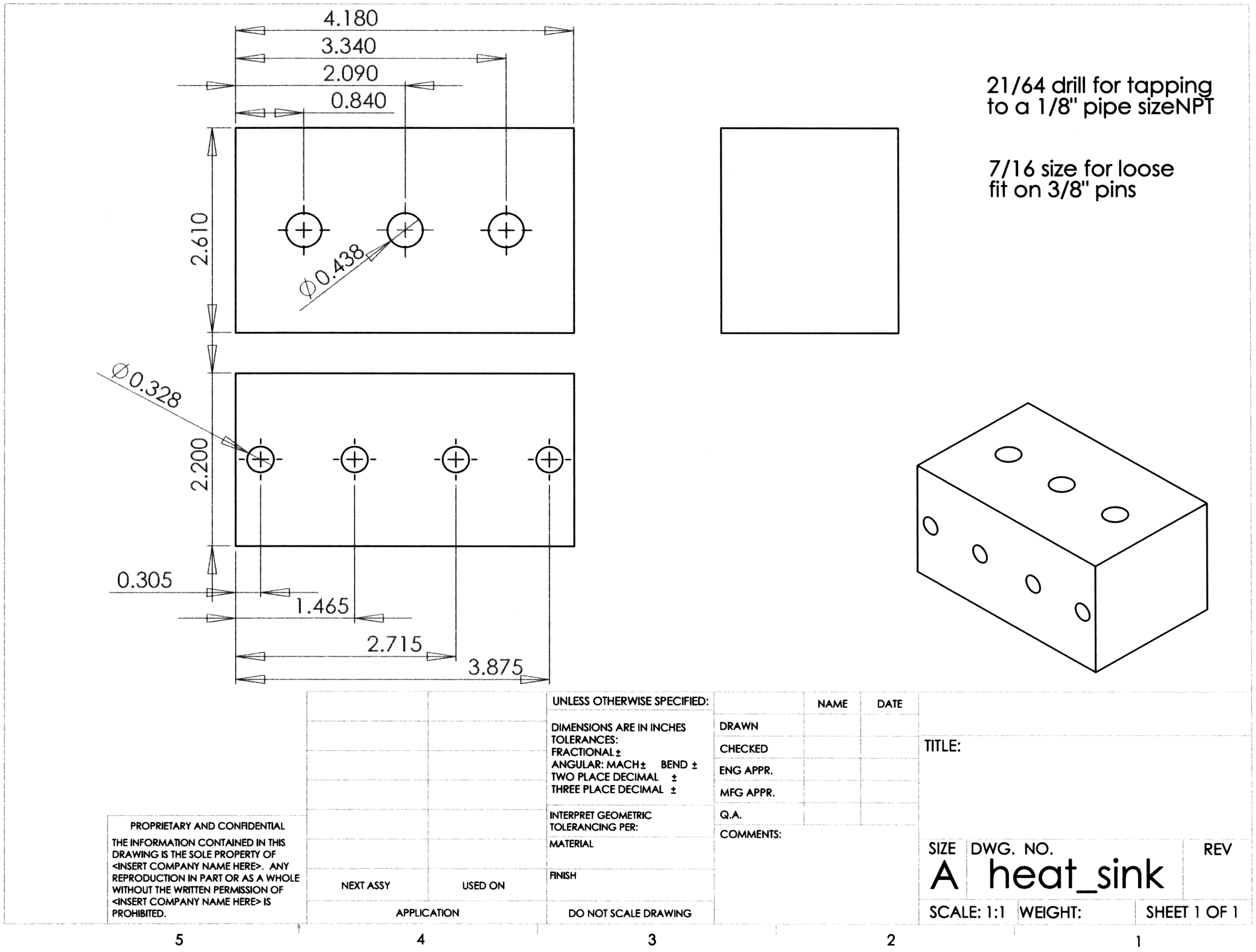
4.180
3.340
2.090
0.840
2.610
⌀0.438
⌀0.328
2.200
0.305
1.465
2.715
3.875
21/64 drill for tapping
to a 1/8" pipe sizeNPT
7/16 size for loose
fit on 3/8" pins
UNLESS OTHERWISE SPECIFIED:
DIMENSIONS ARE IN INCHES
TOLERANCES:
FRACTIONAL±
ANGULAR: MACH± BEND ±
TWO PLACE DECIMAL ±
THREE PLACE DECIMAL ±
INTERPRET GEOMETRIC TOLERANCING PER:
MATERIAL
FINISH
DO NOT SCALE DRAWING
NAME
DATE
DRAWN
CHECKED
ENG APPR.
MFG APPR.
Q.A.
COMMENTS:
TITLE:
SIZE
DWG. NO.
REV
A
heat_sink
SCALE: 1:1
WEIGHT:
SHEET 1 OF 1
NEXT ASSY
USED ON
APPLICATION
PROPRIETARY AND CONFIDENTIAL
THE INFORMATION CONTAINED IN THIS DRAWING IS THE SOLE PROPERTY OF <INSERT COMPANY NAME HERE>. ANY REPRODUCTION IN PART OR AS A WHOLE WITHOUT THE WRITTEN PERMISSION OF <INSERT COMPANY NAME HERE> IS PROHIBITED.
5
4
3
2
1

Figure C-6: Solidworks Heat Sink

Bibliography

[1] Manufacturing. *Merriam-Webster's Collegiate Dictionary*, 11th ed.:1663, Jan 2003.

[2] World Microfluidics/Lab-on-a-chip Markets. *Frost and Sullivan*, Jan 2003.

[3] U.S. Microfluidics/Lab-on-a-chip Markets. *Frost and Sullivan*, May 2006.

[4] Nano & micro imprint technologies technical brochure. *EV Group*, page 12, Oct 2008.

[5] Obducat annual report 2007. *Obducat*, page 76, Jun 2008.

[6] Singapore-Mit Alliance Annual Report 07/08. Jan 2008.

[7] Wikert hydrualic presses technical brochure. *Wikert*, page 7, Dec 2008.

[8] Jenoptik technical brochure. *Jenoptik*, page 1, Apr 2009.

[9] H Becker and C Gartner. Polymer microfabrication technologies for microfluidic systems. *Analytical and Bioanalytical Chemistry*, 390:89–111, Nov 2008.

[10] H Becker and L Locascio. Review: Polymer microfluidic devices. *Talanta*, 56:267–287, Jan 2002.

[11] MB Chan-Park, YC Lam, P Laulia, and SC Joshi. Simulation and investigation of factors affecting high aspect ratio UV embossing. *Langmuir*, 21:2000–2007, Dec 2005.

[12] J Chang and S Yang. Gas pressurized hot embossing for transcription of micro-features. *Microsystem Technologies*, Jan 2003.

[13] J Chang and S Yang. Development of fluid-based heating and pressing systems for micro hot embossing. *Microsystem Technologies*, Jan 2005.

[14] A de Mello. Plastic fantastic? *Lab on a Chip*, Jan 2002.

[15] M Dirckx. Design of a fast cycle time hot micro-embossing machine. *S.M. Thesis*, Jun 2005.

[16] KF Ehmann, D Bourell, ML Culpepper, TJ Hodgson, TR Kurfess, M Madou, K Rajurkar, and RE DeVor. International assessment of research and development in micromanufacturing. *Final Report of the World Technology Evaluation Center (WTEC) Panel on Micromanufacturing*, Oct 2005.

[17] B Ganesan. Process control for micro embossing: initial variability study. *S.M. Thesis*, Jan 2004.

[18] P Gravesen, J Branebjerg, and O Jensen. Microfluidics-a review. *Journal of Micromechanics and Microengineering*, Jan 1993.

[19] DE Hardt, B Anthony, and SB Tor. A teaching factory for polymer microfabrication - μfac. *Proceedings of the 6th International Symposium on Nano-Manufacturing*, Dec 2008.

[20] M Heckele, W Bacher, and K Müller. Hot embossing-the molding technique for plastic microstructures. *Microsystem Technologies*, Jan 1998.

[21] M Heckele and W Schomburg. Review on micro molding of thermoplastic polymers. *Journal of Micromechanics and Microengineering*, Jan 2004.

[22] D Henann and L Anand. A constitutive theory for the mechanical response of amorphous metals at high temperatures spanning the glass transition temperature: Application to microscale thermoplastic forming. *Acta Mater*, 56(13):3290–3305, Jan 2008.

[23] Y Juang, L Lee, and K Koelling. Hot embossing in microfabrication. Part I: Experimental. *Polymer Engineering & Science*, Jan 2002.

[24] S Kalpakjian and SR Schmid. Manufacturing engineering and technology. Jan 2006.

[25] W Liu, T Kimerling, D Yao, and B Kim. Rapid thermal response (RTR) hot embossing of micro-structures. *ANTEC... conference proceedings*, Jan 2004.

[26] A Manz, J Fettinger, E Verpoorte, H Lüdi, HM Widmer, and D Harrison. Micromachining of monocrystalline silicon and glass for chemical analysis systems: A look

into next century's technology or just a fashionable craze? *TrAC Trends in Analytical Chemistry*, 10(5):144–149, 1991.

[27] A Manz, N Graber, and HM Widmer. Miniaturized total chemical analysis systems: a novel concept for chemical sensing. *Sensors and Actuators*, B1:244–248, 1990.

[28] A Mazzeo. Centrifugal casting and fast curing of polydimethylsiloxane (PDMS) for the manufacture of micro and nano featured components. *S.M. Thesis*, Apr 2009.

[29] A Mazzeo and DE Hardt. Toward the manufacture of micro and nano features with curable liquid resins: Mold materials and part-to-part dimensional variation. *Proceedings of the 5th International Symposium on Nanomanufacturing (ISNM)*, Jan 2008.

[30] J Ouellette. A new wave of microfluidic devices. *The Industrial Physicist*, Jan 2003.

[31] M Rossi and I Kallioniemi. Micro-optical modules fabricated by high-precision replication processes. *Proceedings of the OSA Topical Meeting "Diffractive Optics and Micro-optics"*, Jul 2002.

[32] Y Su, J Shah, and L Lin. Implementation and analysis of polymeric microstructure replication by micro injection molding. *Journal of Micromechanics and Microengineering*, Jan 2004.

[33] Q Wang. Process window characterization and process variation identification of micro embossing process. *S.M. Thesis*, page 1, Mar 2006.

[34] X Wang, L Wang, C Liu, L Ma, and Y Luo. Automatic fabrication system for plastic microfluidic chips. *Micro-Nanomechatronics and Human Science*, Jan 2004.

[35] Y Xia and G Whitesides. Soft lithography. *Annual Reviews in Materials Science*, (28):153–184, Jan 1998.

[36] D Yao, AY Yi, L Li, and P Nagarajan. Two-station embossing process for rapid fabrication of polymer microstructures. Dec 2005.